CONTINUOUS FLASH EXTRACTION OF ALCOHOLS FROM FERMENTATION BROTH

Frederick D. Teye

Thesis submitted to the Faculty of the

Virginia Polytechnic Institute and State University

in partial fulfillment of the requirements for the degree of

MASTER OF SCIENCE

in

Biological Systems Engineering

Foster A. Agblevor, Chair

Luke E. Achenie

Chenming Zhang

February 4, 2009

Blacksburg, Virginia

Keywords: Flashing, Tops, Bottoms, saturation temperature, saturation pressure, isothermal flash tank, throttling, critical temperature, critical pressure, gas partition, equilibrium, Joule-Thompson coefficient

Continuous flash extraction of alcohols from fermentation broth

Frederick D. Teye

ABSTRACT

A new method of *in situ* extraction of alcohols from fermentation broth was investigated. The extraction method exploited the latent advantages of the non-equilibrium phase interaction of the fluid system in the flash tank to effectively recover the alcohol. Carbon dioxide gas ranging from 4.2L/min to 12.6L/min was used to continuously strip 2 and 12% (v/v) ethanol solution in a fermentor with a recycle. Ethanol and water in the stripped gas was recovered by compressing and then flashing into a flash tank that was maintained at 5 to 70bar and 5 to 55^{o}C where two immiscible phases comprising CO_2-rich phase (top layer) and H_2O-rich phase (bottom layer) were formed. The H_2O-rich bottom layer was collected as the Bottoms. The CO_2-rich phase was continuously throttled producing a condensate (Tops) as a result of the Joule-Thompson cooling effect. The total ethanol recovered from the extraction scheme was 46.0 to 80% for the fermentor containing 2% (v/v) ethanol and 57 to 89% for the fermentor containing 12% (v/v) ethanol. The concentration of ethanol in the Bottoms ranged from 8.0 to 14.9 %(v/v) for the extraction from the 2 %(v/v) ethanol solution and 40.0 to 53.8 %(v/v) for the 12% (v/v) fermentor ethanol extraction. The Bottoms concentration showed a fourfold increase compared to the feed. The ethanol concentration of the Tops were much higher with the highest at approx. 90% (v/v) ethanol, however the yields were extremely low. Compression work required ranged from 6.4 to 20.1 MJ/ kg ethanol recovered from the gas stream in the case of 12% (v/v) ethanol in fermentor. The energy requirement for the 2% (v/v) extraction was 84MJ/kg recovered ethanol. The measured Joule-Thompson

cooling effect for the extraction scheme was in the range of 10 to 20% the work of compressing the gas. The lowest measured throttle valve temperature was -47^{o}C at the flash tank conditions of 70bar and 25^{o}C. Optimization of the extraction scheme showed that increasing the temperature of the flash tank reduced the amount of ethanol recovered. Increasing the pressure of the flash tank increased the total ethanol recovered but beyond 45bar it appeared to reduce the yield. The 12.6L/min carbon dioxide flow rate favored the high pressure(70bar) extraction whiles 4.2L/min appeared to favor the low pressure(40bar) extraction. The studies showed that the extraction method could potentially be used to recover ethanol and other fermentation products.

DEDICATION

I dedicate this work to my mother Gladys and my father for investing so much in my education. I dedicate it to the rest of the Teye family for their support and atmosphere. I also dedicate this work to Caroline, my fiancée Amy and her family for their hospitality.

ACKNOWLEDGMENTS

I give thanks to the Almighty God who has been my source of strength and inspiration throughout my research and more. The one from whom we derive succour and intelligence. The immense contribution of my supervisor, Dr. Foster A. Agblevor, cannot go unnoticed. At all times he provided me with hints, pieces of information, and guides as to how to proceed with the research. He made as much time not to let wrong placement of punctuations elude him and to that I am grateful. The contributions of my other committee members, Dr. Luke E. Achenie and Dr. Chenming Zhang are deeply appreciated. They were there at all times to listen and guide. I would also like to thank Dr. G. Afrane for the rich academic exposure and helping me discover my potential. The great humour and involvement of my lab mates, Nii and Fred kept me re-energized at all times. Finally, I reserve gratitude to the Department of Biological Systems Engineering and Virginia Polytechnic Institute and State University for investing a great deal of time, money, and other resources towards my research work.

TABLE OF CONTENTS

LIST OF TABLES

LIST OF FIGURES

CHAPTER ONE

INTRODUCTION

1.1 Background

Ethanol production from biomass using biochemical technologies was extensively investigated as an alternative energy source between 1975-1985 when petroleum crude oil prices were high (Almudi 1982; Bungay 1981; Carioca et al. 1981). These researches generated a lot of literature related to the industrial and economic production and use of bioethanol (Cysewski and Wilke 1976; Kosaric et al. 1981; Kosaric et al. 1983; Wilke et al. 1981). However, interest in biomass to ethanol research decreased as oil prices decreased. The potential use of ethanol as octane enhancer in automobile fuels perhaps kept the little research going on in the area after 1985. In the mid 1990s, interest in ethanol research spiked again because of the problems of MTBE (methyltetrabutyl ether) as gasoline additive. Soaring petroleum prices over the last five years have compounded the need for development of cost-effective technologies for alcohols especially ethanol production aimed at achieving better conversion of sugars, minimizing recovery cost and reducing evaporative product losses.

One promising method suitable for large scale application for alcohols is *in situ* gas stripping of fermentation product (Park and Geng 1992). This involves the separation and removal of product as it is formed with a stripping gas. Carbon dioxide has been most researched for gas stripping since it served as free extractant for the process(Park and Geng 1992). Literature on *in situ* gas stripping of alcohol fermentation involved the recovery of alcohols from the gas stream with solid adsorbent, water traps or cold condensers. Absorbing the alcohol in water traps re-introduces water into the process.

Energy is expended to separate the water from the alcohol downstream. Adsorbents have equilibrium capacity for the material they absorb. When they get saturated the adsorbed material would have to be desorbed to regenerate it which requires the use of energy. Cold condensers have also been shown to be ineffective in recovering alcohols from the stripping gas stream (Duboc and von Stockar 1998; Loser et al. 2005).

The ability of carbon dioxide to influence cell growth (Jones and Greenfield 1982) and the capacity of the solvent properties of carbon dioxide to change sharply depending on its concentration and state (Francis 1954) could be exploited to effect the separation of ethanol and water from the carbon dioxide gas stream. This route has the potential of eliminating the above mentioned drawbacks in the recovery process.

In view of this, it is proposed here to extract ethanol by stripping the fermentation media with carbon dioxide at atmospheric pressure or slightly elevated pressures where the performance of microorganisms is not adversely affected. The carbon dioxide mixture will then be compressed and flashed to produce a condensate. This scheme can potentially take advantage of the drastic change in carbon dioxide fluid properties, non-equilibrium phase interaction in the compressor chamber and also the inherently high Joule-Thomson refrigeration effect of carbon dioxide that can condense remnant material in the carbon dioxide gas. The cold gas can be used to provide the cooling needs of the fermentor and other parts of the alcohol fermentation plant where it is needed. This approach will be especially useful in the situation where the fermentation product is valuable and is present in low concentrations. Fermentation of other volatile products other than alcohols could also be recovered using this method. The simplicity of the

proposed scheme makes it promising for small scale application. Sparging carbon dioxide into the fermentor can also produce some stirring effect needed for good fermentation.

1.2 Objectives

The overall goal of this research is to recover fermentation products using near critical flash extraction. Ethanol would be used as a model to study the extraction and the flash recovery of the fermentation product. The specific objectives of the studies are:

1. Investigate the effect of carbon dioxide flow rate, temperature and pressure on the extraction of ethanol from fermentation broth.
2. Use response surface methodology to find optimum operating conditions for ethanol extraction from fermentation broth.
3. Determine energy balance for the extraction system.

CHAPTER TWO

LITERATURE REVIEW

2.1 Introduction

This chapter is an overview of bioethanol production from various feedstocks. Advantages and drawbacks using the different feedstock available for the process are discussed. Process and heat integration methods employed widely in industry to increase the efficiency and recovery of products from fermentation process are discussed. In situ gas stripping of fermentation technology for the recovery of alcohols is discussed.

2.2 Sugars for microbial fermentation

Sources of sugar for alcohol fermentation (sucrose, glucose, and fructose) can be generalized into three main groups: sucrose, starchy and lignocellulosic materials. Sucrose materials (such as sugar cane or sugar beet, etc.) can be converted into alcohols after crushing and extraction, fermentation and purification. Starchy materials like corn, wheat and cassava require an additional hydrolysis step prior to fermentation. Lignocellulosic materials mainly from agricultural residues, industrial or domestic wastes are the cheapest because of their wide availability. However, they are the most expensive to convert because they require pretreatment of the feedstock in addition to hydrolysis to liberate potential fermentable sugars (Cardona and Sanchez 2007; Serra et al. 1987) prior to fermentation and purification. The pretreatment step is needed for the removal of lignin, to make hemicellulose, and cellulose in the biomoass accessible for hydrolysis. Ethanol and other products fermented from lignocellulosic hydrolysate have low yield due to the presence of contaminants that are generated during the pretreatment.

2.3 Process and heat integration

It has long been observed that there is a limit to the ethanol concentration and other alcohols produced by fermentation in a simple batch or in a continuous fermentor because of the toxicity of the product to the alcohol-producing microorganisms. *Saccharomyces cerevisiae* for instance cannot tolerate ethanol concentrations of more than 10-12% volume in the fermentation media. Hence in order to achieve a complete conversion of sugar substrate during fermentation, a dilute glucose solution of about 16% weight is used (Taylor et al. 1995). This leads to large fermentors and high cost in the product recovery stage since large amount of water has to be removed.

To make the production of ethanol and other alcohols from lignocellulosic biomass competitive requires proper process and heat integration in addition to improved conversion technologies. Planning to identify and minimize where there are potential losses is also important. Process integration involving combining different stages in fermentation and recovery into single processes has the potential of reducing energy used, equipment numbers, equipment sizes and increasing product yields. Process integration in fermentation using *in situ* gas stripping of the fermentation product could have the highest impact on the overall process economy (Cardona and Sanchez 2007). The importance of reaction coupled with separation (fermentation and ethanol removal) was highlighted by Maiorella et al. (1984) when they assessed ethanol removal by various methods including membranes and extractive fermentation. Incorporation of gas stripping would be especially useful when used together with improved methods of alcohol production from biomass where enzyme hydrolytic activity is optimized, but ethanol concentration is still a constraint on yeast productivity(Shen and Agblevor 2008).

Energy integration involves a strategic planning for best utilization of the energy that is generated or consumed in a process ultimately to reduce external energy source demand. External energy demand of process plants is usually derived from petroleum.

The proposed ethanol extraction scheme here takes advantage of process and heat integration by using gas stripping technology and flash cooling for fermentor and other cooling needs. There would however be the need for the traditional fermentor slightly modified if carbon dioxide pressures greater than 1atm or the cooling effect generated from the throttling process used in the fermentation. The traditional cooling system (coils or jackets) on the fermentor would have to be removed and instead, an efficient carbon dioxide sparging system put in the bottom. This should ensure good carbon dioxide heat distribution, gas-liquid interaction, and stirring effect in the fermentor. Cooling systems on older fermentors would possibly be redundant. On the other hand, when slightly elevated carbon dioxide pressures would be used, provision for those pressures should be incorporated into the design of the fermentor especially the sealing between the cover and the rest of the fermentor.

Combined fermentation and ethanol recovery were initially reviewed by Park and Geng (1992). They classified separation methods used for ethanol and other alcohols and organics production into product stripping into gas phase (vacuum fermentation, gas stripping), liquid phase (liquid-liquid extraction, aqueous two-phase system) and solid phase (adsorption). These methods rely on partitioning or equilibrium distribution of the product in the gas-liquid, liquid-liquid or liquid-solid systems to achieve the separation. Membranes are sometimes used in conjunction with these systems. The review by Park and Geng (1992) included fermentation under vacuum(Cysewski and Wilke 1977),

pervaporation process(Muller and Pons 1991; Shabtai et al. 1991), liquid-liquid extraction(Kuhn 1980; Matsumura and Markl 1984), perstraction(Christen et al. 1990), and solid adsorption (Lencki et al. 1983). They concluded that gas stripping was attractive for large scale production because it was relatively simple, volatile products were separated in clean forms (not contaminated with the non volatiles) and the stripping gas (carbon dioxide) was a free extractant.

Current method of reaction separation were reviewed by Cardona and Sanchez (2007) They included enzymatic hydrolysis with glucose separation (Gan et al. 2002; Lopez-Ulibarri and Hall 1997; Mandavilli 2000), vacuum fermentation (da Silva et al. 1999), pervaporation, perstraction and membrane distillation(Christen et al. 1990; Gryta et al. 2000; Ikegami et al. 2003) and ethanol removal by liquid-liquid extraction(Offeman et al. 2005; Oliveira et al. 1998)

Gas stripping has enjoyed more research work lately over vacuum fermentation even with the improved patented “Flashferm” vacuum fermentation(Wilke et al. 1982) because carbon dioxide produced during fermentation poses problems in vacuum fermentation. The large amount of non-condensable carbon dioxide produced during fermentation causes severe ethanol condensation and dramatically increases the operating cost of the vacuum pump in vacuum fermentation (Park and Geng 1992). Vacuum fermentation thus requires large compressors. The accumulation of glycerol is however a potential problem in situ gas stripping of ethanol fermentation (Kuhn 1980). This can cause fouling in packed columns attached to the fermentors.

2.4 Fermentation and gas stripping with carbon dioxide

Walsh et al.(1983) and Pham et al. (1989) proposed bubbling of carbon dioxide gas through the fermentor to remove ethanol. Walsh et al.(1983) proposed using carbon dioxide to continuously strip ethanol from fermentation broth and passing the carbon dioxide over an adsorbing bed composed of activated carbon to adsorb the ethanol and some water. Further purification was done by desorbing the adsorbed product into carbon dioxide gas stream by heating and passing the gas over a cellulose material to enrich (remove water) the ethanol in gas stream for condensation. Water cooled condenser was used to condense the ethanol product. The work by Pham et al. (1989) involved continuously stripping ethanol vapor from ethanol solution and rectified it in a coconut shell charcoal packed column with reflux. They used cold condensers for collection of the ethanol.

Thibault et al. (1987) combined the advantages of the stripping power of supercritical carbon dioxide with that of in situ gas stripping of a fermentor with high pressure carbon dioxide up to 7Mpa. It was found that high pressure had a strong inhibitory effect on yeast fermentation of ethanol. This was not only on the initial production of ethanol but also on the final concentration of ethanol. When the pressure was relieved, ethanol production by yeast resumed at its normal rate, showing that pressure effect on yeast was reversible. Because high pressures had strong inhibitory effect on yeast fermentation, the in situ extraction method was improved by using a repetitive cycle of pressurizing and depressurizing (Litalien et al. 1989). They observed a decrease in ethanol concentration (29.0g/l to 15.9g/l) but the viability of yeast cell did not change after several cycles.

Dale et al.(1985) proposed carbon dioxide stripping of ethanol from a fermentor consisting of a packed column of immobilized cells. Their model showed an increase in ethanol productivity as compared to an identical fermentor without gas stripping highlighting the advantage of fermentation coupled with separation. Dale (1992) used a patented technology (Multi-stage continuous stirred reactor separator) consisting of a series of reactors where the broth from one stage to the other was counter currently stripped with carbon dioxide gas to remove ethanol. The stripped gas mixture was contacted with water to absorb the ethanol. Scott and Cooke (1995) used carbon dioxide to strip ethanol and other volatiles in the fermentation medium; the stripped ethanol vapor was passed through a condenser operated at -4^{o}C. Dominguez et al. (2000) showed an improvement in circulation, mass transfer and gas distribution in fermentation-stripping process by using a special gas-lift loop reactor with external side-arm for xylose to ethanol conversion where oxygen was necessary for the fermentation. They used ice-cooled condenser for the product recovery.

Taylor et al. (1995) proposed recycling the contents of a fermentor over a packed column where carbon dioxide was used to strip the ethanol. A refrigerated condenser system was used to recover the ethanol. Their refrigeration system consisted of methanol circulated at -20^{o}C, and the exit gas stream temperature was -8 to -10^{o}C. The researchers reported that the refrigeration system was very expensive. They also experienced fouling of the packed column by the yeast so they developed a scheme for cleaning. Later work by Taylor et al. (2000) integrated this scheme into the dry milling process of ethanol production. They reported a savings of $0.03/gal compared to the conventional dry milling method and

attributed the savings to the ability to ferment concentrated sugars and reduced distillation cost stemming from less water usage.

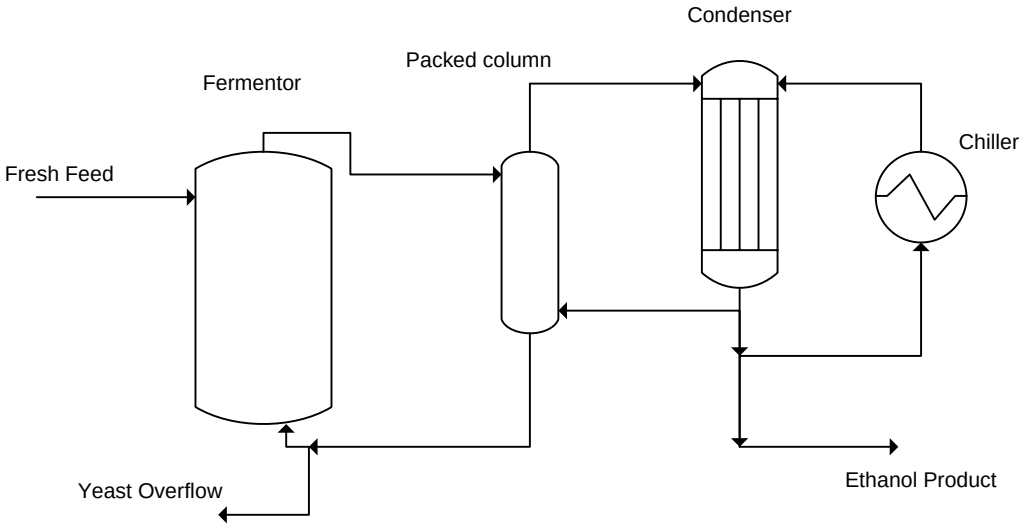

Figure 2.1 In situ carbon dioxide stripping of ethanol from fermentation

In all the cases discussed the recovery of the alcohol was done with water, with an adsorbent, or with refrigeration/ice-cooled bath. Most of the in situ gas stripping of ethanol coupled with fermentation used trap/condensation system similar to the simplified layout in Figure 2.1 as used by Taylor et al. (1998; 2000). The fermentation broth is passed through a packed column where it contacts carbon dioxide gas in a countercurrent manner. Some of the condensate from the condenser is diverted and passed through the refrigeration system (Chiller) and is brought in contact with the CO_2/vapor mixture from the packed column to condense the ethanol vapor.

2.4.1 Condensers on gas stripped fermentation reactors

Gas stripping of alcohols is employed to alleviate the inhibition of the product in bioreactors and also to prevent product losses. Because of their high volatility, ethanol and other volatile alcohols are lost through the exhaust gas stream. The amount of ethanol entrained in the carbon dioxide stream in bioreactors can account for more than 30% of

the ethanol produced (Loser et al. 2005). Loser et al. (2005) reported that the cooler used to reduce water loss does not effectively condense the entrained ethanol. Stripping of ethanol depends on the gas flow rate and the absorbing capacity of the gas (partition coefficient). Neither the stirring rate nor the gas flow in the fermentor significantly affected the partition coefficient of ethanol.

Studies by Duboc and von Stockar (1998) also showed that cold condensers on fermentors had minimal effect on ethanol evaporation. This was because the exiting carbon dioxide gas contacts ethanol-rich condensate on the surface of the condenser. It was shown that ethanol lost through this process was 20-30%.

A graphical representation of the effect of cold condensers on ethanol recovery was presented in the work of Duboc and von Stockar (1998). It was shown that, when the condenser temperature on a fermentor at 30^{o}C was reduced from 30^{o}C to 2 ^{o}C, only 25% of ethanol content in the vapor that entered the condenser was condensed and that the profile was similar when equilibrium was attained as in long condensers, thus the condenser had minimal effect on ethanol loss. However, up to 83% water was condensed. While as the condensation of water increased steeply with decrease in condenser temperature that of ethanol was rather sluggish. They suggested the use of absorption column for the recovery of ethanol from the vapor phase would be more effective than the condensation method.

2.5 Energy in Ethanol recovery

Ethanol recovery and purification methods were grouped by Serra et al. (1987) into conventional or modified conventional systems (distillation system) and non-conventional systems(non-distillation systems) for classification purposes. The

conventional methods of ethanol have been around for many years. The non-conventional systems were mostly developed during the 70's when there was the push to purify chemicals using less oil-derived energy.

2.5.1 Conventional and modified Conventional methods of ethanol concentration

The conventional methods are simple but very heat intensive. These methods of concentrating ethanol are widely used at industrial level to produce the majority of azeotropic ethanol. Dehydration of azeotropic ethanol to anhydrous ethanol requires the addition of other materials like a third entrainer (benzene, pentane, ether etc.) component to break the azeotrope. There are a number of heat optimized configurations (modified conventional method.) of distillation to reduce the energy consumption. These include distillation systems with vapor reuse or vapor recompression. Vapor reuse involves the use of the overhead vapor of one column as the heat source in the reboiler of another column operating at a lower pressure while vapor recompression entails tapping of the latent heat of the overhead vapor into the reboiler of the same column by compressing the vapor to the point of condensation in the reboiler. Heat energy requirement for concentrating ethanol from 6-10%wt to 95%wt with conventional distillation in two to four columns was in the range of 4730 to 8080 kJl^{-1} Product Ethanol (Serra et al. 1987).

2.5.2 Non-conventional methods of ethanol concentration

Non-conventional methods are hardly used on industrial scale. They are mostly used in laboratory or pilot plants where they are used for studies or production of high value product. The discussion by Serra et al. (1987) on non-conventional methods included supercritical or near critical fluid extraction processes (Brignole et al. 1987; Defilippi and

Moses 1982), adsorption on solid materials, water adsorption on molecular sieves (Douglas and Fienberg 1983), water adsorption on adsorbent agents in vapor phase (Hong et al. 1982; Ladisch and Dyck 1979; Ladisch et al. 1984), water adsorption by polymeric compounds in liquid phase(Fanta et al. 1980), ethanol adsorption by polymeric compounds in the liquid phase (Pitt et al. 1983), systems based on membranes (Belanche et al. 1986), liquid-liquid extraction systems (Earhart et al. 1977; Joshi et al. 1984; Munson and King 1984; Roddy 1981) and ethanol recovery by catalytic conversion to gasoline (Aldridge et al. 1984). Energy requirement of some gas extraction methods are shown in Table 2.1.

Table 2.1 Non-conventional ethanol recovery methods

Gas Type	Ethanol Conc. (% w/w)		Energy Usage (kJl^{-1})Product Ethanol	Reference.
	Initial	Final		
Supercritical CO_2 extraction	5	91	4790	Defilippi and Moses (1982)
√	10	91	2300	√
Near critical C_3H_8 extraction	10	99.5	2600	Brignole et al. (1987)

Energies for non conventional methods shown in Table 2.1 are given in heat equivalence with assumption of 33% conversion of heat to work. Hence processes that use electricity or engines for compression, like supercritical and near critical fluid extraction have been corrected to heat energy requirements. The energy consumption of the non-conventional methods are lower than most distillation methods.

2.6 Hypothesis of compressed and flashed carbon dioxide

Carbon dioxide could exhibit a dual antagonistic solubility effect near its critical temperature (Francis 1954). At low concentration of carbon dioxide (<40% wt), it acts as a dissolved gas and mixes well with the solvent or solvent mixture. At high concentration

(>60%wt), it could be a liquid with relatively low affinity (poor solvent) for the same solute species. This happens in the case of compressed carbon dioxide and water mixture. Ethanol is however miscible with liquid carbon dioxide and water. The ternary equilibrium system of ethanol-water-carbon dioxide at high pressures shows a two phase immiscible liquids. The molar concentration of ethanol in the water-rich phase is higher than that in the CO_2-rich phase (Defilippi and Moses 1982). Thus water has higher affinity for ethanol than liquid carbon dioxide.

It is hence hypothesized that during the non-equilibrium compression of the ternary system, the most part of ethanol would preferentially get dissolved in the H_2O-rich phase initially but some would slowly diffuse back into the CO_2-rich phase towards attaining equilibrium. Under this non-equilibrium condition, more ethanol could be recovered in the H_2O-rich phase than would be obtained if the system were at equilibrium and hence result in relatively higher H_2O-rich phase ethanol concentration and more efficient removal of ethanol from the CO_2/vapor mixture. When the CO_2-rich phase is throttled back to atmospheric pressure, the Joule-Thompson cooling effect will potentially condense the remaining material in the carbon dioxide gas stream which would increase the overall recovery of ethanol. This non equilibrium method of ethanol recovery could greatly reduce the energy consumption of the *in situ* gas stripping plant. The diffusion of ethanol into the CO_2-rich phase will however be relatively fast because of the excellent diffusion properties of near critical and supercritical carbon dioxide.

CHAPTER THREE

BACKGROUND OF FERMENTATION AND IN SITU GAS STRIPPING

3.1 Introduction

Understanding the possible stimulation or inhibition of carbon dioxide on microbial growth and metabolism is important for the optimal application of the proposed alcohol extraction scheme and hence is discussed in this chapter. This included the effect of elevated carbon dioxide pressures and the dissolved forms of carbon dioxide in fermentation media. The majority of the focus is on *S. cerevisiae* which is the most widely used yeast in ethanol fermentation. Recommendations are made on the best use of elevated carbon dioxide pressures for optimal fermentation and in situ gas stripping. Factors affecting the solubility of carbon dioxide in the fermentation media and methods for predicting the amounts of dissolved carbon dioxide in fermentation media are discussed. The amounts of the dissolved forms of carbon dioxide determine the possible biochemical effects of the gas on fermentation microorganisms. The ternary equilibrium gas compression phenomenon is modeled in this chapter to compare with the non equilibrium experimental results. This included analysis of the composition of the gas from a gas-stripped ethanol fermentor. Compression of the ternary ethanol-water-carbon dioxide mixture is modeled for equilibrium distribution and yield of ethanol in the condensate. Compression energy in gas stripping is discussed. The amount of Joule-Thompson refrigeration that can be harnessed is given. Some conclusions are reached.

3.2 Carbon Dioxide inhibition

Alcoholic product, carbon dioxide and to a lesser extent glucose can have inhibitory effect on yeast physiology and metabolism. Carbon dioxide uptake or evolution is associated with many microorganisms' metabolic pathways. Increasing ethanol productivity is inevitably accompanied by higher carbon dioxide production therefore it is more important to thoroughly understand the effect of higher concentration of carbon dioxide on these microorganisms than it is for ethanol. Except for auto-trophic organisms, carbon dioxide concentration effects on the physiology of microorganisms have not been extensively studied. Carbon dioxide pressures(pCO_2) below 0.15-0.2atm are either neutral or stimulate microbial growth; while higher pressures tend to adversely affect growth and metabolism (Jones and Greenfield 1982). The fact that carbon dioxide has inhibitory effect on many microorganisms has been industrially exploited for food preservation (Dixon and Kell 1989).

The amount of dissolved carbon dioxide that is stimulatory or inhibitory is microbial dependent. Jones and Greenfield (1982) showed that the degree of carbon dioxide inhibition on growth of microorganisms could be different from its effect on metabolism. Carbon dioxide cell inhibition was more pronounced when solutes like glucose, ethanol etc were present in the medium(Gill and Tan 1979; Kunkee and Ouch 1966). At constant pCO_2 , cell growth and metabolic activity inhibition are higher in the presence of these solutes than with carbon dioxide alone in the fermentation broth. The inhibition is a complex interaction between cell environment, especially membrane-affecting species like ethanol, high osmotic pressure, ionic strength and dielectric effect(Jones and Greenfield 1982). This was true because the dissolved solutes themselves did not affect

cell activity. Carbon dioxide inhibition of cells could result from interaction with the plasma-membrane (growth inhibition) or internal metabolic pathways (metabolic inhibition) (Jones and Greenfield 1982). Carbon dioxide interacts with the lipid in the plasma-membrane of the cell thereby affecting its transport mediation properties (permeability) for species in and out of the cell. This phenomenon has been shown to be responsible for inhibition due to elevated pCO_2 (Esplin et al. 1973; Poole-Wilson 1978). The dissolved forms of CO_2 ($CO_{2(aq)}, HCO_{3(aq)}^{-}$) play an important role in cellular metabolism. Jones and Greenfield (1982) showed that the concentrations and ratios of these species in solution could be inhibitory or stimulatory to cellular carboxylation or decarboxylation reactions.

3.2.1 Effect of elevated pressures of carbon dioxide on microorganisms

The rate of fermentation, yeast growth, and the production of fusel oils are reduced by increasing the pressure of carbon dioxide in the fermentation medium (Arcayledezma and Slaughter 1984; Jones and Greenfield 1982; Kunkee and Ouch 1966).

In ethanol fermentation studies conducted by Norton and Krauss (1972) (25 ^{o}C, pH 4.5 , 0% ethanol, 5% glucose) it was observed that the exponential growth rate of *S. cerevisiae* was reduced when $pCO_2 >$ 0.5atm and completely stopped when $pCO_2 \geq$ 2.7atm. Additional evidence showed that although cell division was inhibited, cell metabolism was not affected when $pCO_2 \leq$ 12-13atm since ethanol production rate did not change. Studies conducted on *Streptococcus faecelis* showed that at gas pressures (>41atm) microbial growth was inhibited by all gases (Fenn and Marquisr 1968).

Straskrabova, Paca et al. (1980) observed that excessive removal of carbon dioxide from fermentation media caused abnormal and depressed cell growth as a result of reduced

levels of carbon dioxide within the cells. Scott and Cooke (1995) observed that *S. cerevisiae* cell size (>3um) increased by 14% for carbon dioxide stripped ethanol fermentation after 21 days. After one hour of exposure to high carbon dioxide pressure, the average cell size of *S. cerevisiae* increased while that of *Schizosaccharomyces pombe* decreased (Lumsden et al. 1987). The experiment by Lumsden et al. (1987) and other researchers led to the conclusion made by Dixon and Kell (1989) that high carbon dioxide pressures inhibited the division and production of new bud cells in *S. cerevisiae*; however the metabolic rate of production of carbon dioxide was unaffected. Thibault et al. (1987) showed that when elevated pCO_2 was relieved during *S. cerevisiae* fermentation, the yeast resumed normal rate of ethanol production; showing that pressure effect on yeast was reversible. Ethanol could be optimally produced from yeast by appropriate use of elevated pCO_2 where cell viability and ethanol productivity were kept high while cell mass yield was suppressed(Jones and Greenfield 1982).

3.2.2 Effect of dissolved forms of carbon dioxide on microorganisms

Carbon dioxide in aqueous media can exist as carbonic acid, bicarbonate ions or carbonate ions. This dissociation is represented as (Knoche 1980)

$$CO_{2(aq)} + H_2O \leftrightarrow H_2CO_3 \leftrightarrow HCO_3^- + H^+ \leftrightarrow CO_3^{2-} + 2H^+ \qquad (3.1)$$

The equilibrium constants of these aqueous species depend on the pH and temperature of the solution. At ethanol fermentation conditions (pH 4.0-7.0 and 20-50^oC) carbonate ions are minimal hence the above equation could be written as (Yagi and Yoshida 1977)

$$CO_2 + H_2O \leftrightarrow H_2CO_3 \leftrightarrow HCO_3^- + H^+ \qquad (3.2)$$

The latter aqueous forms of carbon dioxide could be assumed with some accuracy when investigating the effect of aqueous carbon dioxide on the physiology of specific

fermentation microorganisms. Under ethanol fermentation conditions (pH 4.0- 5.5), one part of dissolved $[CO_2]_{aq}$ is in equilibrium with 0.001 parts of $[H_2CO_3]$ and 0.003 – 0.08 parts of $[HCO_3^-]$ (Dean 1979), hence dissolved carbon dioxide in the fermentation medium would exist mainly as $[CO_2]_{aq}$. The concentration of $[HCO_3^-]$ increases with increased pH (4 to 7) of fermentation solution.

Jones and Greenfield (1982) showed that even though elevated $pCO_{2(g)}$ on yeast fermentation was primarily of physico-chemical nature there are possible biochemical effects of the aqueous forms ($CO_{2(aq)}$ and HCO_3^-) at the appropriate concentration and that inhibition was a complex function of the relative concentrations of $CO_{2(aq)}$ and HCO_3^-. Extensive quantitative studies of the effect of these two species have not been done on any single microorganism. Their effect is further complicated by the specific cell membrane make up and diffusivity of these species across the cell plasma membrane.

$CO_{2(aq)}$ is easily transported across cell membrane compared to HCO_3^- (Typical membrane permeability:($D(CO_{2(aq)})$ 0.3-0.6cms^{-1}, $D(HCO_3^-)$ 10^{-8}-10^{-7}cms^{-1}) hence the net carbon dioxide flux across cell membrane is determined by the difference in intracellular and extracellular $CO_{2(aq)}$ (Gutknecht et al. 1977).

The normal intracellular pH of yeasts, most bacteria and nearly all mammalian cells is approximately 7.0 (Ryan and Ryan 1972). For *S. cerevisiae*, in an external medium (pH 4.0-7.0), cell internal condition is buffered (pH 6.0-7.0) (Ryan and Ryan 1972) and $[HCO_3^-]/[CO_{2(aq)}]$ internally is in the range 0.25-2.5 (Jones and Greenfield 1982).

3.2.2.1 Factors affecting carbon dioxide solubility in fermentation media

The solubility of carbon dioxide is affected by temperature, pressure and dissolved solutes. The relationship between concentration and partial pressure of carbon dioxide in aqueous media at constant temperature can be expressed by Henry's law (Butler 1982)

$$[CO_2]_{aq} = K_H \, pCO_2 \qquad (3.3)$$

Where K_H = the Henry's Law constant (mol/l atm) and pCO_2 = the partial pressure of CO_2 (atm).

If fermentation pressures are close to atmospheric pressures, Henry's law could be used to characterize the pressure dependence of carbon dioxide solubility in the medium without introducing appreciable errors (Schumpe et al. 1982). Within the temperature range of microbial fermentation, gas solubility in aqueous media decreases with increase in temperature. When temperature is increased from 25^{o}C to 35^{o}C , Henry's Law constant for carbon dioxide in water decreases from 32.93 to 25.11 mM CO_2/atm (Dean 1979).

Dissolved electrolytes (ionic species) and non-electrolytes (sugars, alcohols etc) in aqueous solution affect the solubility of gases in the media. Salts and non-electrolytes reduce the amount of gas that can dissolve in the aqueous medium.

The Bunsen coefficient (α) is another solubility parameter that is widely used to characterize the solubility of gases. It is defined as the volume of gas reduced to 0^{o}C and 101.3kPa absorbed by a unit volume of solvent at a gas partial pressure of 101.3kPa. In dilute solution of mixed electrolytes and non electrolytes, the solubility of a gas in aqueous medium could be written as (Schumpe et al. 1982)

$$\log(\alpha_o / \alpha) = \sum_i H_i I_i + \sum_j K_j c_j \qquad (3.4)$$

Where α_o is the Bunsen coefficient of the gas in the aqueous medium with no solutes dissolved, α is the Bunsen coefficient of the gas in the aqueous medium with all solutes dissolved, H_i is gas specific empirical constant for salting-out of ion i, I_i is ionic strength of ion i, K_j is gas specific empirical constant for the organic solute j, c_j is the concentration of the organic solute j.

The ionic strength of the ions is defined as

$$I_i = \frac{1}{2} c_i z_i^2 \tag{3.5}$$

Where c_i is the molar concentration of ionic species i, z_i is the ionic charge of ionic species i.

At low solubilities, the Bunsen coefficient, molar concentration and Henry's Constants are related by

$$\log(\alpha_o/\alpha) = \log(c_o/c) = \log(K_{Ho}/K_H) \tag{3.6}$$

The presence of organic liquids in the aqueous medium could be accounted for by the use of the gas solubility in the aqueous organic solution as α_o, c_o or K_{Ho}. This holds for small concentrations of organic solvents as long as the aqueous nature of the medium is not affected (Schumpe and Deckwer 1979). Ion-specific constant for salting-out (H_i) and empirical constants for organic solutes (K_j) for carbon dioxide are given in the work by Schumpe et al. (1982) and are independent of temperature (10-40^{o}C).

Dissolved proteins, anti-foams, oils and microbial cells have the ability to adsorb gases and hence increase the solubility of gases in fermentation media(Baburin et al. 1981). Thus actual solubilities of carbon dioxide could be higher than calculated values attributed to salting out effect of electrolytes and non-electrolytes alone.

Many cellular enzymes involved in carboxylation or decarboxylation are either stimulated or inhibited by $[HCO_3^-]$ in 10-100mM at the anion sensitive sites and the $[HCO_3^-]/[CO_{2(aq)}]$ ratio partly determines the relative rates at which these two classes of enzymes function(Jones and Greenfield 1982). Hence where these classes of enzymes are essential for high product yield, high concentration of the ionic species of carbon dioxide need to be thourougly experimented. The glycolitic production of ethanol by *S. cerevisiae* happens not affected by $pCO_2 \leq 13$atm.

3.3 Estimation of ethanol concentration in stripping gas

The gas from a carbon dioxide stripped ethanol fermentation medium will comprise of carbon dioxide, water, and ethanol in addition to small quantities of impurities like lower and higher alcohols as well as other volatile metabolic by-products. Glycerol, sugars and other yeast nutrients will remain in the broth since they have relatively low volatilities. The major dissolved components of the fermentation broth would be sugars and ethanol. Yeast nutrients are usually in minute quantities. Since fermentable sugars like glucose have high molecular weight and are used in dilute concentrations (<16%wt) in fermentations, the liquid phase molar composition of these species which is the essential parameter for gas phase estimation are low (<2%mol/mol). The volatile components of the fermentation medium can thus be assumed as comprising water and ethanol alone for the purpose of gas phase estimation.

3.3.1 Equilibrium concentration of species

The mole fraction of a volatile species i in a gaseous phase in contact with a liquid phase at equilibrium when the solution behaves ideally or if the mole fraction of the species in the liquid phase approaches unity is related by Raoult's Law given by Equation 3.7

$$y_i = \frac{P_i}{P} = x_i \frac{P_i^{sat}}{P} \tag{3.7}$$

Where y_i is the mole fraction of species i in the vapor phase, x_i is the mole fraction of species i in the liquid phase, P is the total pressure of the systems(mmHg), P_i is the partial pressure of species i in the gas phase(mmHg) and P_i^{sat} is the saturation vapor pressure of species i at the temperature of the system(mmHg). P_i^{sat} for each species can be calculated using the Antoines equation, Table 3.1a (Holland and Liapis 1983).

In real fermentation systems, this is not usually the case since mole fraction of species of interest could be far less than unity. In this case it is important to use the modified Raoult's Law(Gmehling and Onken 1977)

$$y_i = \frac{P_i}{P} = \gamma_i x_i \frac{P_i^{sat}}{P} \tag{3.8}$$

Where γ_i is the activity coefficient of species i in the liquid phase. The law holds well for up to moderate pressures. For non-ideal solution, the activity coefficient (γ_i) can be predicted by the Wilson equation (1964) given by Equation 3.9

$$\ln \gamma_i = -\ln\left(x_i + \Lambda_{ij} x_j\right) + x_j \left(\frac{\Lambda_{ij}}{x_i + \Lambda_{ij} x_j} - \frac{\Lambda_{ji}}{x_j + \Lambda_{ji} x_i} \right) \tag{3.9}$$

$$\Lambda_{ij} = \frac{v_j^L}{v_i^L} \exp\left(-\frac{\lambda_{ij} - \lambda_{ii}}{RT} \right) \tag{3.10}$$

$v_i^L =$ Molar volume of pure liquid component i

$\lambda_{ij} =$ Interaction energy between component i and j, $\lambda_{ij} = \lambda_{ji}$

The molar volume of the water and ethanol can be calculated from Table 3.1b (Holland and Liapis 1983). For ethanol(1) and water(2) mixtures, Gmehling and Onken (1977) gave $\lambda_{12} - \lambda_{11} = 325.0757\, cal/mol$ and $\lambda_{21} - \lambda_{22} = 953.2792\, cal/mol$.

Table 3.1a Parameters for Antoine's equation

$$\log P_i^{sat} = A_i - \left(\frac{B_i}{C_i + t} \right) \quad (P_i \text{ in mmHg, t in } ^\circ c)$$

Component	Ethanol	Water
A	8.04494	7.96681
B	1554.30	1668.21
C	222.65	228.00

Table 3.1b Liquid molar volume constants

$V_i = a_i + b_i T + c_i T^2$ (V_i in cm^3/g.mol, T in ºR)

Component	Ethanol	Water
a	53.70027	22.88676
b	-17.282×10^{-3}	-20.231×10^{-3}
c	49.382×10^{-6}	21.159×10^{-6}

Microorganisms used for ethanol fermentation have low alcohol tolerance. *S. cerevisiae* for example can only tolerate 10-12% v/v (3.3-4.0% mol) ethanol in the fermentation broth. The concentration of ethanol especially in the fermentation of lignocellulosic materials is usually low because of the high amounts of solid contaminants generated from the pretreatment stage which limits the amount of sugars that can be dissolved in the fermentation medium. At such low concentrations of ethanol, the activity coefficient of ethanol is called activity coefficient at infinite dilution ($\gamma_E = \gamma_E^\infty$). When the concentration of a species in the liquid phase of a systems at equilibrium with a gas phase approaches unity ($x_i \to 1$), the systems behave like an ideal solution and $\gamma_i \to 1$ and hence Raoult's law is obeyed. When the species composition in the liquid phase is low, the modified Raoult's Law becomes important because the deviation becomes more pronounced. One of the several estimates of the activity coefficient at infinite dilution for

ethanol(γ_E^{∞}) in ethanol/water mixture was given by Gmehling and Onken (1977) as 6.97. The calculated activity coefficient of ethanol and water using the modified Raoult's Law, Wilson equation and Antoine's correlations at 30°C (ethanol: $x_E = 0.01, \gamma_E = 7.08$; water: $x_W = 0.99$, $\gamma_W = 1.0$) show good agreement with the experimental data.

3.3.2 Experimental species partition coefficient

In real gas stripping situations, the systems are far from equilibrium for the species that are present in small amounts before the gas exits the system, hence an empirical relation of the form below is used to replace the modified Raoults law (Duboc and von Stockar 1998)

$$y_E = K_{E,\exp} x_E \qquad (3.11)$$

Where y_E is the mole fraction of ethanol in the gas phase, x_E is the mole fraction of ethanol in the liquid phase and $K_{E,\exp}$ is the partition coefficient of ethanol that is experimentally determined, which is strongly dependent on temperature and contact times between the liquid and the gas phases.

Because the average time of contact is short, equilibrium is not attained. Surfactants such as antifoam can slow down the rate at which equilibrium is achieved in the system due to the creation of an extra interface through which species have to diffuse from the liquid into the vapor phase. The dynamic approach of equilibrium for ethanol at 30°C was investigated by Duboc and von Stockar (1998); by passing air through ethanol solution with or without fermentation medium antifoam and measuring the gas ethanol content directly with an infrared analyzer. The researchers found that the ethanol concentration in the exit gas stream stabilized after 15-20 seconds.

The researchers did not observe any clear influence of typical fermentation media components (such as 0.1mL/L antifoam, 2g/L KH_2PO_4, 4g/L $(NH_4)_2SO_4$, 10g/L glucose and cells) on the partition of ethanol. The partition coefficient was hence considered constant at a constant temperature and stirring rate in their experiment.

Duboc and von Stockar (1998) gave the following correlation for ethanol/water mixture in a fermentor at 30°C from experimental results.

$$y_E = 0.532 x_E \qquad (3.12a)$$

The partition coefficient of ethanol was not affected by the aeration rate used in their experiment (0.63-1.3vvm). A similar experiment conducted to determine the partition coefficient for water at 30°C showed that the thermodynamic concentration of water vapor was the same as the partition concentration; hence thermodynamic equilibrium of water was achieved fast. Loser et al. (2005) reported a lower value for $K_{E,\exp}$ but in their experimental ethanol partition was determined indirectly by fitting various models and following the ethanol loss from the fermentor which was susceptible to systematic error and hence less reliable.

If dilute ethanol solution is stripped with carbon dioxide for a short time, the total amount of material in the fermentor would remain approximately constant (N_o) but the ratio of the final to initial mole fraction of ethanol $\left(\frac{x_{e(f)}}{x_{e(i)}}\right)$ would be significantly different from unity. If the CO_2 is not recycled and since the composition of water in the exiting CO_2/vapor phase will be approximately constant (equilibrium composition), ethanol carried away in the gas stream for a differential time can be related by

$$-N_o \Delta x_e = k x_e \frac{Q_{CO_2}}{1 - y_w - k x_e} \Delta t \qquad (3.12b)$$

Where

Q_{CO_2} is flow of carbon dioxide (mole/min)

k is the partition coefficient of ethanol

N_o is total amount of material (water and ethanol) initially in fermentor (mole)

Δt is the stripping time (min)

Δx_e is the change in liquid phase ethanol mole fraction

y_w is vapor phase water mole fraction(constant equilibrium composition)

Equation 3.12b can be re arranged as

$$-\left(\frac{1 - y_w - k x_e}{k x_e}\right) dx_e = \frac{Q_{CO_2}}{N_o} dt \qquad (3.12c)$$

Integrating from initial to final ethanol fraction (x_e) and initial to final time (t)

$$-\int_{x_{e(o)}}^{x_e} \left(\frac{1 - y_w - k x_e}{k x_e}\right) dx_e = \int_0^t \frac{Q_{CO_2}}{N_o} dt \qquad (3.12d)$$

$$-\left[\frac{(1 - y_w)}{k} \ln x_e - x_e\right]_{x_{e(o)}}^{x_e} = \frac{Q_{CO_2}}{N_o} t \qquad (3.12e)$$

Rearranging gives

$$k = \frac{(1 - y_w) N_o}{Q_{CO_2} t + N_o (x_{e(o)} - x)} \ln\left(\frac{x_{e(o)}}{x}\right) \qquad (3.12f)$$

The partition coefficient can thus be determined from batch experiment data using equation 3.12f. The need to use experimentally determined partition coefficient for the estimation of the gas phase ethanol composition appears to be more important at

relatively lower concentration of ethanol in the liquid phase since the deviation of the ethanol partition concentration (Equation 3.12a) from the equilibrium value is larger (Table 3.2). Even though the partition concentration of ethanol is attained rapidly, equilibrium is reached extremely slowly.

Table 3.2 Calculated composition of the gas phase in contact with ethanol in water solution at 1atm and 30°C

EtOH Solution		Gas Phase composition %(y_i)			Deviation of EtOH Non-equilibrium from Equilibrium (%)
%(v/v)	%(x_i)	Equilibrium Water	Equilibrium EtOH	Non-equilibrium EtOH	
1.9	0.59	4.15	0.45	0.31	31.1
2.0	0.62	4.14	0.47	0.33	29.8
10.0	3.28	4.05	1.97	1.74	11.7
12.0	3.99	4.03	2.23	2.13	4.5

3.4 Compression of ternary mixture of water-ethanol-carbon dioxide system

When the mole fractions of volatile impurities in the stripped gas phase are low which is usually the case in alcohol fermentation, the CO_2 extraction and compression of ethanol from the fermentation broth can be modeled as a ternary system (carbon dioxide, ethanol and water). After compression, the vapor will be in contact with a condensate as shown in Figure 3.1. The H_2O-rich phase would be the bottom layer and the CO_2-rich phase would be the top layer since gas or liquid carbon dioxide is relatively less dense than water (Table 3.3). The feed is the gas stripped from the fermentation. The composition of the vapor and liquid in contact with each other at equilibrium depends on the pressure and temperature of the flash drum. Equilibrium phase diagrams are usually used to represent the compositions of the vapor and liquid phases in contact with each other.

Table 3.3 Saturated carbon dioxide density

t (^oC)	p(bar)	Density (kg/m^3) Liquid	Gas
-3.15	32.03	947.0	88.5
6.85	41.6	885.0	122.0
16.85	53.15	805.8	172.4
26.85	67.1	680.3	270.3

(Abstracted from Table 2-241, Perry, Green et al (1997))

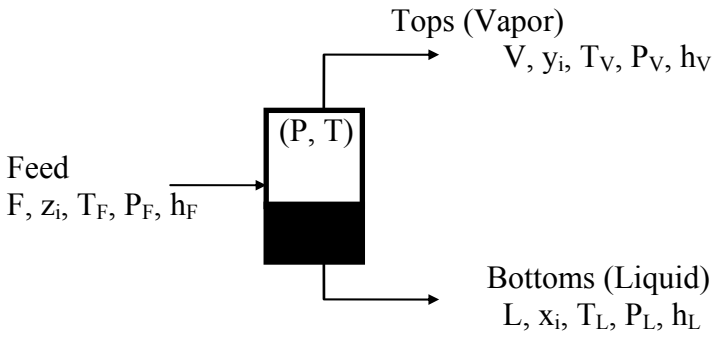

Figure 3.1 Schematic diagram of isothermal flash drum

Where F, L and V are the molar flow rates of the feed, liquid and vapor streams respectively. z_i, x_i and y_i are the respective fractional mole composition of species i, in the feed, liquid and vapor streams. T is temperature of the system and P is the total drum pressure.

If we assume thermal and mechanical equilibrium in the tank, then

$T_V = T_L$ and $P_V = P_L$

For a total material balance on the systems:

$$F = V + L \tag{3.13}$$

And for component balance:

$$Fz_i = Vy_i + Lx_i \tag{3.14}$$

Summation of mole fractions of all phases (feed, vapor and liquid)

$$\sum_i x_i = 1 \text{ (Liquid)} \qquad \sum_i y_i = 1 \text{ (Vapor)} \qquad \sum_i z_i = 1 \text{ (Feed)}$$

The ratio of the mole fraction of a species i in the vapor phase to its mole fraction in the liquid phase is its K-value defined as:

$$K_i = \frac{y_i}{x_i} \tag{3.15}$$

Defining vapor fraction as

$$\psi = \frac{V}{F} \tag{3.16}$$

Substituting Equation 3.16 in Equations 3.13 and 3.14 yield

$$L = F - \psi F \tag{3.17}$$

and

$$z_i = \frac{V}{F} y_i + \frac{F - \psi F}{F} x_i = \psi y_i + x_i - \psi x_i \tag{3.18}$$

Substituting Equation 3.15 in Equation 3.18 gives

$$z_i = \psi y_i + x_i - \psi x_i = \psi K_i x_i + x_i - \psi x_i = (\psi K_i + 1 - \psi) x_i$$

$$x_i = \frac{z_i}{(\psi K_i + 1 - \psi)} \tag{3.19}$$

Substituting for liquid mole fraction (Equation 3.19) in K-value (Equation 3.15) gives

$$y_i = \frac{K_i z_i}{(\psi K_i + 1 - \psi)} \tag{3.20}$$

Difference in mole fraction summation

$\sum_i y_i = 1$ And $\sum_i x_i = 1$ gives

$$\sum_i (y_i - x_i) = 0 \tag{3.21}$$

Substituting Equation 3.19 through Equation 3.20 in Equation 3.21 yields Rachford Rice equation (Rachford and Rice 1952)

$$\sum_i (y_i - x_i) = \sum_i \frac{K_i z_i}{(\psi K_i + 1 - \psi)} - \sum_i \frac{z_i}{(\psi K_i + 1 - \psi)} = \sum_i \frac{K_i (z_i - 1)}{(\psi K_i + 1 - \psi)} = \sum_i \frac{K_i (z_i - 1)}{\psi (K_i + 1) + 1} = 0$$

$$f(\psi) = \sum_i \frac{K_i (Z_i - 1)}{\psi (K_i - 1) + 1} = 0 \tag{3.22}$$

The solution to this equation can be obtained using the Newton-Raphsons iteration (Equation.3.23).

$$\psi_{i+1} = \psi_i - \frac{f(\psi_i)}{f^1(\psi_i)} \tag{3.23}$$

3.5 Energy of compression

3.5.1 Polytropic Compression

In actual compression processes the situation is neither isothermal or adiabatic hence a polytropic compression is usually used to characterize the systems. Polytropic specific work of compression is given by Equation 3.24 (Perry, Green et al. (1997) Ch. 10)

$$\hat{W}_p = \frac{zRT_1}{(n-1)} \left[\left(\frac{p_2}{p_1} \right)^{\frac{n-1}{n}} - 1 \right] \qquad \frac{J}{mol} \tag{3.24}$$

Where z is compressibility factor, R the gas constant (J/K.mol), p_1 the initial pressure (Pa), p_2 the final pressure (Pa), T_1 the initial temperature of the gas (K) and n the

polytropic index. The polytropic index *n* depends on the nature of the gas and details of the compression process and is given by Equation 3.25.

$$\frac{n}{n-1} = \frac{\gamma}{\gamma-1}\eta_p \tag{3.25}$$

Where $\gamma = \frac{C_p}{C_v}$, η_p is the polytropic efficiency (this is the one usually stated by compressors manufacturer), C_p is the specific heat at constant pressure(J/mol) and C_v is the specific heat at constant volume(J/mol). Equation 3.25 can be transformed into Equation 3.26.

$$n = \frac{\eta_p \cdot \gamma}{1 + \eta_p \cdot \gamma + \gamma} \tag{3.26}$$

3.5.1.1 Multistage Polytropic Compression

The Compressors that attain higher compression ratio are usually multi-staged to enable some intercooling between stages to minimize the work of compression. Consider a two stage compression process ($p_1 \rightarrow p_2 \rightarrow p_3$) with complete inter-stage cooling so that the temperature of the gas exiting the first stage is cooled back to that of the initial before entering the second stage. The polytropic work will be given by Equation 3.27.

$$\hat{W}_p = \frac{zRT_1}{(n-1)}\left(\left[\left(\frac{p_2}{p_1}\right)^{\frac{n-1}{n}} - 1\right] + \left[\left(\frac{p_3}{p_2}\right)^{\frac{n-1}{n}} - 1\right]\right) \qquad \frac{J}{mol} \tag{3.27}$$

The intermediate pressure P_2 that minimizes work is such that $p_2^{opt} = \sqrt{p_1 p_3}$ (by differentiation)

$$\frac{p_2}{p_1} = \frac{p_3}{p_2} = \left(\frac{p_3}{p_1}\right)^{1/2} \tag{3.28}$$

To minimize work, compression ratios have to be identical. This can be extended for n stages as:

$$\frac{p_2}{p_1} = \frac{p_3}{p_2} = \cdots = \frac{p_{n+1}}{p_n} = \left(\frac{p_{n+1}}{p_n} \right)^{1/n} \tag{3.29}$$

The actual work of compression is

$$\hat{W}_c = \frac{\hat{W}_p}{\eta_p} \qquad \frac{J}{mol} \tag{3.30}$$

Where $\hat{W}_c$ is actual work done, (J/mol); $\hat{W}_p$ is polytropic work, (J/mol); and η_p is the polytropic efficiency.

Since the stripped gas phase of the scenarios studied comprised mostly carbon dioxide (>90% mol), compression simulation with the assumption that the CO_2/vapor mixture behaved as CO_2 alone would not introduce appreciable errors. Data on carbon dioxide was extracted from other sources for the simulation of the compression of the stripped gas (see Table 3.4). The average compressibility factor (0.78) was used in energy calculation where the pressure was 40 to 60bar. Where pressure was lower than 40bar compressibility factor ranging in 1.0 – 0.83 by interpolation was used.

Typical Polyprotic efficiency of carbon dioxide compressor $\eta_p = 0.9$ was assumed.

Table 3.4 Thermo physical properties of carbon dioxide

Parameter	Value	Reference
Compressibility(z)	0.83-0.73	At 50 ^oC and 40 to 60bar (Table 2-167 of Perry, Green et al (1997)
Specific volume(v)	0.5650m^3kg^{-1}	At 300K (Table 2-242 of Perry, Green et al (1997)
Specific heat(Cp)	37.11 $Jmol^{-1}K^{-1}$	At 25^oC (Table 2.1 of P.W (1986)
Specific heat(Cv)	28.46 $Jmol^{-1}K^{-1}$	At 25^oC (Table 2.1 of P.W (1986)
Gas Constant(R)	8.314 J $K^{-1}mol^{-1}$	

If the running time for the compressor is known then the total work of compression of the CO_2/Vapor mixture is give by Equation 3.31

$$Work(J) = \frac{Flw_{CO_2}}{y_{CO_2} \times M_{CO_2} \times v} \times \hat{W}_c \times t \qquad (3.31)$$

Where

$\hat{W}_c$ is actual work of compression of CO_2 (J mol^{-1})

v is the specific volume of CO_2 (L g^{-1})

Flw_{CO_2} is the flow rate of CO_2 (L min^{-1})

y_{CO_2} is the mole fraction of CO_2 in the CO_2/Vapor mixture leaving the fermentor

M_{CO_2} is the molar mass of carbon dioxide(g mol^{-1})

t is time of run (min)

Compression energy is defined as the total work (kJ) of gas compression per unit mass of total pure ethanol collected in condensates (Tops and Bottoms) from the flash tank and is given by Equation 3.32a

$$Compres.\ Energy(J/g) = \frac{Work}{M_{EtOH} \times L \times x_{EtOH}} \qquad (3.32a)$$

Where

$Work$ is total work of compression of the CO_2/Vapor mixture (J)

L is the molar amount of the Bottoms condensate (mol)

x_{EtOH} is the mole fraction of ethanol of the Bottoms condensate

M_{EtOH} is the molar mass of ethanol(g mol^{-1})

If the feed molar amount is known the compression energy could be written as Equation 3.32b

$$Compres.\ Energy(J/g) = \frac{\hat{W}_c}{M_{EtOH} \times \left(L/F\right) \times x_{EtOH}} \qquad (3.32b)$$

Where F is the molar amount of the CO_2/Vapor Feed mixture (mol)

$\hat{W}_c$ is actual work of compression of CO_2 (J mol^{-1})

Only the liquid condensate of the Bottoms is considered in compression energy equation since the Tops is assumed flashed off. However more liquid could possibly be obtained by the Joule-Thompson cooling if the Tops were throttled. Bottoms ethanol yield (%) is defined as percentage of ethanol stripped by carbon dioxide (in the CO_2/vapor Feed stream) that was recovered in the liquid condensate (Bottoms) from the flash tank (Equation 3.33).

$$Yield(\%) = \frac{L \times x_{EtOH}}{F \times z_{EtOH}} \times 100\% \tag{3.33}$$

x_{EtOH} is the mole fraction of ethanol of the Bottoms condensate

L is the molar amount of the Bottoms condensate (mol)

z_{EtOH} is the mole fraction of ethanol of the CO_2/vapor Feed stream

F is the molar amount of the CO_2/vapor Feed stream (mol)

3.6 Joule-Thomson cooling

Joule-Thomson cooling is the adiabatic cooling or heating that accompanies the expansion of a real gas. The process through the throttling valve is an isenthalpic process if it is well insulated. The Joule-Thomson coefficient is given by

$$\frac{\Delta T}{\Delta P} \approx \left(\frac{\delta T}{\delta P} \right) = \mu_{JT} \tag{3.34}$$

The saturation point of a fluid is the set of temperature and pressure at which the fluid would be in both liquid and gaseous forms coexisting. When a fluid is saturated, a slight increase in the pressure or decrease in the temperature of the system would change the fluid into the liquid phase. On the other hand a slight increase in the temperature or

decrease in the pressure of the system will change the fluid into the gaseous phase. Some physical properties like the density and the diffusivity of the fluid change dramatically when the fluid changes phase from the liquid to the gaseous phase and vice versa. Tables 3.5 and 3.6 were produced with the online public tool by Lemmon et al. (2005). Table 3.5 shows the conditions at which carbon dioxide would exit as a two phase mixture (liquid and gas). This was used to approximate the state of the Tops in the flash tank containing the compressed CO_2/vapor mixture. Pure carbon dioxide Joule-Thompson coefficients (Table 3.6) were used to estimate the refrigeration that can be attained by flashing the Tops from the flash tank from the proposed scheme.

Table 3.5 Saturation temperature and pressure for carbon dioxide

t (^oC)	5.0	5.3	10.0	14.3	15.0	18.3	20.0	22.0	25.0	28.7	30.0	31.0
p (bar)	39.7	40.0	45.0	50.0	50.9	55.0	57.3	60.0	64.3	70.0	72.1	73.8

Table 3.6 Joule-Thomson coefficient (^oC/bar) of gas carbon dioxide

	P(bar)					
t (^oC)	1	20	40	55	60	70
10	1.2488	1.2656	1.2774	0.0660*	0.0611*	0.0529*
20	1.1417	1.1526	1.1557	1.1130	0.1372*	0.1069*
25	1.0932	1.1019	1.1021	1.0717	1.0384	0.1714*
30	1.0479	1.0546	1.0524	1.0276	1.0065	0.8814
40	0.9653	0.9689	0.9635	0.9437	0.9309	0.8865
50	0.8923	0.8935	0.8862	0.8688	0.8592	0.8306
60	0.8273	0.8266	0.8180	0.8024	0.7945	0.7729

(*Liquid state values)

Cooling effect is defined as the heat change that accompanies throttling of a gas. When the throttled gas is pure CO_2 cooling effect is given by Equation 3.35.

$$Cool_{Effect}(J) = \frac{Flw_{CO_2}}{M_{CO_2} \times v} \times C_p \times \Delta T_p \times t \tag{3.35}$$

Where

Flw_{CO_2} is the flow rate of CO_2 (L min^{-1})

v is the specific volume of CO_2 (L g^{-1})

C_p is the specific heat capacity of CO_2 (J mol^{-1} K^{-1})

ΔT is the predicted Joule-Thomson cooling with respect to CO_2 (K).

t is the time span of throttling (min)

The Joule Thomson-cooling temperature change can be evaluated from Equation 3.36a.

$$\Delta T_p = \mu_{JT} \Delta P \qquad (3.36a)$$

The final and initial temperatures of the fluid undergoing throttling define as T_f and T_i respectively are related by 3.36b

$$T_f = T_i - \Delta T \qquad (3.36b)$$

CO_2 constitutes (>98%) of CO_2/vapor mixture that leaves the flash tank as Tops. In this situation Equation 3.35 could be used without introducing large margin of error.

Refrigeration energy is defined as the heat effect (J) of gas throttling per unit mass of total pure ethanol collected in condensates (Tops and Bottoms) from the flash tank.

$$Refrig.\,Energy(J/g) = \frac{Cool_{Effect}}{M_{EtOH} \times L \times x_{EtOH}} \qquad (3.37)$$

Where

$Cool_{Effect}$ is cooling effect as defined in Equation 3.35 (J)

L is the molar amount of the Bottoms condensate (mol)

x_{EtOH} is the mole fraction of ethanol of the Bottoms condensate

M_{EtOH} is the molar mass of ethanol(g mol^{-1})

3.7 Concluding remarks

Considering the discussion of the effect of carbon dioxide on yeast, it is essential that the proposed method of in situ gas stripping coupled with fermentation should not be done at pressures greater than normal atmospheric pressures during the initial stages of fermentation when cell mass accumulation is important. Slightly pressurized carbon dioxide could be used to stop yeast division without affecting ethanol fermentation during gas stripping. When cell mass concentration is high and the rate of fermentation is high then pCO_2 can be slightly increased above atmospheric pressures to take advantage of its higher extractive power. There is an added advantage of slightly higher pCO_2 on the fermentation at later times since it serves to indirectly stop further cell division so that more sugars can be converted into alcohols instead of cell mass. In this way ethanol production from biomass using yeast could be maximized. Since cell exponentially division diminished between 0.5 and 2.7atm this scheme can be implemented without the need for ultra high pressure equipment.

CHAPTER FOUR

IN SITU RECOVERY OF ETHANOL FROM ETHANOL/WATER MIXTURE

4.1 Introduction

This chapter presents the materials, method and experimental design for the fermentation and in situ carbon dioxide stripping. The flow sheet of the experiment is shown along with details of equipment and materials used. Equilibrium simulation of ethanol recovery by compression and flashing of the stripped CO_2/vapor mixture and the compression energy is presented. Raw data generated from the experimental runs are shown. Processed results from the experiments are compared with those simulated to verify the hypothesis. The influence of the most significant factors (Temperature, Pressure and Flow rate) affecting the recovery of ethanol in the condensate were studied. Influence of different saturation states of carbon dioxide on the recovery of ethanol and optimization of the variables of interest was done using response surface methodology.

4.2 Experimental Methods

4.2.1 Materials and Apparatus

- A 4L glass cylinder (13.78cm diam. x 30cm high) with dome flanged top and gum gasket seal was used as the simulated fermentor. The top had an embedded porous material (polyurethane foam) to prevent entrainment of fermentor liquid content. It was fabricated by a glass blower in the Chemistry Department of Virginia Polytechnic and State University. It had a magnetic stirrer and a temperature control device (Temp Controllr Auto 2-Aaa Btry, Fisher Scientific, Suwanee, GA, USA). Gas was introduced at the bottom through a sparger with 1mm holes.

Pressure in the fermentor was maintained at atmospheric by tuning the exit gas valve.

- A 500ml aluminum pressure tank (DOT-E7737-1800, Catalina Cylinders Hampton, VA, USA) with a dial temperature gauge (Thrm Bi 2"/12", Fisher Scientific, Suwanee, GA, USA) and a dial pressure gauge (0-2000psi, McMaster-Carr, Atlanta, GA, USA) was used as the flash tank. The tank was immersed in a water bath that was maintained at a constant temperature with a Fisher Scientific temperature controller (Temp. Controll Auto 2-Aaa Btry, Fisher Scientific, Suwanee, GA, USA). The bath was either heated with an incorporated immersion heater when needed to be kept above ambient temperatures or cooled by circulating the water over ice. The Throttling valve attached to the flash tank was stainless steel.
- The separator was a glass cylinder (5cm diam x 20cm high) with a porous plug at the top to prevent entrainment. It was fabricated by a glass blower in the Chemistry department of Virginia Polytechnic and State University.
- A Bauer air compressor (Model JRII/2HP/20Amp, Bauer compressor, Norfolk, VA, USA) was slightly modified to fit experimental needs. Fluid was allowed to go through only the first and second compression chambers and then out of the compressor. High pressure tubings (stainless steel braided FEP 3000psi, Cole-Parmer, Vernon Hills, IL, USA) were used to connect the gas from the compressor to the flash tank.
- Commercial 99.9% purity compressed carbon dioxide cylinder (CD AN200, Airgas, Radford, VA, USA) equipped with a flow meter (Manostat 36-547-305

Bel-Art Products, Pequannock, NJ, USA) was used as the gas supply. Coalescing filter (Norgren (R) Filter, Sigma-Aldrich Inc., Saint Louis, MO, USA) was used on the carbon dioxide recycle line whenever applicable.

- A NI data acquisition Instrument (NI USB-6008, National Instruments Austin, TX, USA) equipped with miniature bead thermistors (AVX NI24, AVX Corporation, Myrtle Beach, SC, USA) was used for temperature data acquisition.

4.2.2 Methods

4.2.2.1 Effect of temperature, pressure and saturation state of carbon dioxide on ethanol recovery

The experimental setups are schematically shown in Figure 4.1a and 4.1b. Photos of the apparatus are shown in Figures 4.2a, 4.2b and 4.2c. The fermentor was filled with 4L of 12% (v/v) ethanol/water mixture and maintained at 30^{o}C and atmospheric pressure. Carbon dioxide from the supply cylinder mixed with recycled gas was passed through a coiled-tube immersed in water at 25^{o}C before introduction into the fermentor through a ring-type sparger. The flow rate of fresh and recycled carbon dioxide into the fermentor was maintained at 8.4 L/min. The carbon dioxide supply cylinder was kept open throughout each experiment to serve as flow buffer to prevent pressure fluctuations in the recycle line. The CO_2/vapor mixture that left the fermentor was at 30^{o}C. The extraction with carbon dioxide was carried out for one hour for each experiment. The exit gas from the fermentor was compressed to a set pressure ranging from 5-60bar and flashed into the flash tank which was maintained at a set temperature that ranged from 6-55 (±1 ^{o}C). The pressure in the flash tank was maintained by fine tuning the throttling valve.

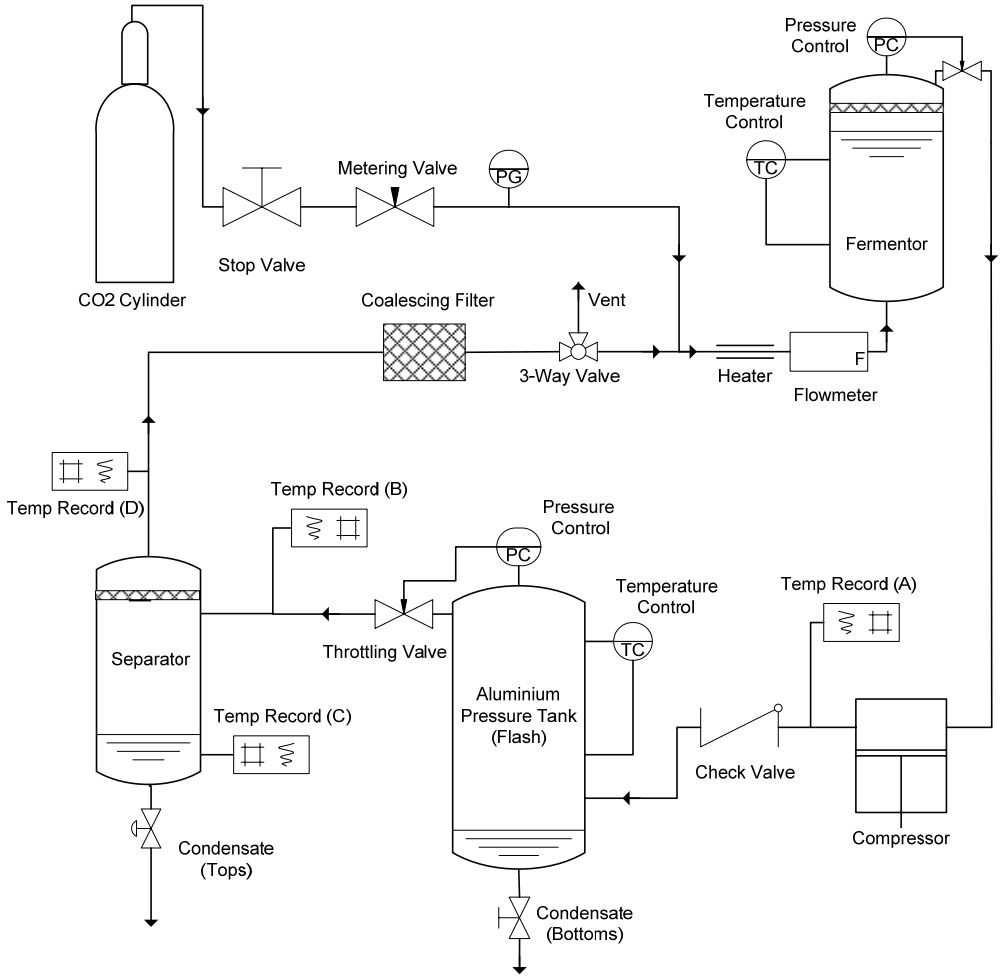

Figure 4.1a Schematic diagram of continuous flash extraction of ethanol from fermentation broth (Isothermal flash tank layout)

In the case of the isothermal flash tank layout (IFTL) as shown in Figure 4.1a the liquid (condensate) from the bottom of the flash tank was collected as the Bottoms fractions at the end of the experiment. The CO_2/vapor mixture from the flash tank was continuously throttled through a stainless steel valve which caused cooling and condensation because of the Joule-Thompson effect. The cooled mixture was introduced into the separator where the condensate (Tops) was deposited and the CO_2 was passed through a porous

material to remove any entrained liquid. The CO_2 was then passed through a coalescing filter before recycling. Each experiment was run three times.

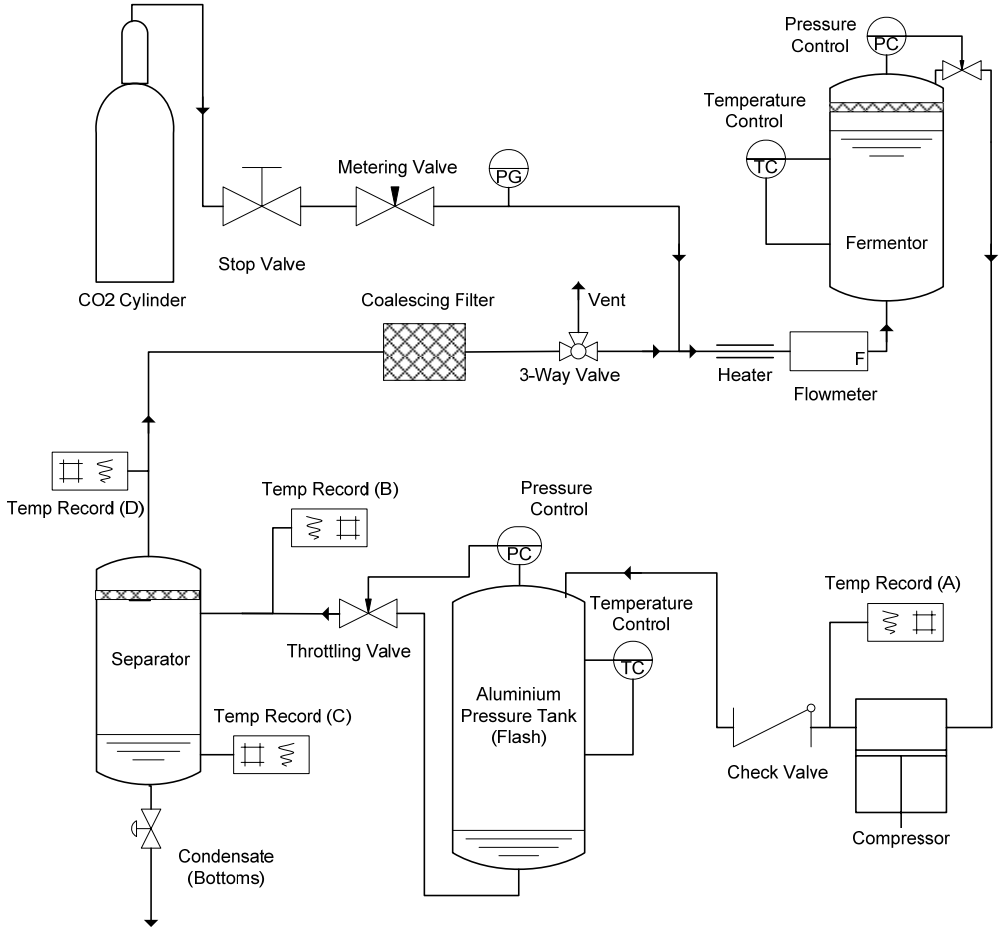

Figure 4.1b Schematic diagram of continuous flash extraction of ethanol from fermentation broth (Reversed layout)

Most of the experiments were run with the IFTL (Figure 4.1a) as described above where the compressed gas from the compressor entered the flash tank from the bottom and exited from the top. Some experiments were done with the reversed layout (RL) (Figure 4.1b) where the compressed gas from compressor entered flash tank from top and exited from the bottom.

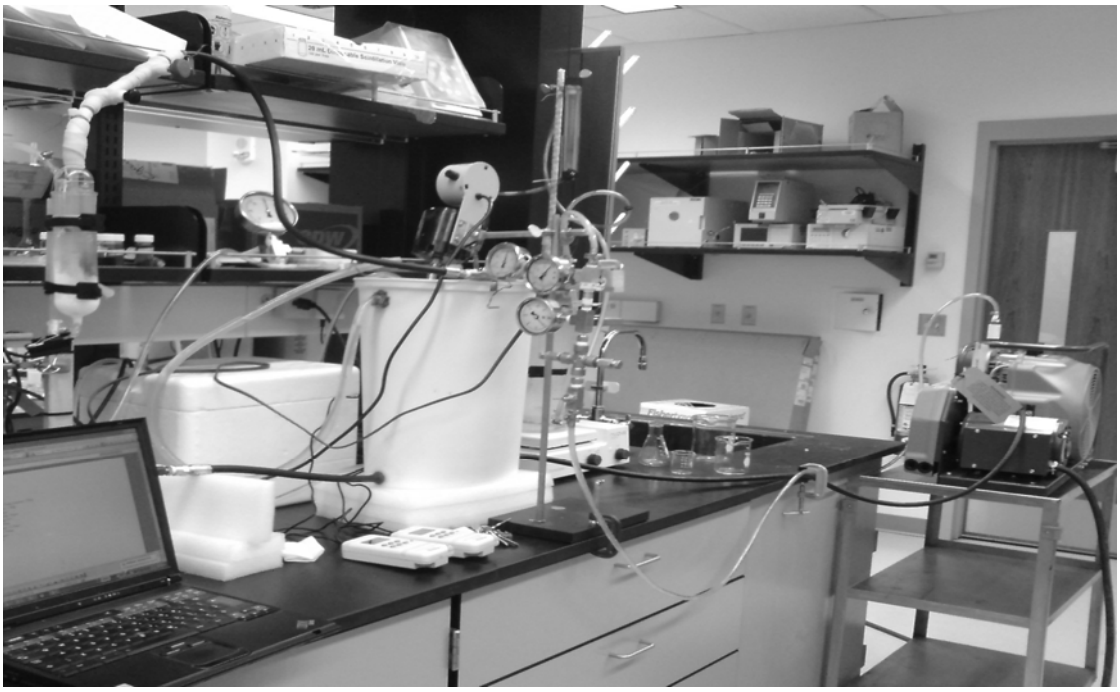

Figure 4.2a System showing Compressor, Pressure Tank bath and Separator

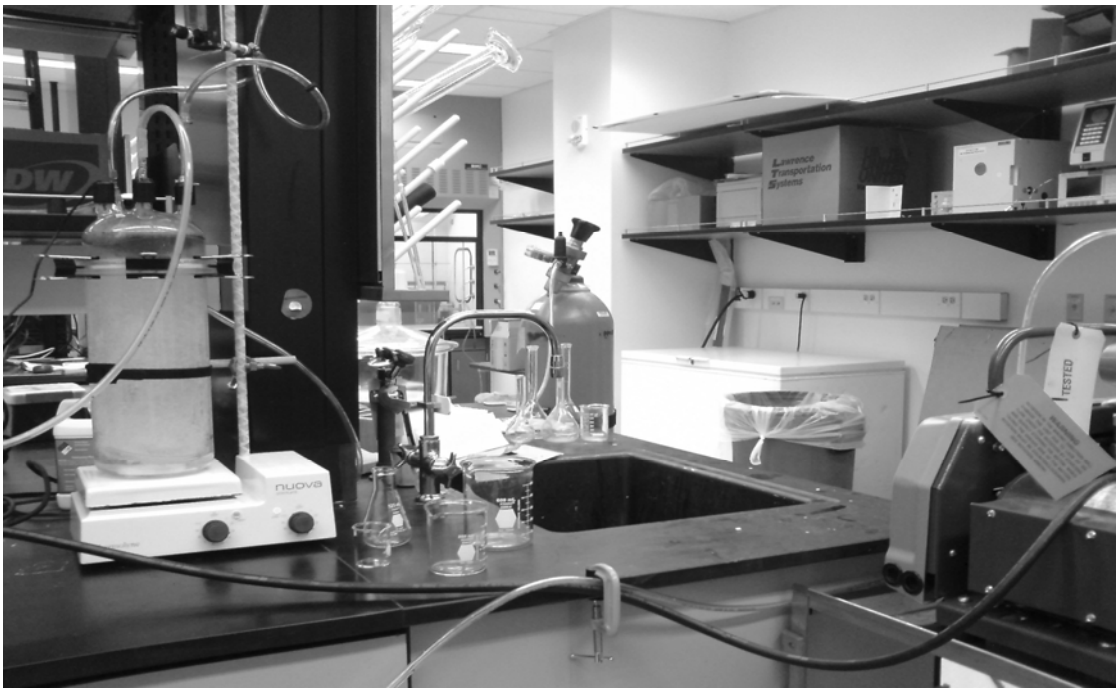

Figure 4.2b Fermentor and Carbon dioxide cylinder

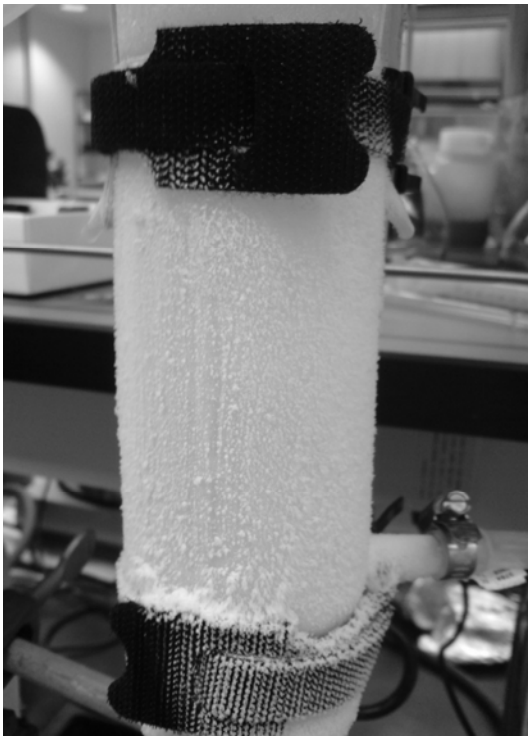

Figure 4.2c Frozen Separator

The goal of this arrangement (RL) was to investigate the situation where all material in the flash tank (liquid and gas) was mixed before throttling to prevent formation of separate liquid and gas phases. A single product stream was hence continuously collected (Bottoms) unlike the two streams (Tops and Bottoms) for the IFTL. The particular configuration used is stated in the run results as Isothermal flash tank layout (IFTL) or reversed layout (RL).

4.2.2.2 Optimization of temperature, pressure and flow rate on ethanol recovery

The physical state of carbon dioxide in the flash tank significantly affected the recovery phenomenon. The pressure which determined the degree of cooling attained from the Joule-Thompson effect in turn determined the amount of remnant material in the throttled gas phase that could be condensed. The extent of interaction of liquid and vapor phases in

the flash tank and the approach of the interaction to equilibrium depend on the flow rate of carbon dioxide.

The experimental procedure for the optimization runs was similar to the single effect runs using the isothermal flash tank configuration (Fig. 4.1a). But in this case the fermentor was filled with 2% (v/v) ethanol solution. Experiments were run for an hour each. Carbon dioxide flow rate to the fermentor ranged from 4.2-12.6 L/min at atmospheric pressure for the optimization process. The flow rate ensured at least 15secs residence time in the fermentor so that the stable partition vapor phase composition of ethanol was attained.

The flash tank pressure and temperature ranged from 40-70bar and 10-40^{o}C respectively. The pressure and temperature ranges included conditions where carbon dioxide could exist as gas, liquid or near critical liquid (slightly below the critical point). Carbon dioxide at supercritical conditions was not chosen because the Joule-Thompson coefficient drops rapidly (Lemmon et al. 2005) and density rises dramatically like in the case of liquid carbon dioxide and hence lower cooling effect and high product entrainment. Supercritical carbon dioxide also has high solubility for solutes compared to the gas so would increase entrainment of ethanol from flash tank. Near critical liquid carbon dioxide conditions however was included since it has properties not as extreme as supercritical carbon dioxide and also favorable Joule-Thompson coefficient.

The Box-Behnken response surface methodology for three factors was used for the optimization of the three input parameters. Other popularly used designs in this category include the central composite and other modified forms of the central composite designs. These design methods have the ability to find optimal minima and maxima response

points for a given range of input factors if they exist by rigorously modeling for second order terms which explains the curvature in the response fitting.

One important difference between the central composite design and the Box-Behnken design for three factors is that the central composite has input factor points at the vertices of the design cube while the Box-Behnken design avoids the vertices (Figure 4.2d). The Box-Behnken design rather has design points midway on the sides of all edges of the design cube. This was the reason for choosing the Box-Behnken design for the study. Vertex points like the extreme gas flow rate and high pressures were avoided due to the possibility of instability of the experimental system. Liquid or near critical carbon dioxide flowing at high rates were difficult to control through the stainless steel throttling valve on the experiment.

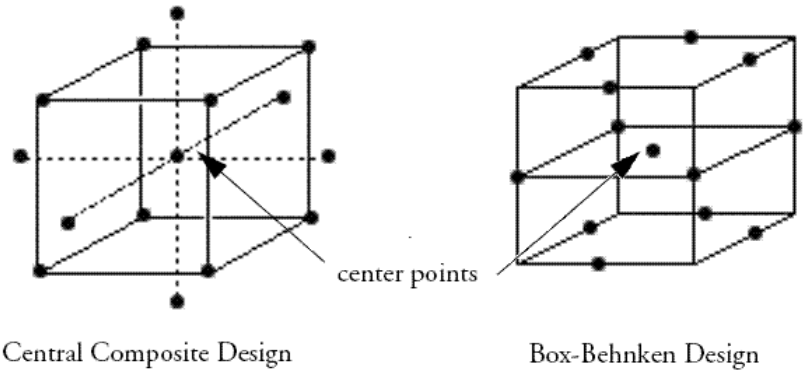

Figure 4.2d Three-parameter surface response design of experiment

The nominal parameters for the Box-Behnken design for the optimization scheme is shown in Table 4.1a. These intervals encompassed saturation conditions for carbon dioxide knowing that the best conditions for ethanol recovery were those near the saturation pressures and temperatures of carbon dioxide.

Table 4.1a Box-Behnken three parameter design

Design Code	Temperature (^oC)	Pressure (bar)	Flow rate (ml/min)
-1	10	40	4200
0	25	55	8400
1	40	70	12600

4.2.2.3 Analytical method

Tops and Bottoms condensates collected were weighed at the end of each run. Aliquots were analyzed using a Shimadzu 10Avp high performance liquid chromatography (HPLC) unit with UV-detector (Shimadzu Scientific, Columbia, MD, USA) set to wavelength of 190nm. Samples were analyzed on a Benson Polymeric BP-100 H+ Carbohydrate column (300 mm x 7.8 mm, Benson Polymeric, Reno, NV, USA). Eluent was 2.5mM H_2SO_4 at a flow rate of 0.6ml/min. Samples were prepared by filtering through a 0.25µm PTFE syringe filter and 20µL samples were injected onto the column at 25^oC. The analysis time was 30min. Ethanol was identified by comparing sample peaks with standard ethanol standard. Three ethanol calibration curves were prepared spanning 2-12 %(v/v), 12-60 %(v/v) and 60-95 %(v/v) (Figures 4.3 through 4.5). The concentration of ethanol (%v/v) used for the calibration was the percentage of the volume of pure ethanol dissolved in a unit volume of solution (ethanol + water) at 25^oC. Percentage ethanol concentration of Tops and Bottoms condensates where not stated explicitly in all the results was less than unity (% (v/v) ± 1). Ethanol concentration was converted from (%(v/v)) to (%(w/w)) at 25^oC using the correlation shown in Figure 4.6a

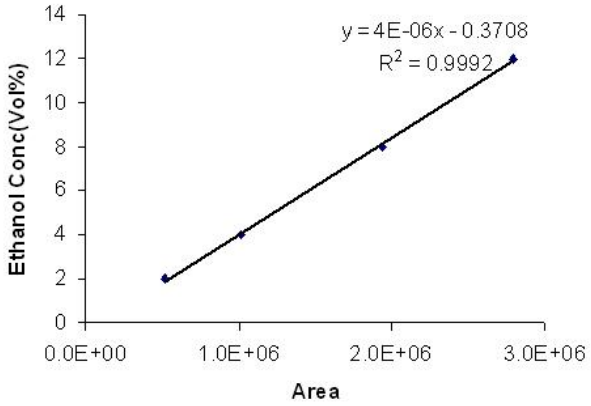

Figure 4.3 Dilute ethanol calibration curve (2-12% (v/v))

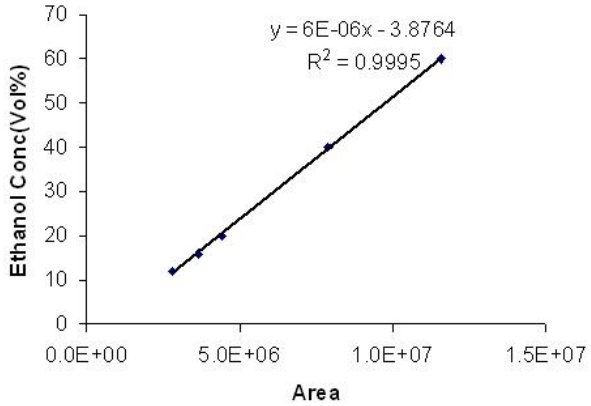

Figure 4.4 Ethanol/Water calibration curve (12-60% (v/v))

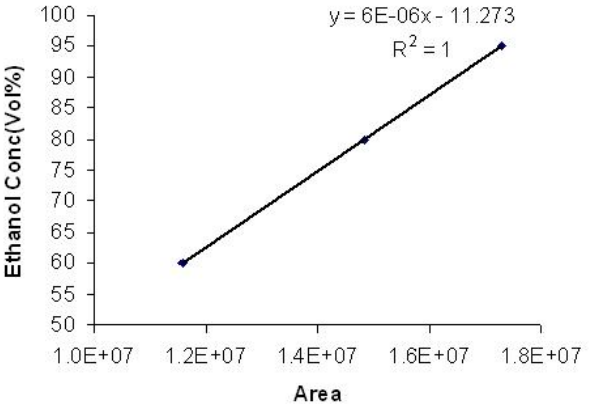

Figure 4.5 Ethanol/Water calibration curve (60-95% (v/v))

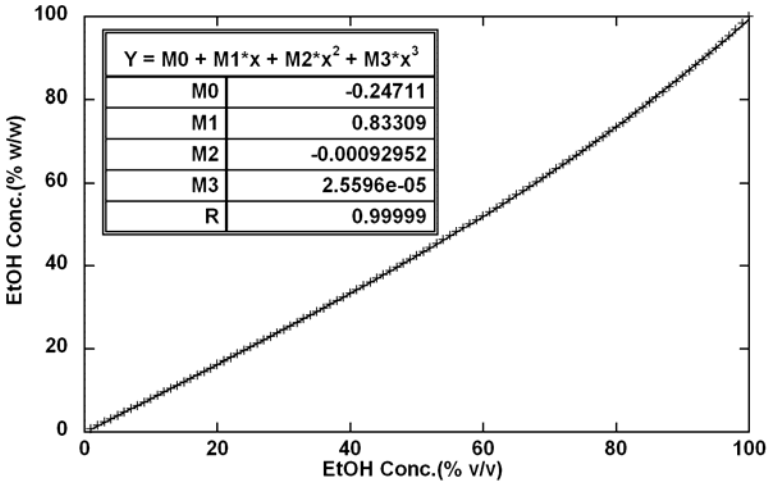

Figure 4.6a Ethanol Concentration in water weight vs. volume basis at 25^{o}C

The partition coefficient of ethanol was determined by stripping ethanol/water solution in the 4L fermentor with carbon dioxide at 8400ml/min and taking samples at 30mins interval for HPLC analysis of the ethanol concentration. The batch stripping without recycle data was fitted to $k = \frac{(1-y_w)N_o}{Q_{CO_2}t + N_o(x_{e(o)} - x)} \ln\left(\frac{x_{e(o)}}{x}\right)$ as shown in Figure 4.6b.

The average determined partition coefficient of ethanol was 0.518 ± 0.059. This was similar to the coefficient value (0.532) reported by Duboc and von Stockar (1998). The concentration of ethanol in the fermentor did not change vastly from one determination to the other since the extraction time intervals were not long and hence concentration determinations were likely to undergo slight experimental errors. However since the five ethanol concentration determinations and hence the partition coefficients were sequential, experimental errors that could possibly arise in one determination was nullified in the next. This could be seen in Figure 4.6b as the slight oscillation of the initial few partition coefficients about the average line. The overall average was thus the most important and reliable partition coefficient of ethanol.

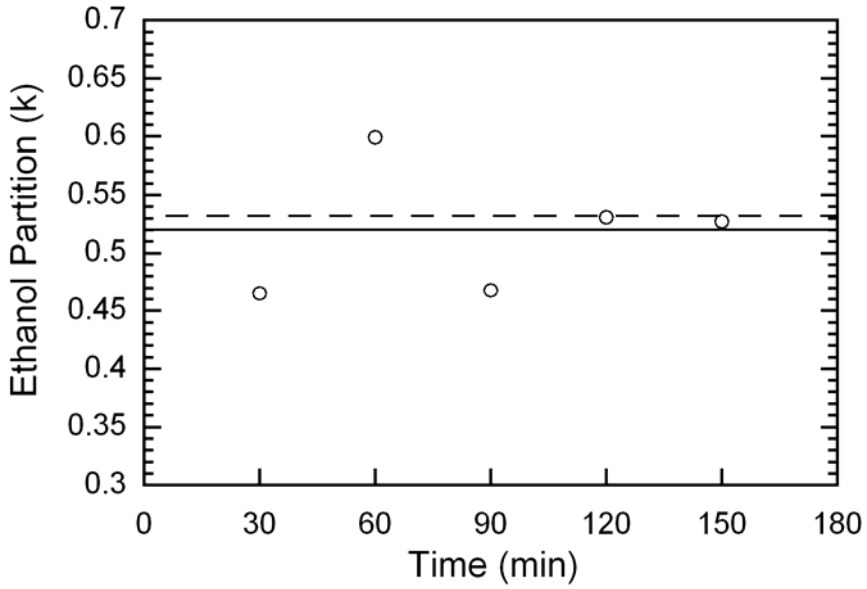

Figure 4.6b Ethanol partition coefficient from batch stripping experiment (Fermentor: 12%(v/v), 30^{o}C at CO_2 flow: 8400ml/min.(this experiment(o), average of this experiment (———), Duboc and von Stockar 1998 (– – – –))

Two similar other experiments were done with the flow rate of carbon dioxide varied from 4200ml/min to 12600ml/min. The average partition coefficient of ethanol was 0.525 ± 0.027 for CO_2 flow rate of 4200ml/min and 0.542 ± 0.049 for CO_2 flow rate of 12600ml/min. The coefficients at 4200ml/min and 8400ml/min were similar but that at 12600ml/min seemed slightly higher than those at the lower flow rates however, the difference was not statistically significant. The seemingly higher coefficient at 12600ml/min could probably be due to the increased tendency of liquid entrainment by the gas flowing at high rate. The ethanol partition coefficient was hence constant (0.528) up to 3vvm carbon dioxide flow rate. The proposed partition coefficient of ethanol (0.532) by Duboc and von Stockar (1998), which appears essentially the average of our experimental result, was used to calculate the concentration of ethanol in the stripped gas phase leaving the fermentor.

Ethanol distribution was hence characterized with experimental partition coefficient while equilibrium distribution was used for water. The compositions of the CO_2/vapor leaving the fermentor that were used for yields and compression energy calculations for the experimental runs are shown in Table 4.1b.

Table 4.1b Calculated exit gas composition at stable partition (1atm and 30 ^oC)

EtOH Solution		Gas Phase composition %(y_i)			EtOH Distribution
%(v/v)	%(x_i)	Ethanol	Water	CO_2	
2.0	0.62	0.33	4.14	95.53	Partition
12.0	3.99	2.13	4.03	93.85	Partition

Tops and Bottoms ethanol yields (%) are defined as the percentages of ethanol stripped by carbon dioxide (from ethanol partition in CO_2) from the broth that was recovered in the respective liquid condensates (Equation 4.1). Total ethanol yield was the sum of the Tops and Bottoms ethanol yields.

$$Yield(\%) = \frac{Conc_{EtOH} \times Ms}{\frac{1}{v} \times Flw_{CO_2} \times t \times \frac{M_{EtOH} \times y_{EtOH}}{M_{CO_2} \times y_{CO_2}}} \tag{4.1}$$

Where

$Conc_{EtOH}$ is the ethanol concentration of the Tops or Bottoms liquid condensate (% w/w)

Ms is the weight of the Tops or Bottoms liquid condensate (g)

v is the specific volume of carbon dioxide(L/g)

Flw_{CO_2} is the flow rate of carbon dioxide (L/min)

y_{EtOH} is the mole fraction of ethanol in the gas phase leaving the fermentor

y_{CO_2} is the mole fraction of carbon dioxide in the gas phase leaving the fermentor

M_{EtOH} is the molar mass of ethanol(g/mol)

M_{CO_2} is the molar mass of carbon dioxide(g/mol)

t is time span of run (min)

Compression energy is defined as the total work of gas compression per unit mass of total pure ethanol collected in condensates (Tops and Bottoms) from the flash tank (Equation 4.2).

$$Compres.\ Energy(J/g) = \frac{Work}{Ms_{Top} \times \frac{Conc_{EtOH(Top)}}{100} + Ms_{Bot.} \times \frac{Conc_{EtOH(Bot.)}}{100}} \qquad (4.2)$$

Where

$Conc_{EtOH(Top)}$ is the ethanol concentration of the Tops condensate (% w/w)

$Conc_{EtOH(Bot.)}$ is the ethanol concentration of the Bottoms condensate (% w/w)

Ms_{Top} is the weight of the Tops condensate (g)

$Ms_{Bot.}$ is the weight of the Bottoms condensate (g)

$Work$ is the total compression work as define in Equation 3.31 and re-stated below

$$Work(J) = \frac{Flw_{CO_2}}{y_{CO_2} \times M_{CO_2} \times v} \times \hat{W}_c \times t$$

Where

$\hat{W}_c$ is actual work of compression of CO_2 (J mol^{-1})

v is the specific volume of CO_2 (L g^{-1})

Flw_{CO_2} is the flow rate of CO_2 (L min^{-1})

y_{CO_2} is the mole fraction of CO_2 in the CO_2/Vapor mixture leaving the fermentor

M_{CO_2} is the molar mass of carbon dioxide(g mol^{-1})

t is time of run (min)

Refrigeration energy defined as the heat effect (J) of gas throttling per unit mass of total pure ethanol collected in condensates (Tops and Bottoms) from the flash tank were computed using Equation 4.3.

$$Refrig.\,Energy(kJ/kg) = \frac{Cool_{Effect}}{Ms_{Top} \times \frac{Conc_{EtOH(Top)}}{100} + Ms_{Bot.} \times \frac{Conc_{EtOH(Bot.)}}{100}} \tag{4.3}$$

Where

$Conc_{EtOH(Top)}$ is the ethanol concentration of the Tops condensate (% w/w)

$Conc_{EtOH(Bot.)}$ is the ethanol concentration of the Bottoms condensate (% w/w)

Ms_{Top} is the weight of the Tops condensate (g)

$Ms_{Bot.}$ is the weight of the Bottoms condensate (g)

$Cool_{Effect}$ is cooling effect as defined in Equation 3.35 and re-stated below

$$Cool_{Effect}(J) = \frac{Flw_{CO_2}}{M_{CO_2} \times v} \times C_p \times \Delta T_m \times t$$

Where

Flw_{CO_2} is the flow rate of CO_2 (L min^{-1})

v is the specific volume of CO_2 (L g^{-1})

C_p is the specific heat capacity of CO_2 (J mol^{-1} K^{-1})

t is the time span of throttling (min)

ΔT_m is the measured Joule-Thomson cooling (K).

The measured Joule-Thomson cooling (ΔT_m) is defined as

$$\Delta T_m = T_{i(m)} - T_{f(m)} \tag{4.4}$$

Where

$T_{i(m)}$ is the measured temperature of the flash tank(K)

$T_{f(m)}$ is the measured temperature of the throttling valve(K)

The Predicted Joule-Thomson cooling is given by

$$\Delta T_p = \mu_{JT} \Delta P = T_{i(m)} - T_{f(p)} \tag{4.5}$$

Where

$T_{i(m)}$ is the measured temperature of the flash tank(K)

$T_{f(p)}$ is the predicted temperature of the throttling valve(K)

ΔP is the pressure drop across the throttling valve(bar)

Predicted temperature of the throttling valve ($T_{f(p)}$) is hence given by

$$T_{f(p)} = T_{i(m)} - \mu_{JT} \Delta P \tag{4.6}$$

For temperature predictions, if the flash tank was at pressures lower than the saturation pressure of CO_2, ΔP was taken as the difference between the flash tank pressure (P_1) and the atmospheric pressure (P_2). Where the flash tank pressures were higher than the saturation pressure of CO_2, ΔP was taken as the saturation pressure (P_1) less the atmospheric pressure (P_2). μ_{JT} was the average of the gas phase Joule-Thompson coefficients of CO_2 ranging from 1bar to P_2 (of closest to P_2) in Table 3.13. For instance the carbon dioxide system at 55bar and 10 ^oC was assumed to be at 45bar and 10 ^oC for predicting cooling. Hence the true temperatures could be lower than those predicted for such situations.

4.3 Results and Discussion

4.3.1 Effect of pressure on ethanol separation

The masses and ethanol concentrations of the liquid collected from the Bottoms and Tops are shown in Figure 4.7. When the flash tank pressure was increased from 5bar to 45bar the mass of liquid collected from the Bottoms was almost constant (40.11 ± 0.85g). Similarly the concentration of ethanol from the Bottoms was also constant at (52.66 ± 1.59% (v/v)). On the contrary no ethanol was collected from the top fraction. As the flash tank pressure was increased from 50bar to 60bar both the mass and concentration of the ethanol in the Bottoms decreased rapidly. The Bottoms mass collected decreased by 38.20% and the corresponding concentration of ethanol decreased from 53.8% (v/v) to 42.2% (v/v). As the Bottoms fraction decreased, there was a corresponding increase in the mass of the Tops fraction (Table 4.2a). There was however an inverse relationship between the mass of Tops liquid collected and its concentration. As the mass of liquid in the Tops increased from 0.5g to 13g, the ethanol concentration decreased from 87.4 %(v/v) to 70.1 %(v/v). At 60bar flash tank pressure, 35% of the liquid had ethanol concentration of 70.6% (v/v) while at 55bar, 24% of the liquid had ethanol concentration 75% (v/v). Only 1.4% of the liquid collected at 50bar had ethanol concentration of 87% (v/v). The redistribution of the Tops and Bottoms fractions occurred at pressures near the saturation pressure of carbon dioxide (50.8bar). This showed the difference in the interaction of the CO_2-rich (Tops) and H_2O-rich (Bottoms) phases at some critical pressure in the flash tank. At pressures lower than the saturation pressure of carbon dioxide, minimal ethanol was entrained from the Bottoms into the Tops because the CO_2-rich phase which was in the gas phase was of low density and hence had poor interaction

for mass transfer with the H_2O-rich liquid phase. Thus, no Tops liquid was collected within the pressure range of 5bar to 45bar even though gases had better diffusivities than liquids. At 60bar when the CO_2-rich phase was in the liquid form, although it was a poor medium for water, it was relatively good medium for ethanol. Compounded with the better liquid-liquid interaction of the Tops and Bottoms and the improved diffusivity of liquid carbon dioxide at 60bar, ethanol was rapidly removed from the H_2O-rich phase into the CO_2-rich phase towards attaining equilibrium. This resulted in the quick depletion of ethanol from the Bottoms into the Tops observed at 60bar. The total mass of liquid collected remained approximately the same because both the flow rate and pressure of the extracting fluid (CO_2) were constant. There appeared to a limit to the total maximum amount of ethanol that can be recovered with increased pressure. The maximum total ethanol recovered was 89.5% at 45bar. The total ethanol yield seemingly increased with increase in flash tank pressure up to 45bar and then dropped steeply at higher pressures. The seemingly increase of total ethanol yield with increased pressure up to 45bar could possibly be due to more effective separation of the CO_2-rich and H_2O-rich phases with increased pressure below the saturation point of carbon dioxide (50.85bar). The total ethanol recovered drops sharply when the saturation pressure of the CO_2-rich phase (50.85bar) was exceeded. When more material was carried in the Tops as in the case when the flash tank pressure was increased from 50 to 60bar and the saturation pressure of the CO_2-rich phase was exceeded, the Joule-Thompson cooling was possibly not enough to effectively condense the remaining material in the Tops and resulted in the sharp drop in total ethanol recovered decreased (Figure 4.8a). The throttle valve temperature decreased while the compressor exit temperature increased with increased

flash tank pressure from 5 to 45bar. This was due to the increased work of compression and Joule-Thompson cooling effect with increased pressure.

Table 4.2a Isothermal and Constant flow run showing effect of pressure on ethanol recovery (At 15 ^{o}C two phase pressure of CO_2 is 50.85bar; Fermentor EtOH, 12%(v/v); Temp, 30 ^{o}C; Configuration, IFTL; Run time, 1hr)

CO_2 Flow (ml/min)	Flash Tank Press. (bar)	Flash Tank Temp (ºC)	Tops Amount (g)	Bottoms Amount (g)	Tops Ethanol (%(v/v))	Bottoms Ethanol (%(v/v))
8400	5	15	0.0000	39.0824	n/a	49.98
8400	10	15	0.0000	39.4810	n/a	51.44
8400	20	15	0.0000	39.6865	n/a	53.52
8400	30	15	0.0000	40.2800	n/a	53.60
8400	40	15	0.0000	40.8213	n/a	53.65
8400	45	15	0.0000	41.3280	n/a	53.75
8400	50	15	0.5672	39.5474	87.38	53.80
8400	55	15	9.6747	29.2116	74.95	44.49
8400	60	15	13.1064	24.4391	70.56	42.19

Table 4.2b Yields and energy consumption of isothermal and constant flow run (A, Compressor; B, Throttle valve)

CO_2 Flow (ml/min)	Flash Tank Press. (bar)	Flash Tank Temp (ºC)	Tops Ethanol Yield (%)	Bottoms Ethanol Yield (%)	Total Ethanol Yield (%)	Temp. Recorder (^{o}C)		Energy (kJ/kg)
						A	B	
8400	5	15	0.00	78.04	78.04	46	18	6412
8400	10	15	0.00	81.38	81.38	47	15	8665
8400	20	15	0.00	85.50	85.50	48	7	10764
8400	30	15	0.00	86.92	86.92	49	-2	11801
8400	40	15	0.00	88.18	88.18	none	none	11952
8400	45	15	0.00	89.46	89.46	53	-19	12258
8400	50	15	2.21	85.70	87.91	none	none	12915
8400	55	15	30.97	51.39	82.35	none	none	14217
8400	60	15	38.94	40.61	79.55	none	none	15130

Figure 4.8b shows the compression energy input with pressure. The total ethanol yield also increased with increase in energy input up to 12258KJ/kg (Table 4.2b). Above 12.25MJ/kg, the yield of ethanol decreased thus at constant carbon dioxide flow rate of

8.4 L/min, the total ethanol yield was maximum at 89% and occurred near the saturation pressure of carbon dioxide.

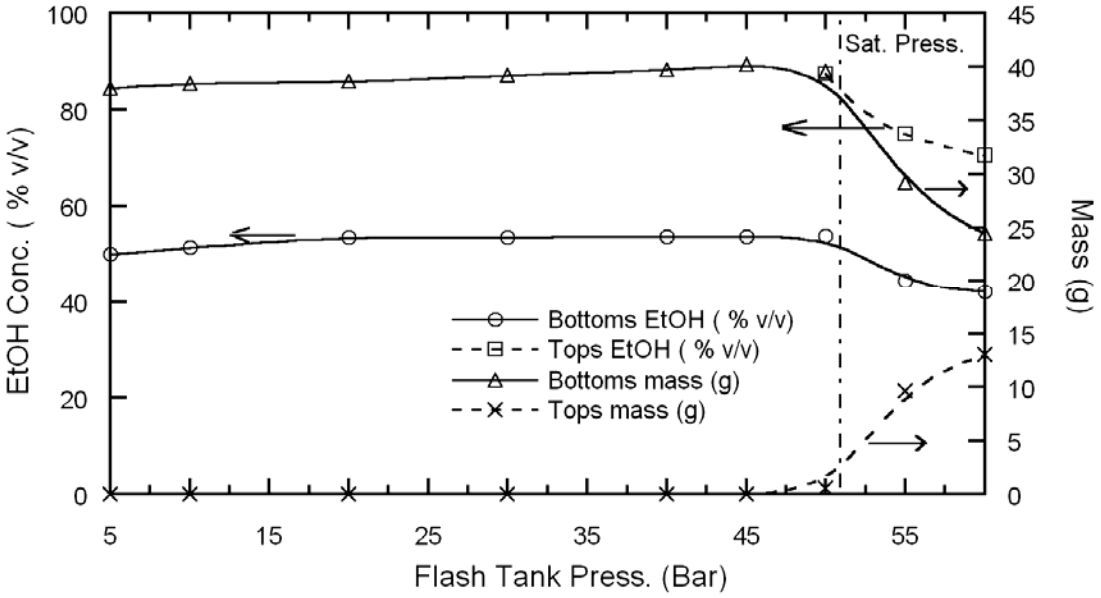

Figure 4.7 Mass and ethanol concentration of Tops and Bottoms as function of pressure (isothermal)

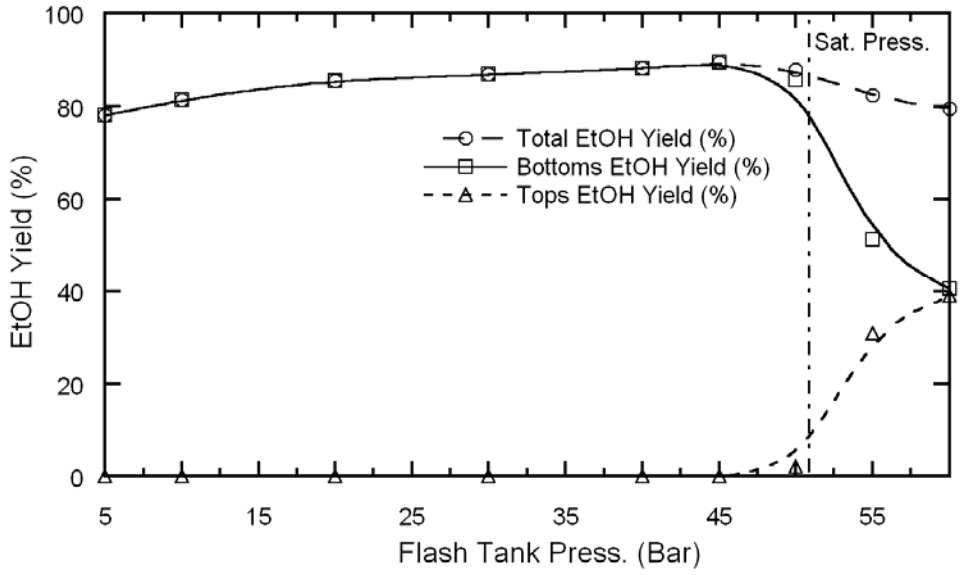

Figure 4.8a Ethanol yield as function of pressure (isothermal)

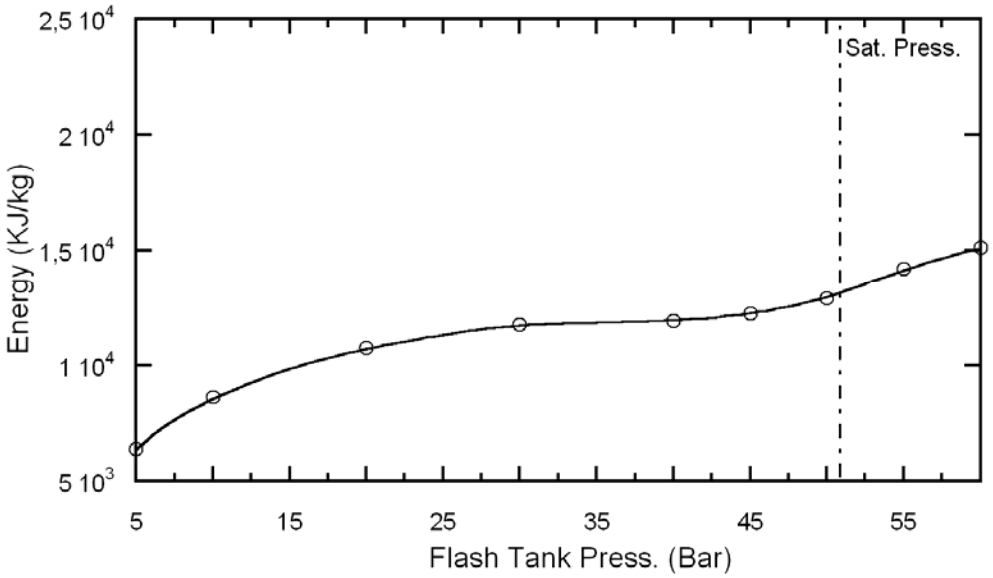

Figure 4.8b Compression energy as function of pressure (isothermal)

4.3.2 Effect of flash tank temperature on ethanol separation

The collected liquid masses and ethanol concentrations of the liquids from experiment are shown in Figure 4.9. Ethanol recovered in Tops and Bottoms are shown in Figure 4.10a and compression energies are shown in Figure 4.10b. As the flash tank temperature increased, the ethanol concentration increased for both Tops and Bottoms. However, above 25^{o}C, the Tops ethanol remained constant while the Bottoms ethanol concentration decreased (Figure 4.9). The Tops ethanol seemed relatively constant (89.92 ± 0.51% (v/v)) when temperature was above 25 ^{o}C. This upper limit of ethanol concentration was also reported by Defilippi and Moses (1982) in a pilot plant studies of supercritical carbon dioxide extraction of ethanol from water where the product concentration was limited to 84-89wt%(88.7-92.5%(v/v)). It was observed that the azeotropic composition of ethanol in water could not be broken with supercritical or liquid carbon dioxide extraction.

Table 4.3 Isobaric and Constant flow run showing effect of temperature on ethanol recovery (At 55bar two phase temperature CO_2 is 18.27 °C; Fermentor EtOH, 12%(v/v); Temp, 30 °C; Configuration, IFTL; Run time, 1hr)

CO_2 Flow (ml/min)	Flash Tank Press. (bar)	Flash Tank Temp (ºC)	Tops Amount (g)	Bottoms Amount (g)	Total Amount (g)	Tops Ethanol (%(v/v))	Bottoms Ethanol (%(v/v))
8400	55	15	9.6747	29.2116	38.8863	74.95	44.49
8400	55	25	1.2322	39.7202	40.9524	89.99	50.78
8400	55	35	0.6833	36.1635	36.8468	89.41	48.67
8400	55	45	1.0359	32.3615	33.3974	89.68	43.58
8400	55	55	2.0329	31.0372	33.0701	90.60	40.03

Table 4.4 Yields and energy consumption of isobaric and constant flow run

CO_2 Flow (ml/min)	Flash Tank Press. (bar)	Flash Tank Temp (ºC)	Tops Ethanol Yield (%)	Bottoms Ethanol Yield (%)	Total Ethanol Yield (%)	Energy (kJ/kg)
8400	55	15	30.97	51.39	82.35	14217
8400	55	25	5.00	80.70	85.70	13662
8400	55	35	2.75	70.12	72.87	16067
8400	55	45	4.18	55.67	59.86	19561
8400	55	55	8.32	48.77	57.09	20509

The ethanol yield in the Tops decreased initially (91%) with increase in flash tank temperature from 15 to 35°C, however above 35°C, it appears to slightly increase (approx. twice the yield at 35°C). The dramatic drop in the Tops liquid when the flash tank temperature as increased from 15°C to 35°C could be also be attributed to the density effect of the CO_2-rich phase (Tops) in the flash tank. Although the vapor pressure of ethanol and the diffusivity of the CO_2-rich phase increased with increased temperature from 15°C to 35°C, the effect of phase change and hence density of the CO_2-rich phase within the temperature interval had the dominant effect. The liquid CO_2-rich phase at 15°C resulted in more material being carried into the Tops. The trend between 35 to 55°C could be due to the exponential increase in vapor pressure of ethanol with increasing

temperature overshadowing the cooling effect. At constant pressure, an increase in flash tank temperature would cause a proportional increase in the exit temperature of the throttled gas and hence it was expected that the Tops ethanol yield would decrease monotonically with increase in the flash tank temperature. Both Bottoms and total ethanol yields on the other hand increased with flash tank temperature reaching maxima at 25^{o}C and then decreased above this temperature. The maximum Bottoms ethanol yield was 80.70% while as the total yield was 85.70%. There was a favorable balance at flash tank temperature of 25^{o}C since ethanol evaporation from the Bottoms was at minimum and at the same time condensation of remnant ethanol in the Tops was effective. Compression energy decreased initially reaching a minimum at 25^{o}C where it was 13.6MJ/kg. Energy increased above 25^{o}C reaching 20MJ/kg at 55^{o}C (Figures 4.10b).

It appears from Figures 4.8a and 4.10a that the maximum Total and Bottoms ethanol yields were attained at conditions where the CO_2-rich phase possibly existed as gas not far from its saturation temperature and pressure. This maximum yield condition was expected since carbon dioxide in the gas phase is of lower density and had relatively lower tendency to entrain both ethanol and water out of the flash tank ethanol than when it is in the liquid phase.

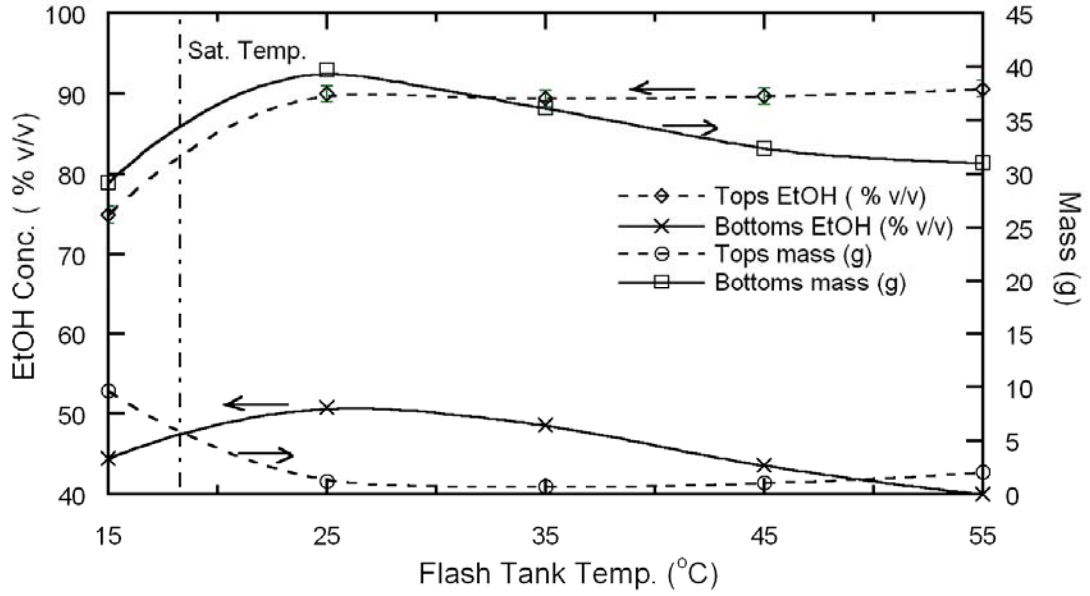

Figure 4.9 Mass and ethanol concentration of Tops and Bottoms as function of temperature (Isobaric)

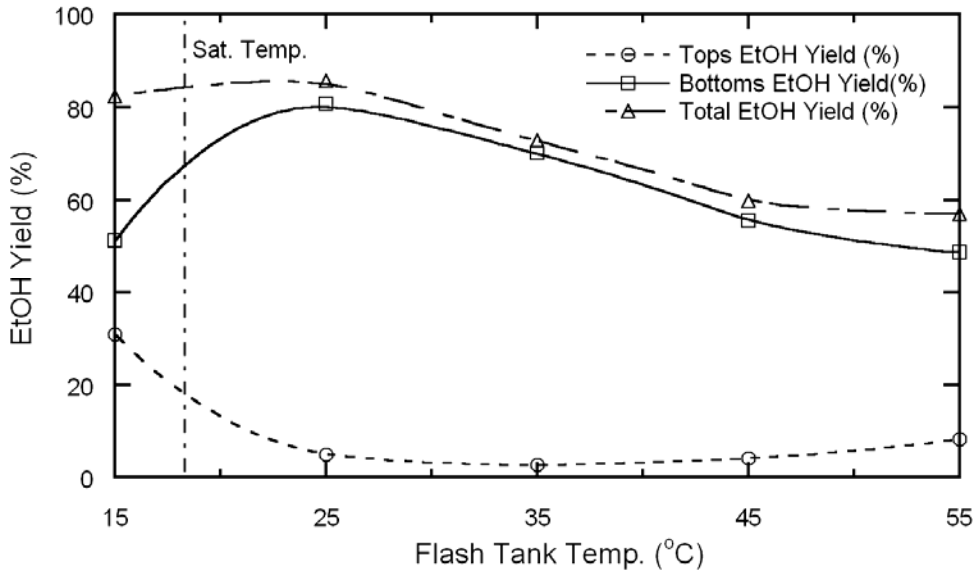

Figure 4.10a Ethanol yield as function of temperature (Isobaric)

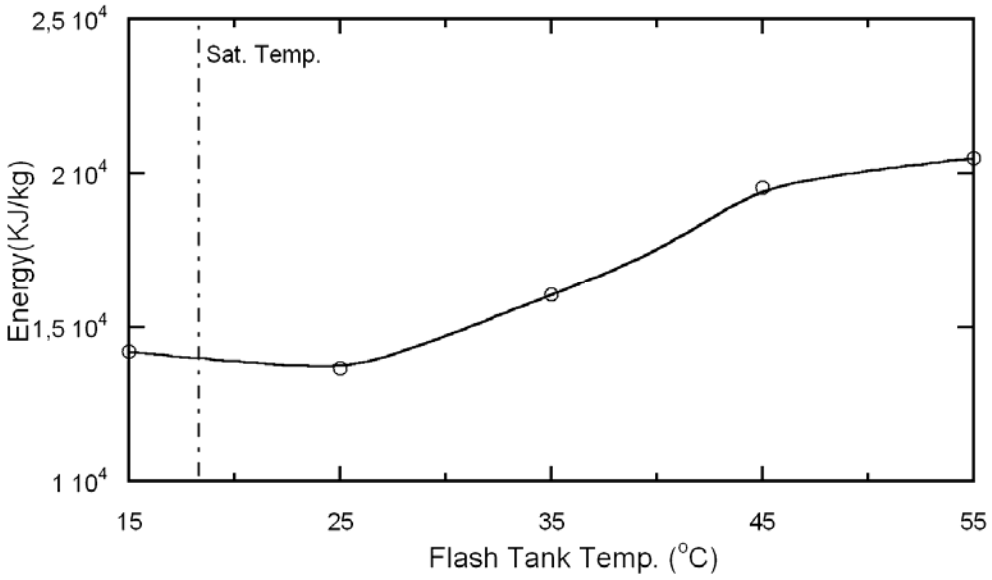

Figure 4.10b Compression energy as function of temperature (Isobaric)

4.3.3 Effect of saturation states of carbon dioxide

With the deductions from the studies on the effect of pressure and temperature on the extraction of ethanol, different sets of temperatures and pressures at which carbon dioxide would exist as near saturated vapor were experimented for the effect on ethanol extraction. The Bottoms ethanol masses and concentrations for the two different conditions were similar (Table 4.5a). The Bottoms ethanol concentration averaged 53.44 ± 0.51% (v/v). It was expected that at higher temperatures the Bottoms ethanol concentration would be relatively lower but higher pressures seemed to have nullified the effect. Total ethanol yields were also similar averaging 88.26 ± 0.49% (Table 4.5b). Compression energy was 8% lower at the lower temperature condition. There appears to be a tradeoff between pressure and temperature with the runs at the two conditions. It can be concluded that the extraction phenomenon at near saturated vapor carbon dioxide was similar irrespective of the saturation condition set at the flash tank.

Table 4.5a Effect of runs at different saturation conditions of carbon dioxide (At 40 and 50bar, two phase temperatures of CO_2 were respectively 5.3 and 14.3°C; Fermentor EtOH, 12%(v/v); Temp, 30 °C; Configuration, IFTL; Run time, 1hr)

CO_2 Flow (ml/min)	Flash Tank Press. (bar)	Flash Tank Temp (ºC)	Tops Amount (g)	Bottoms Amount (g)	Tops Ethanol (%(v/v))	Bottoms Ethanol (%(v/v))
8400	40	6	0.0000	41.5053	n/a	53.08
8400	50	15	0.5672	39.5474	87.38	53.80

Table 4.5b Yields and energy consumption of runs at different two phase conditions

CO_2 Flow (ml/min)	Flash Tank Press. (bar)	Flash Tank Temp (ºC)	Tops Ethanol Yield (%)	Bottoms Ethanol Yield (%)	Total Ethanol Yield (%)	Energy (kJ/kg)
8400	40	6	0.00	88.60	88.60	11895
8400	50	15	2.21	85.70	87.91	12915

4.3.4 Simulated ethanol recovery from compression and flashing

Scenarios with 2%(v/v) or 12%(v/v) ethanol in water stripped with carbon dioxide were simulated using the equations developed previously (Chapter three) to compare with the experimental results of the IFTL. The case of 2%(v/v) was included for the purpose of comparison with the optimization of the IFTL extraction scheme in latter sections. The initial CO_2/Vapor feed stream compositions to compression stage investigated are shown in Table 4.6a.

Table 4.6a Calculated exit gas phase composition at stable partition or equilibrium at 1atm and 30 °C

EtOH Solution		Gas Phase composition %(y_i)			EtOH Distribution
%(v/v)	%(x_i)	Ethanol	Water	CO_2	
2.0	0.62	0.33	4.14	95.53	Partition
2.0	0.62	0.47	4.14	95.39	Equilibrium
12.0	3.99	2.13	4.03	93.85	Partition

At 2%(v/v) ethanol in fermentor, the composition of ethanol in the vapor with the assumption of ethanol partition is approximately 30% less than that at equilibrium. The composition with the assumption that equilibrium distribution is attained for ethanol will only be approached at extended contact times between carbon dioxide gas and the fermentation medium. This condition will rarely be attained in practical carbon dioxide stripping process but is added to give an upper limit mark.

Figures 4.11 shows the equilibrium tie lines of the three sets of CO_2/vapor compositions simulated on the ternary two-liquid phase diagram for ethanol-water-carbon dioxide at 25^{o}C and the saturation pressure of CO_2 (65atm) adapted from Defilippi and Moses (1982). The two solid lines in Figure 4.11 are equilibrium data on the system.

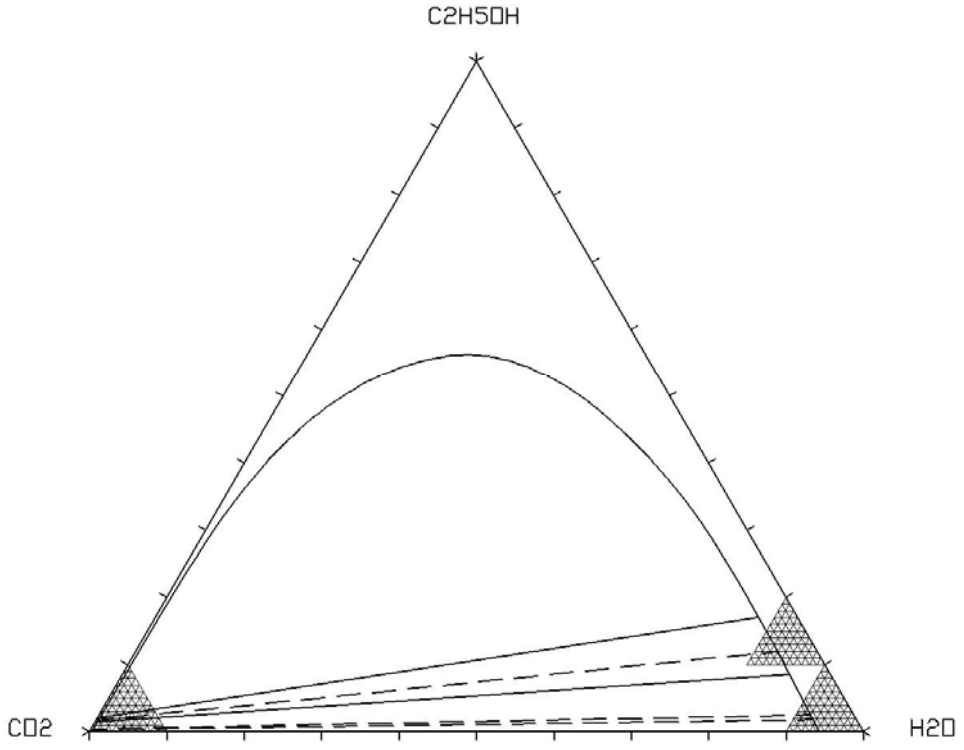

Figure 4.11 Equilibrium tie-line plot for ethanol-water-CO_2, mixtures at 25^{o}C and 65 atm. The three dashed lines are for Feeds (EtOH-0.33%, H_2O-4.14%, CO_2-95.53%; EtOH-0.47%, H_2O-4.14%, CO_2-95.39%; and EtOH-2.13%, H_2O-4.03%, CO_2-93.85)

The calculated composition of the H_2O-rich phase (Bottoms) in contact with the CO_2-rich phase (Tops) and the Solution of Rachford Rice equation (Equation 3.22) for the Bottoms and Tops flow rates for the flash tank are shown in Table 4.6b. It can be seen that CO_2 > 98% in the CO_2-rich phase (Tops) in equilibrium with the H_2O-rich phase (Bottoms) thus the Tops could be approximated with the properties of pure carbon dioxide.

Table 4.6b Calculated Flash tank Tops and Bottoms molar flow rates and component material balance at 25 ^oC and 65atm

Species	Mole fractions			Molar flows	
	Feed(z_i)	y_i	x_i	Vy_i	Lx_i
EtOH	0.0033	0.0027	0.0176	0.0026	0.0007
H_2O	0.0414	0.0026	0.9260	0.0025	0.0389
CO_2	0.9553	0.9947	0.0564	0.9529	0.0024
Total	1.0000	1.0000	1.0000	0.9580	0.0420
EtOH	0.0047	0.0038	0.0247	0.0036	0.0010
H_2O	0.0414	0.0026	0.9192	0.0025	0.0387
CO_2	0.9539	0.9936	0.0561	0.9518	0.0024
Total	1.0000	1.0000	1.0000	0.9579	0.0421
EtOH	0.0213	0.0167	0.1189	0.0159	0.0054
H_2O	0.0403	0.0028	0.8210	0.0027	0.0372
CO_2	0.9385	0.9805	0.0521	0.9361	0.0024
Total	1.0000	1.0000	1.0000	0.9547	0.0453

It can be deduced from Table 4.6b that when the fermentor (30^oC) is stripped with carbon dioxide and compressed to 65atm at 25^oC and flashed, if equilibrium is attained in the flash tank, the carbon dioxide free liquid condensate (Bottoms) would have ethanol content of 1.76 – 2.52% mole (5.72 – 7.80%(v/v)) with ethanol recovery of 21.2-21.3% of the feed ethanol content in the case of 2% (v/v) ethanol solution in fermentor and for 12%(v/v) solution would be 12.68%mole (32.96%(v/v)) with ethanol recovery of 25.4%. Carbon dioxide free vapor leaving the fermentor for 2% (v/v) ethanol fermentor content would be 7.38-10.19mol% (20.87-27.52%(v/v)) and for 12% (v/v) ethanol fermentor content would be 34.57mol% (65.31%(v/v)).

The calculated Bottoms ethanol yield from compression of CO_2/vapor mixtures from fermentor containing 2 or 12% (v/v) ethanol in water to 65bar and 25^oC are similar (21.2 and 25.4% respectively) whiles compression energy for 2% (v/v) is about 5.4 to 7.7 times that of 12% (v/v) for the simulated cases (Table 4.6c). Running the fermentor at the highest possible ethanol concentration would promise compression energy savings.

Table 4.6c Calculated compression and Bottoms EtOH yields at 25^oC and 65atm

Compressed gas composition			Bottom EtOH Yield	Compression Energy
Ethanol (mol %)	Water (mol %)	CO_2 (mol %)	(%)	(kJ/kg Ethanol)
0.33	4.14	95.53	21.2	394000
0.47	4.14	95.39	21.3	276000
2.13	4.03	93.85	25.4	51000

The refrigeration energy attained from the Joule-Thompson effect could be up to 20% of the compression energy and the final temperature of throttled carbon dioxide gas could reach -38^oC assuming throttled gas were all CO_2 (Table 4.6d). The energies in Table 4.6d are on the basis of 1 mole of compressed CO_2 gas.

Table 4.6d Compression and refrigeration energies of CO_2 at 25^oC and 65atm

Compression Work $kJmol^{-1}$	Cooling effect $kJmol^{-1}$	Final temp. (^oC)
12.140	2.315	-38

4.3.4.1 Comparison of the simulated equilibrium and the experimental IFTLs

Comparison of the simulated Bottoms ethanol yield and that from experimental results at 15^oC and 25^oC for 12%(v/v) ethanol in fermentor are shown in Table 4.6e. The Bottoms ethanol yield of the experiment was 1.6 to 3.2 times that of simulation. The Bottoms ethanol concentration of experiment was 28 to 54% higher than the simulated. It is evident from the data that the compression process in the compressor transfers the

ethanol mostly into the aqueous layer first and the phases in the flash tank were far from equilibrium. The tendency of ethanol to diffuse from the Bottoms back from into the Tops increases tremendously when the Tops (CO_2-rich phase) was in the liquid form. The rapid tendency for ethanol to diffuse from the Bottoms (H_2O-rich phase) into the Tops (CO_2-rich phase) towards equilibrium when the CO_2-rich phase was in the liquid form as compared to when it was in the gas form can be seen in the experimental results at 15^oC (Table 4.6e). At 15^oC and 45bar when the CO_2-rich phase was in the gas phase, there was no Tops collected and the ethanol yield in the Bottoms was 89.5% but at 60bar when the CO_2-rich phase was in the liquid phase 35% of the total liquid condensate was collected as Tops. The Bottoms ethanol yield at 60bar dropped steeply to 40.6% a decrease in yield of 55% that at 45bar. The difference in the Bottoms ethanol yield was not too large when the CO_2-rich phases of the experiment and simulated systems were both liquids (15^oC, 60bar; 25^oC, 66bar). At 15^oC and 60bar, the Bottoms ethanol yield was only 1.6 times higher than that of the simulated equilibrium yield at 25^oC and 66bar. At 25^oC and 55bar, when the CO_2-rich phase was gas, the Bottoms ethanol yield reached a maximum of 3.2 times that of the simulated equilibrium yield at 25^oC and 66bar. In the case where the CO_2-rich phases were both gas, the Bottoms ethanol yield at 15^oC, 45bar was however slightly higher (11%) than that at 25^oC, 55bar because the vapor pressure of ethanol was relatively lower at 15^oC and there was a higher tendency of ethanol to remain in the Bottoms (H_2O-rich phase). Since the compression of the ternary system of gas was fast and the residence time in the flash tank was small, the phase interaction for mass transfer was minimal and hence equilibrium was only approached in the experiments. If equilibrium were attained in the flash tank at 15^oC and 60bar, the Bottoms ethanol yield

would further fall below 40.6%. It would however be expected that the equilibrium Bottoms ethanol yield at 15^{o}C and 60bar would be slightly higher than the simulated yield at 25^{o}C and 66bar (25.4%) since the vapor pressure of ethanol decreases with decrease in temperature as discussed and thus there would be an increased tendency of ethanol to preferentially remain in the H_2O-rich phase (Bottoms). Since the Bottoms ethanol yields were higher when the CO_2-rich phase in the flash tank was in the gas phase as compared to when it was in the liquid phase and also during compression, the gas can only be changed in the direction of from the gaseous phase into the liquid phase, it can be concluded that the non equilibrium compression of the ternary system of ethanol-water-carbon dioxide initially transfers the ethanol into the Bottoms (H_2O-rich phase). The compressed ternary gas system would however tend towards equilibrium when the two phases in contact with each other are allowed to be in contact for extended time.

Table 4.6e Bottoms ethanol concentration and recovery for simulation and IFTL (experiment)

	Simulation	Experiment		
Fermentor EtOH (%v/v)	12	12	12	12
Flash Tank Press.(bar)	65.9	55	60	45
Flash Tank Temp.(^{o}C)	25	25	15	15
CO_2-rich phase	Liquid	Gas	Liquid	Gas
Bottom EtOH (%v/v)	33.0	50.8	42.2	53.8
Bottom EtOH Yield (%)	25.4	80.7	40.6	89.5

4.3.5 Reversed configuration

Experimental results for the reversed configuration as described in process flow description section at 30^{o}C and three different pressures are shown in Tables 4.7a and 4.7b. In this configuration, no Tops fraction was collected. Thus the total product collected was equal to the Bottoms fraction. The Bottoms ethanol concentration were similar averaging 49.17 ± 0.15 %(v/v) for a fermentor containing 12%(v/v) ethanol in

water. The Bottoms ethanol concentration was approximately four time that in the fermentor. It can be seen from Figure 4.12 that increasing flash tank pressure did not have marked effect on the concentration of ethanol in the Bottoms. However, there was 5% increase in Bottoms mass with increase in flash tank pressure. Figure 4.13 shows that the total ethanol yield increased linearly with increase in flash tank pressure. This trend was possibly due to the linear dependence of cooling effect with pressure together with the fact that there was a single stream product collection system so that increased cooling resulted in proportional increase in material condensation.

Table 4.7a Isothermal and Constant flow run showing effect of increasing pressure on ethanol recovery for reversed layout(Fermentor EtOH, 12%(v/v); Temp, 30^{o}C; Configuration, RL; Run time, 1hr)

CO_2 Flow (ml/min)	Flash Tank Press. (bar)	Flash Tank Temp (ºC)	Tops Amount (g)	Bottoms Amount (g)	Tops Ethanol (%(v/v))	Bottoms Ethanol (%(v/v))
8400	50	30	0.00	37.6981	n/a	49.00
8400	55	30	0.00	38.7791	n/a	49.20
8400	60	30	0.00	39.8508	n/a	49.30

Table 4.7b Yields and energy consumption of Isothermal and Constant flow run for reversed layout

CO_2 Flow (ml/min)	Flash Tank Press. (bar)	Flash Tank Temp (ºC)	Tops Ethanol Yield (%)	Bottoms Ethanol Yield (%)	Total Ethanol Yield (%)	Energy (kJ/kg)
8400	50	30	0.00	73.65	73.65	15416
8400	55	30	0.00	76.10	76.10	15385
8400	60	30	0.00	78.38	78.38	15356

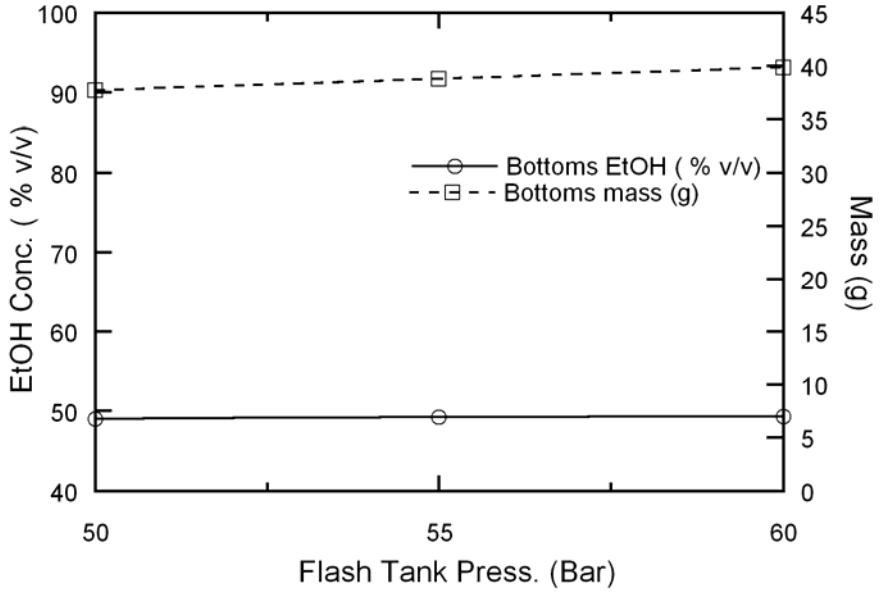

Figure 4.12 Mass and ethanol concentration of Tops and Bottoms (Reversed layout)

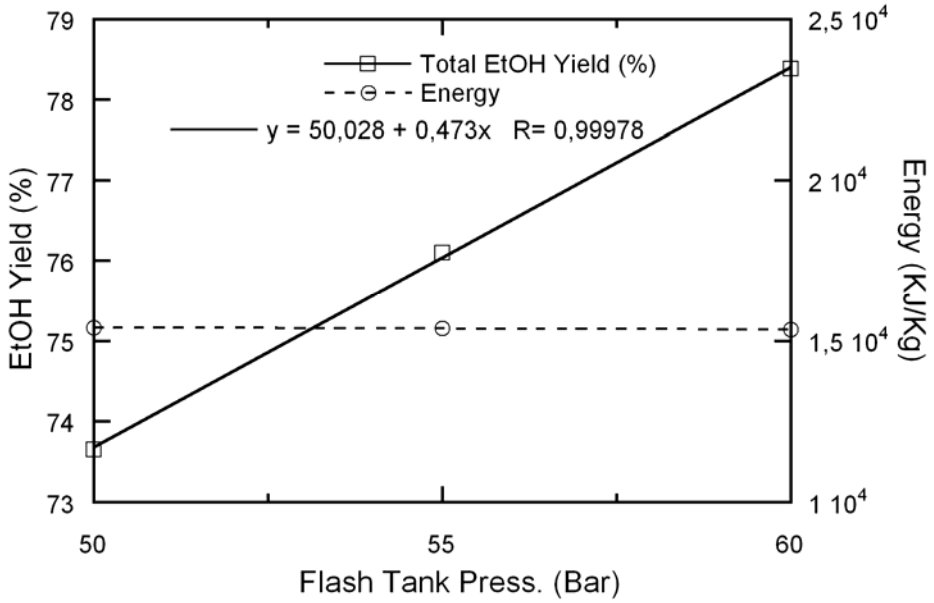

Figure 4.13 Ethanol yield and compression energy (Reversed layout)

Comparison of data of the isothermal flash tank layout and the reversed layouts are shown in Tables 4.8a and 4.8b. The Bottoms ethanol concentrations were similar at 49.55 ± 1.09 %(v/v) for both configurations. The mass of Bottoms liquid collected for the

reversed layout was higher than the average value of those collected for the isothermal flash tank (Figures 4.14) layouts. Even though it appears from Figures 4.15 that the Bottoms ethanol yield of the RL was higher than the average value of those of the IFTL, it is seen that the total ethanol yield for the RL was lower than the average of the two IFTL since more ethanol was recovered in the Tops in the case of the IFTL. The masses of the Tops were small (<1.3g) but were rich in ethanol (approx. 90 %(v/v)). It seems that the main advantage of the IFTL over the RL was the ability to recover extra ethanol in the Tops but this might not be statistically significant since the Tops masses were low compared to the Bottoms. The IFTL might seem advantageous when the goal is to further concentrate the ethanol since it is a step ahead in concentrating the product. An added advantage of the isothermal flash tank scheme was that the throttling valve did not contain a mixture of gas and liquid and hence could be controlled more easily. Energies of the two layouts ranged from 13 to 16MJ/kg (Figure 4.16).

Table 4.8a Isobaric and Constant flow comparison of the IFTL and RL layouts on ethanol recovery (Fermentor EtOH, 12%(v/v); Temp, 30°C; Run time, 1hr)

Type	CO_2 Flow ml/min	Flash Tank Press. (bar)	Flash Tank Temp (°C)	Tops Amount (g)	Bottoms Amount (g)	Tops EtOH % (v/v)	Bottom EtOH % (v/v)
IFTL	8400	55	25	1.232±0.043	39.720±0.337	89.99	50.78
IFTL	8400	55	35	0.683±0.027	36.164±0.219	89.41	48.67
RL	8400	55	30	0.000±0.000	38.779±0.410	n/a	49.20

Table 4.8b Yields and energy consumption of the IFTL and RL layouts

Type	CO_2 Flow ml/min	Flash Tank Press. (bar)	Flash Tank Temp (°C)	Tops EtOH Yield (%)	Bottoms EtOH Yield (%)	Total EtOH Yield (%)	Energy (kJ/kg)	Total mass (Tops + Bottom) (g)
IFTL	8400	55	25	5.00	80.70	85.70	13662	40.952
IFTL	8400	55	35	2.75	70.12	72.87	16067	36.847
RL	8400	55	30	0.00	76.10	76.10	15385	38.779

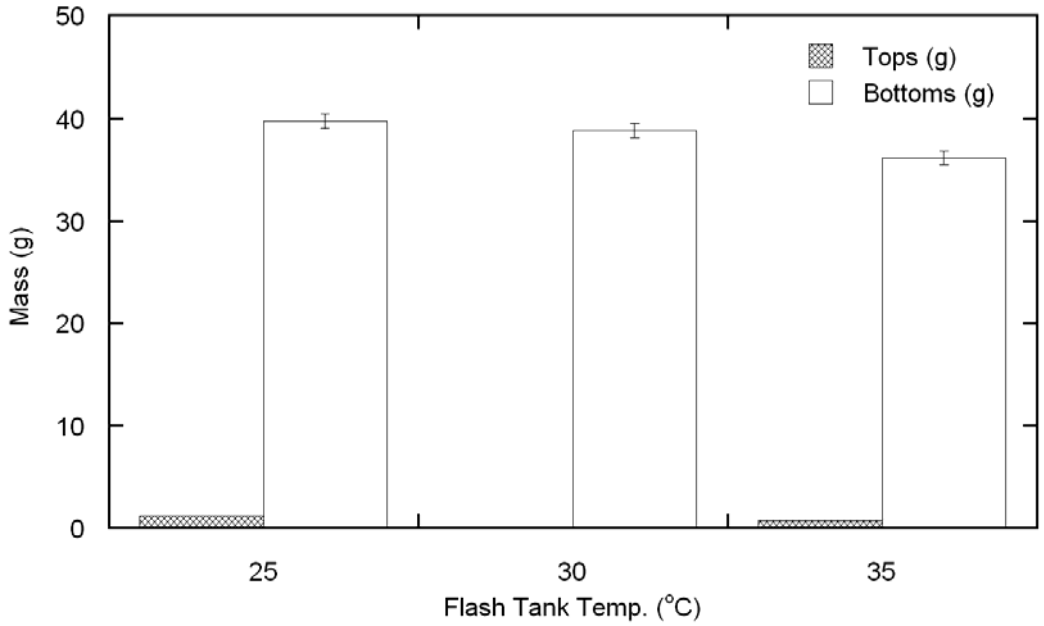

Figure 4.14 Masses of Tops and Bottoms of isothermal flash tank and reversed layouts (Isothermal flash tank; 25 and 35°C, reversed 30°C)

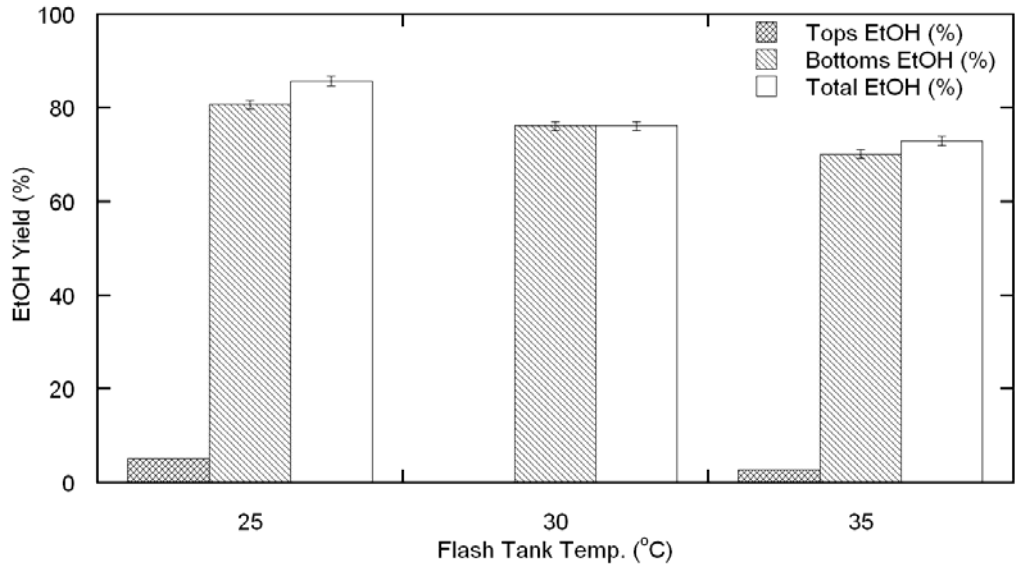

Figure 4.15 Yields of isothermal flash tank and reversed layouts (Isothermal flash tank; 25 and 35°C, reversed 30°C)

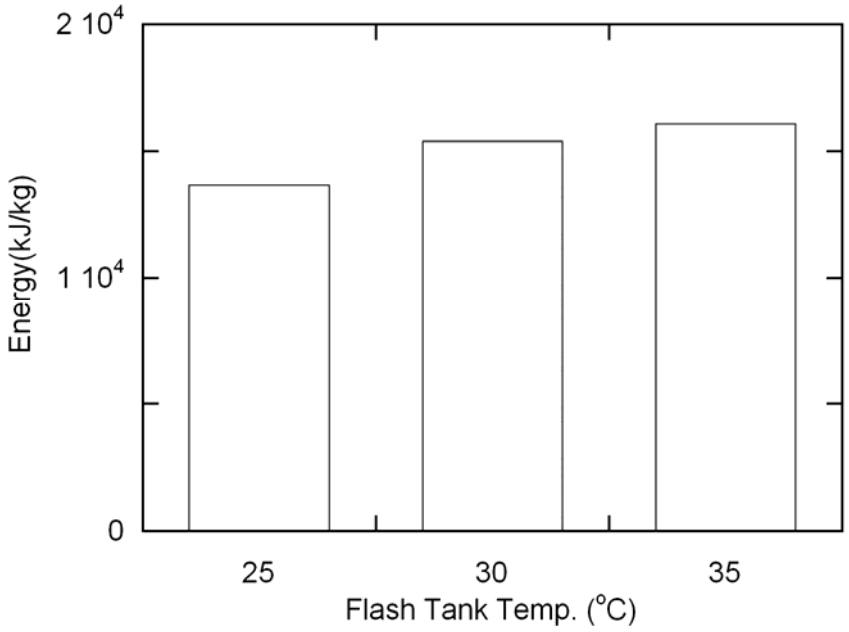

Figure 4.16 Compression energy as function of temperature (Isothermal flash tank; 25 and 35°C, reversed 30°C)

4.3.6 Optimization of flow rate, temperature and pressure on separation

Results of the Box-Behnken optimization design runs for 2%(v/v) ethanol in the fermentor are shown in Table 4.9, 4.10, 4.11 and 4.12. The Bottoms ethanol concentration ranged from 8.91 to 14.89 %(v/v). The Tops ethanol concentration averaged 67.42 ± 3.14 %(v/v) (Table 4.9). The range of the total ethanol yield was 46.03% at (8.4L/min, 40bar, 40°C) to 80.18% at (4.2L/min, 40bar, 25°C) and averaged 64.69 ± 11.13%. The average compression energy was 120.0MJ/kg (Table 4.10). The measured temperature of the compressed CO_2/vapor mixture exiting the compressor (Recorder B) prior to entering the flash tank (where it was maintained at a set temperature and pressure) ranged from 37 to 67°C(Table 4.11). This temperature appeared to increase with increased flow rate or flash tank pressure as was expected since

total compression work increase with increased flow rate and pressure. The temperature however decreased with increase in flash tank temperature.

Table 4.9 Condensate masses and ethanol concentrations of Tops and Bottoms for Box-Behnken design (Fermentor EtOH, 2%(v/v); Temp, 30°C; Configuration, IFTL; Run time, 1hr)

CO_2 Flow Nominal (ml/min)	Flash Tank Press. (bar)	Flash Tank Temp (°C)	Tops Amount (g)	Bottoms Amount (g)	Tops Ethanol (%(v/v))	Bottoms Ethanol (%(v/v))
4200	40	25	0.00 ± 0.00	11.70 ± 0.87	n/a	13.67
4200	55	40	0.00 ± 0.00	10.45 ± 0.55	n/a	10.44
12600	55	40	0.72 ± 0.06	30.38 ± 0.59	65.19	8.91
4200	70	25	0.48 ± 0.15	8.93 ± 0.77	60.06	9.58
12600	40	25	0.10 ± 0.04	28.84 ± 2.01	69.80	11.87
12600	70	25	1.61 ± 0.18	31.24 ± 1.89	68.87	9.14
8400	55	25	0.60 ± 0.33	17.60 ± 1.44	66.91	11.93
8400	70	40	0.83 ± 0.11	17.64 ± 0.36	69.97	8.04
8400	40	40	0.00 ± 0.00	18.99 ± 1.33	n/a	9.75
8400	70	10	1.09 ± 0.14	21.56 ± 1.92	69.14	10.00
8400	40	10	0.00 ± 0.00	20.08 ± 1.83	n/a	14.89
4200	55	10	0.39 ± 0.09	8.83 ± 0.50	68.11	14.75
12600	55	10	1.57 ± 0.28	29.09 ± 1.82	68.72	12.29

Table 4.10 Condensate Ethanol Yields and compression energy consumption

CO_2 Flow Nominal (ml/min)	Flash Tank Press. (bar)	Flash Tank Temp (°C)	Tops Ethanol Yield (%)	Bottoms Ethanol Yield (%)	Total Ethanol Yield (%)	Energy (kJ/kg)	Total mass (Tops + Bottom) (g)
4200	40	25	0.00	80.18	80.18	84840	11.70
4200	55	40	0.00	54.38	54.38	138978	10.45
12600	55	40	8.51	44.75	53.26	141896	31.10
4200	70	25	15.59	42.50	58.09	140290	9.41
12600	40	25	1.26	57.03	58.29	116710	28.94
12600	70	25	20.38	47.25	67.63	120508	32.85
8400	55	25	10.94	52.45	63.39	119219	18.20
8400	70	40	15.97	34.89	50.86	160235	18.47
8400	40	40	0.00	46.03	46.03	147808	18.99
8400	70	10	20.75	53.66	74.41	109516	22.65
8400	40	10	0.00	75.01	75.01	90697	20.08
4200	55	10	14.77	65.35	80.12	94322	9.22
12600	55	10	19.82	59.60	79.42	95153	30.66

Table 4.11 Temperature Recorder readings at various points and throttled gas state (A, Compressor; B, Throttle valve; C, Separator; D, Recycle line)

CO_2 Flow ml/min	Flash Tank Press. (bar)	Flash Tank Temp. (^oC)	CO_2 Sat. Press. (bar)	Temp. Recorder (^oC)				Visual observation of Tops
				A	B	C	D	
4200	40	25	64.3	37	-7	5	12	No product
4200	55	40	n/a	38	-12	2	13	Little white Vapor
12600	55	40	n/a	60	-20	-10	-1	Little white Vapor
4200	70	25	64.3	43	-44	-40	-12	Plenty of white powder
12600	40	25	64.3	56	-15	-4	2	Little white vapor
12600	70	25	64.3	60	-47	-46	-40	Plenty of white powder
8400	55	25	64.3	49	-26	-20	-3	Medium white powder
8400	70	40	n/a	52	-30	-25	-4	Plenty of white powder
8400	40	40	n/a	48	-3	4	10	No product
8400	70	10	45.0	59	-42	-40	-30	Plenty of white powder
8400	40	10	45.0	55	-15	-8	4	No product
4200	55	10	45.0	47	-42	-40	-10	Medium white powder
12600	55	10	45.0	67	-42	-40	-35	Plenty of white powder

Table 4.12 Measured and Predicted Joule-Thompson cooling and refrigeration energy

CO_2 Flow Nominal (ml/min)	Flash Tank Press. (bar)	Flash Tank Temp (^oC)	Measured Throttle Valve Temp (^oC)	Predicted Throttle Valve Temp (^oC)	Ratio of Meas. Cooling. to Compression Energy
4200	40	25	-7	-18.96	0.11
4200	55	40	-12	-12.82	0.16
12600	55	40	-20	-12.82	0.19
4200	70	25	-44	-44.22	0.20
12600	40	25	-15	-18.96	0.14
12600	70	25	-47	-44.22	0.21
8400	55	25	-26	-35.07	0.16
8400	70	40	-30	-26.01	0.20
8400	40	40	-3	1.36	0.15
8400	70	10	-42	-46.88	0.15
8400	40	10	-15	-40.56	0.09
4200	55	10	-42	-46.88	0.16
12600	55	10	-42	-46.88	0.16

The temperature difference between the throttle valve and the separator ranged from 1 to 14^{o}C. The temperature difference decreased as more powdery material (dry ice) was observed in the separator. This could be attributed to the increased heat needed to

sublime the dry ice in the separator. The measured refrigeration ranged from 9-21% of the work of compression (Table 4.12).

The Bottoms ethanol yield decreased when the pressure increased from 40 to 70bar at 10ºC and 8.4L/min CO_2 (Figure 4.17). A similar trend was observed at 15ºC (Figure 4.8a) when the pressure was increased above the saturation pressure of carbon dioxide even though the Bottoms and total ethanol yields initially increased slightly with increase in pressure. On the contrary, even though the Bottoms ethanol yield decreased by 32% at 40ºC when pressure was increased from 40 to 70bar, it was relatively less drastic as compared to the 40% drop in yield at 10ºC so resulted in a slight increase in the total ethanol yield at 40ºC with increased flash tank pressure (overshadowing the fact that the Tops ethanol yield was relatively higher at 10ºC). The sharp difference in the margin of the decrease in the Bottoms ethanol yields was probably due to the absence of any drastic property change of carbon dioxide within the pressure interval at 40ºC as a result of the nonexistence of phase transition (liquid to gas). The Bottoms and total ethanol yields at 10^oC were higher than those at 40^oC. It can be seen from Figure 4.18a that at 25^oC and 40bar the total ethanol yield at 4.2L/min was 38% higher than that at 12.6L/min but on the contrary, at 70bar the total ethanol yield at 4.2L/min was 14% lower than that at 12.6L/min. This shows a major interaction of carbon dioxide flow rate and flash tank pressure. The elevated fluid agitation in the compressor and the increased volumetric flow rate of the gas form CO_2-rich phase at high gas flow rate could have caused an inefficient separation of the aqueous phase from the form carbon dioxide rich phase so that it resulted in the lower total ethanol yield at 12.6 L/min compared to that at 4.2 L/min at 40bar and 25^oC. However, at 70bar and 25^oC where the carbon dioxide rich

phase was liquid and relatively denser with improved extractive power for ethanol, the extended interaction time of the two phases in the flash tank at 4.2 L/min might have cause more ethanol diffusing into the carbon dioxide rich phase toward attaining equilibrium. This could have resulted in the lower total ethanol yield at 4.2 L/min compared to 12.6 L/min at 70bar overshadowing the fact that at 40bar, the total yield at 4.2 L/min was relatively higher.

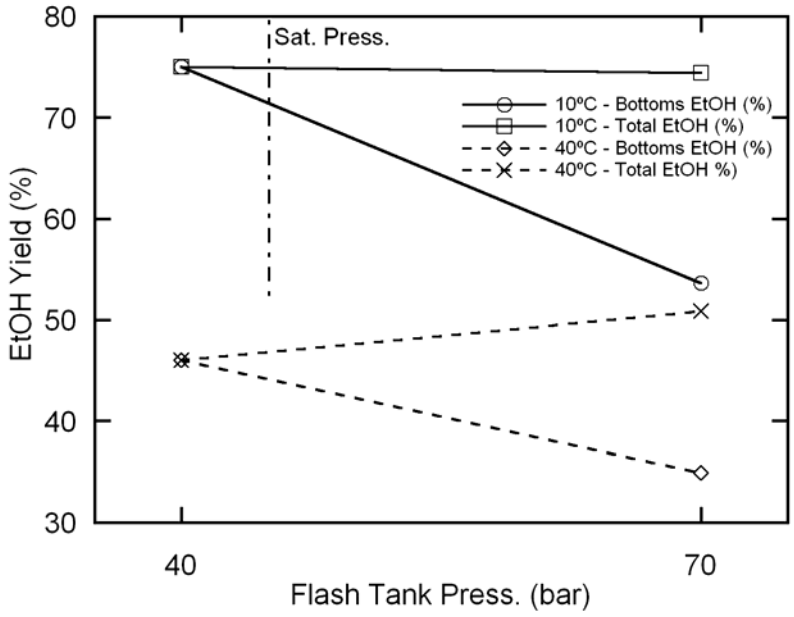

Figure 4.17 Ethanol yields at flash tank temperatures of 10 and 40 ºC as function of flash tank pressure at CO_2 flow rate of 8400ml/min

Both the Bottoms and total ethanol yields decreased with temperature (Figure 4.18b), even though the Bottoms ethanol yield at 12.6 L/min were lower compared to those at 4.2 L/min, the total ethanol yields were comparable. Stemming from Figure 4.18a, it would be expected that at 10^oC where carbon dioxide was dense, the yields at 4.2 L/min would be lower than those at 12.6 L/min due to longer interaction time in the flash tank

but the decreased flash tank temperature may have slowed this phenomenon as a result of lower diffusivity.

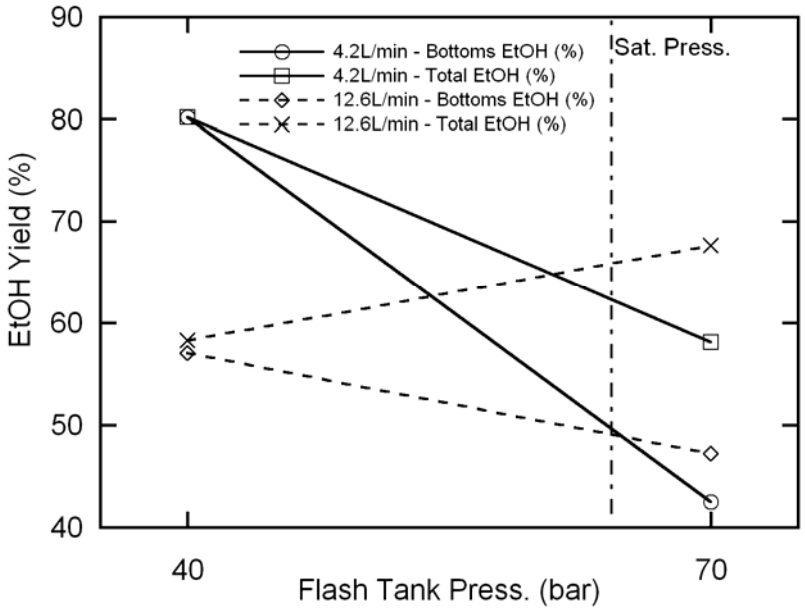

Figure 4.18a Ethanol yields at flash tank temperature of 25 ºC as function of flash tank pressure.

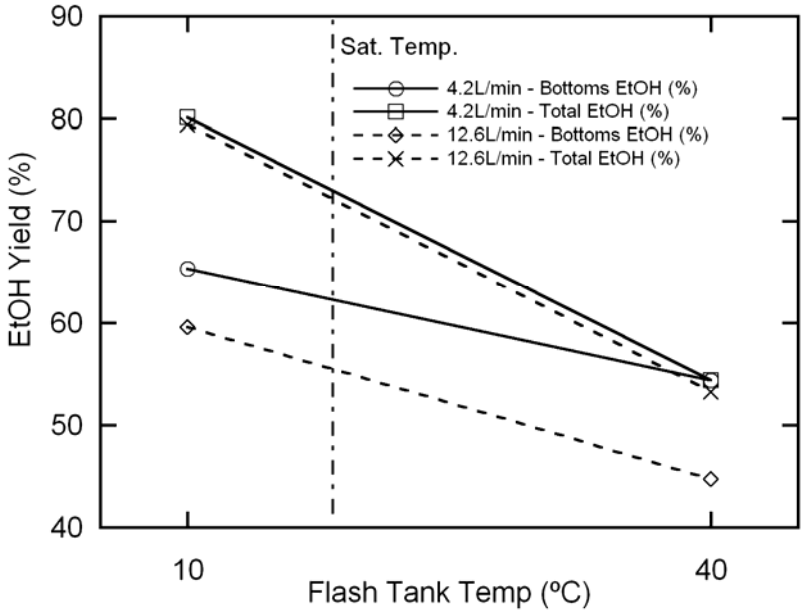

Figure 4.18b Ethanol yields at flash tank pressure of 55bar as function of flash tank temperature.

The measured throttle valve temperatures appeared to slightly decrease with increased flow rate of carbon dioxide (Figure 4.18c). This trend could be a feature of the high gas flow rates suppressing the effect of heat transfer to the throttling valve from the surroundings or the Joule-Thompson throttling effect being more efficient with increased gas flow. The deviations of the measured temperatures at the two flow rates (4.2 and 12.6L/min) ranged from 0 to 8^{o}C.

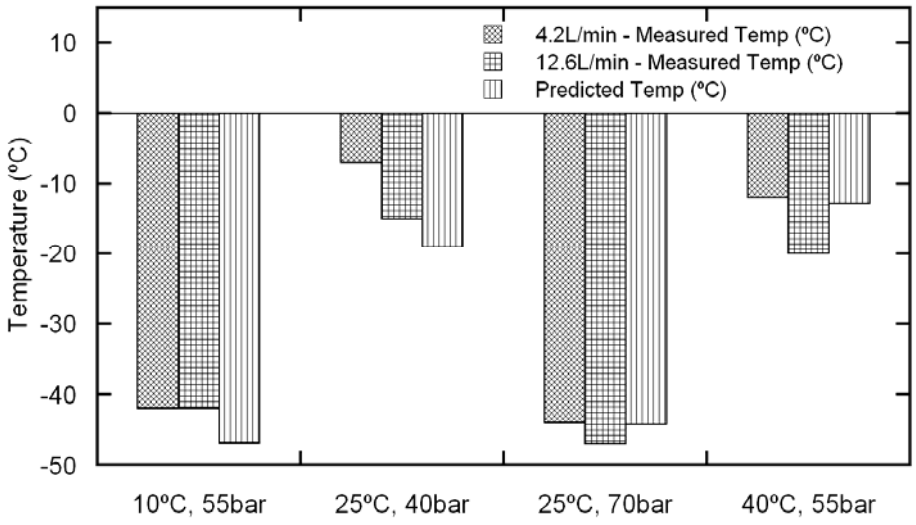

Figure 4.18c Measured and predicted throttle valve temperatures at carbon dioxide flow rates of 4.2L/min and 12.6L/min.

The experimental Joule-Thompson coefficients at 25^{o}C computed as the slopes of the temperature versus pressure plots were 1.066 to 1.233^{o}C/bar (Figure 4.18d). These were comparatively within the range of the theoretical Joule- Thompson coefficient of pure carbon dioxide at 25^{o}C. The experimental Joule-Thompson coefficient at 25^{o}C and carbon dioxide flow rate of 12.6L/min appeared to be slightly lower than that at 4.2L/min contrary to what was expected since the heat interaction of the throttling valve with the surrounding was attenuated at high gas flow rates. This was likely due to relatively higher measured liquid (condensate) content of the Tops at high gas flow rates at constant

flash tank temperature and pressure (Table 4.9). The liquid condensates (ethanol and water) of the Tops have the tendency to reduce the extent of the Joule-Thompson cooling due to carbon dioxide since they have higher specific heat capacities compared to the gaseous carbon dioxide and moreover do not produce significant cooling effect as carbon dioxide.

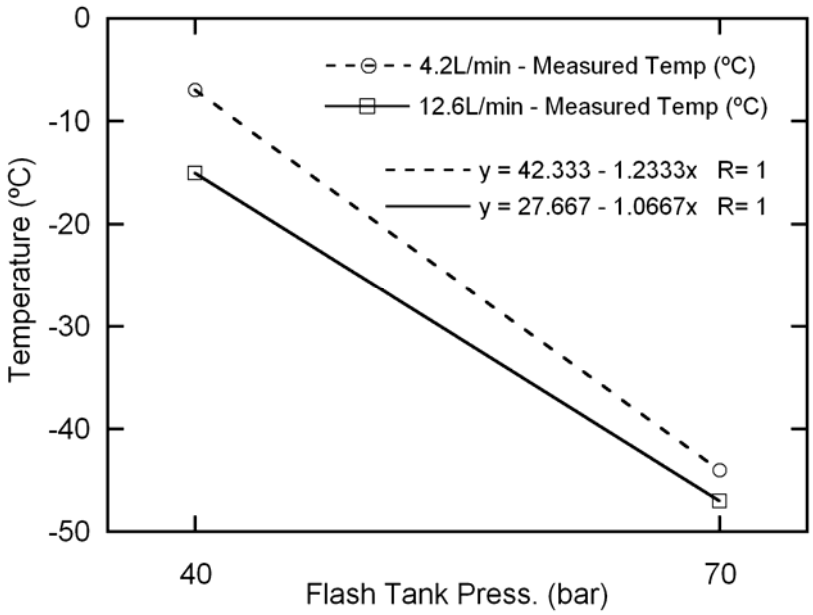

Figure 4.18d Measured throttle valve temperature as function of flash tank pressure (flash tank temperature: 25 ºC).

Table 4.13 Effect Tests of main parameters and interactions for Bottoms, Tops and Total ethanol yields and work of compression

Source	Bottoms Yield (Prob > F)	Tops Yield (Prob > F)	Total Yield (Prob > F)	Work Energy (Prob > F)
Flow (ml/min)(4200,12600)	0.1163	0.2311	0.3071	0.4731
Press (bar)(40,70)	0.0140	0.0121	0.5139	0.0185
Temp (^{o}C)(10,40)	0.0175	0.0996	0.0029	0.0020
Flow (ml/min)*Press (bar)	0.0834	0.7284	0.0309	0.0326
Flow (ml/min)*Temp (^{o}C)	0.7456	0.7334	0.9622	0.8885
Press (bar)*Temp (^{o}C)	0.4184	0.6412	0.5534	0.6723
Flow (ml/min)*Flow (ml/min)	0.3530	0.9955	0.2407	0.2434
Press (bar)*Press (bar)	0.9321	0.6346	0.6677	0.5645
Temp (^{o}C)*Temp (^{o}C)	0.9215	0.9649	0.8562	0.3563

4.3.6.1 Response of Bottoms Yield

Table 4.13 shows that pressure and temperature were the two main factors that had significant influence (95% confidence level) on the ethanol recovered in the Bottoms since they defined the physical state of carbon dioxide. Interaction of flow and pressure was significant at 90% confidence level. It seems from the cube plot of Figure 4.19 that pressure increment from 40 to 70bar resulted in decreased Bottoms ethanol yields. When pressures increased from 40 to 70bar the Bottoms ethanol yield decreased by 46% and 16% at 10^{o}C a seemingly steeper drop compared to 43% and 2% at 40^{o}C. This could be the result of CO_2-rich phase change present at 10^{o}C when pressure was increased from 40 to 70bar as already discussed. Given a constant increase in the pressure of a fluid system, there would be a relatively drastic change in the density and other fluid properties when the fluid undergoes a phase change (liquid to gas and vice versa) as compared to when the fluid phase remained homogeneous (gas or liquid alone). The change of the CO_2-rich phase to liquid when the pressure was increased to 70bar at 10^{o}C resulted in better liquid-liquid interaction with the H_2O-rich phase than the gas-liquid interaction of the CO_2-rich phase at 70bar at 40^{o}C with the H_2O-rich phase. The improved two-phase liquid-liquid interaction caused increased entrainment of ethanol from the Bottoms (H_2O-rich phase) at 70bar and 10^{o}C than at 70bar and 40^{o}C even though the vapor pressure of ethanol and the diffusivity of carbon dioxide were relatively higher at 70bar and 40^{o}C as was discussed earlier. As was also seen from Figure 4.8a the Bottoms ethanol yield decreased when the pressure increased above 45bar for flash tank temperature between 10 and 40ºC. This was irrespective of whether the flash tank was at sub or super critical temperature of carbon dioxide (31ºC). Figure 4.19 also shows that the Bottoms ethanol yields decreased with

increased temperature as was already shown (Figure 4.10a). The Bottoms ethanol yields decreasing with increasing temperature were due to the increasing vapor pressure of ethanol with increased temperature. At higher temperatures more ethanol was carried away in the Tops carbon dioxide gas phase. It appears that the extraction process at 40bar and 70bar were different considering the trend with flow rate. Whiles the ethanol recovered in the Bottoms decreased with increasing flow rate at 40bar, it appeared to increase slightly with flow rate at 70bar (Figure 4.19). This was attributed to the interaction of the densities of the two phases in contact with each other and the retention time in the flash tank. Ethanol recovered in the Bottoms ranged from 40-85%. Figures 4.20, 4.21 and 4.22 are constant flow rate slices of the cube plot of Figure 4.19 showing the detailed yield curves. The yield cube (Figure 4.19) was swept rigorously but did not have occurrences of any buried maxima or minima points within.

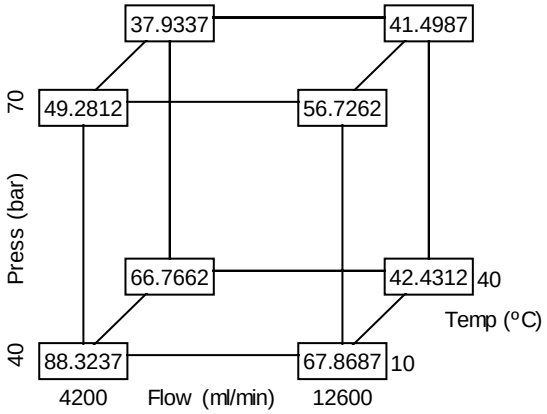

Figure 4.19 Cube Plot showing the Bottoms Yield (% Ethanol) at all extreme parameter conditions

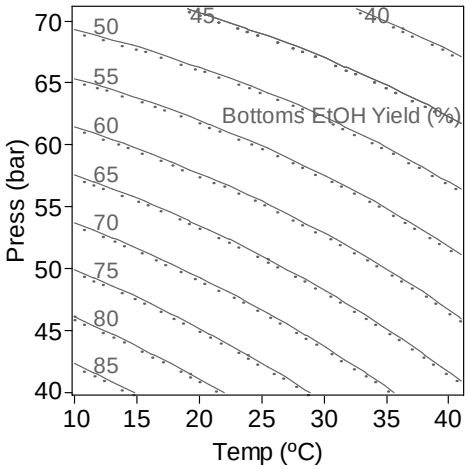

Figure 4.20 Contour plot of Bottoms Yield (%) as function of temperature and pressure at 4200ml/min

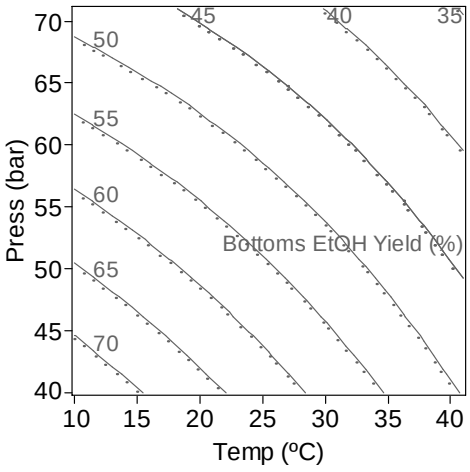

Figure 4.21 Contour plot of Bottoms Yield (%) as function of temperature and pressure at 8400ml/min

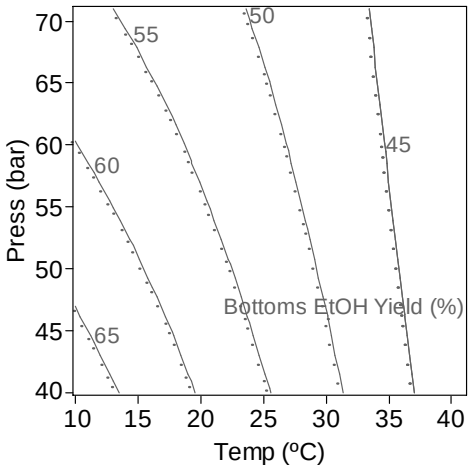

Figure 4.22 Contour plot of Bottoms Yield (%) as function of temperature and pressure at 12600ml/min

They show that the maximum Bottoms yield of ethanol was at the 40bar and 10°C as expected since this pressure (40bar) is below the saturation pressure (45bar) of carbon dioxide at 10°C. Effect of pressure on Bottoms yield is minimized as flow rate increased.

4.3.6.2 Response of Tops ethanol yield

In the case of the ethanol yield in the Tops, Table 4.13 shows that pressure was the main factors that had significant effect on the amount of ethanol collected in the Tops(at 95% confidence level). Temperature becomes marginally significant main factor at 90% confidence level. There was no evidence of interaction effect of any of the main factors. Figure 4.23 shows that ethanol yield in the Tops increased with increased pressure from 40 to 70bar as was previously shown (Figure 4.8a). More material was condensed from the exiting gas phase due to the increased Joule-Thomson cooling effect associated with increasing pressure and the possible increased entrainment of the aqueous phase from the

flash tank into the separator as a result of the elevated densities of carbon dioxide at 70bar. Constant flow rate cuts of cube plot of ethanol yield (Figure 4.23) are shown in Figures 4.24, 4.25 and 4.26. The Tops ethanol yield decreased with increasing flash tank temperature. Although there was cooling, the outlet throttle temperature was relatively higher at increased flash tank temperature and probably not cold enough to condense as much product from the carbon dioxide gas. The Tops ethanol yield increased slightly with increasing carbon dioxide flow rate from 4200ml/min to 12600ml/min. Heat loss or gain from throttle valve appeared to be attenuated at higher carbon dioxide flow rates and hence throttle valve temperatures were lower at higher flow rate (Figure 4.18c). The colder throttle temperature could have resulted in the increased Tops ethanol yield with increasing flow rate as seen in Figures 4.24, 4.25 and 4.26 but this was not statistically significant at 90% confidence level. The yield cube (Figure 4.23) did not have any occurrences of obscured maxima or minima points within.

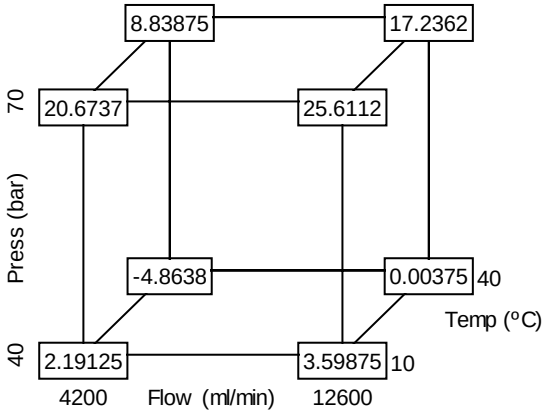

Figure 4.23 Cube Plot showing the Tops Yield (% Ethanol) at all extreme parameter conditions

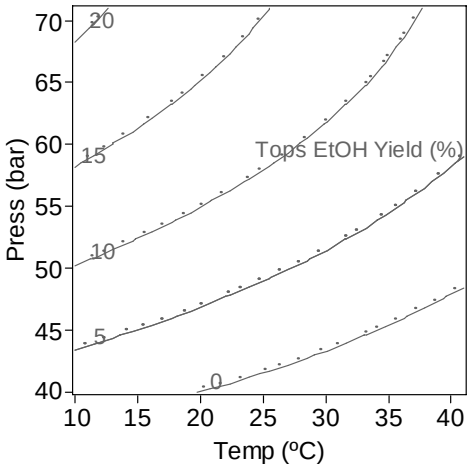

Figure 4.24 Contour plot of Tops Yield (%) as function of temperature and pressure at 4200ml/min

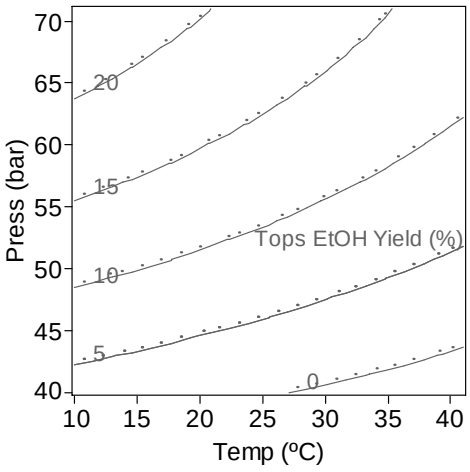

Figure 4.25 Contour plot of Tops Yield (%) as function of temperature and pressure at 8400ml/min

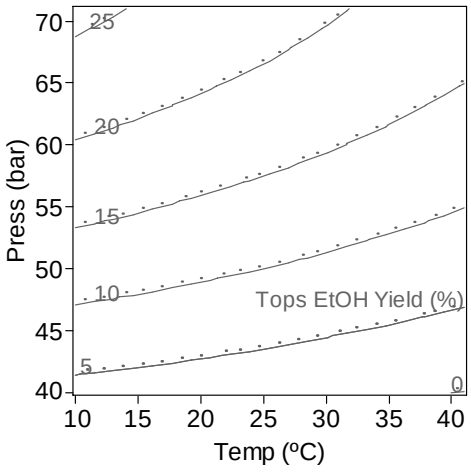

Figure 4.26 Contour plot of Tops Yield (%) as function of temperature and pressure at 12600ml/min

4.3.6.3 Response of Total ethanol yield

Table 4.13 shows temperature as the only significant main factor that determined the total ethanol yield at 95% confidence level. Interaction of flow and pressure was also significant at this level. The total ethanol yield was the sum of the ethanol yields of the Bottoms and the Tops. Figure 4.27 show decrease in total recovered ethanol with increasing temperature of the flash tank. This was due to more ethanol escaping in the gas phase at higher temperature as a result of increased ethanol vapor pressure and the Joule-Thompson cooling not enough to cool the exiting gas to very low temperatures since the initial gas temperatures were relatively higher. The interaction of flow and pressure can be seen in Figures 4.28, 4.29 and 4.30 where the maximum total ethanol yield at 4200ml/min was at 40bar and 10^{o}C but at 12600ml/min it was at 70bar and 10^{o}C. CO_2. The contour curves of the total ethanol yield cube (Figure 4.27) did not have any occurrences of hidden maxima or minima yield points within.

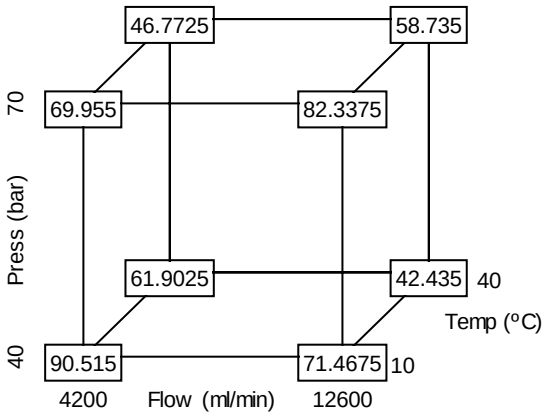

Figure 4.27 Cube Plot showing the Total Yield (% Ethanol) at all extreme parameter conditions

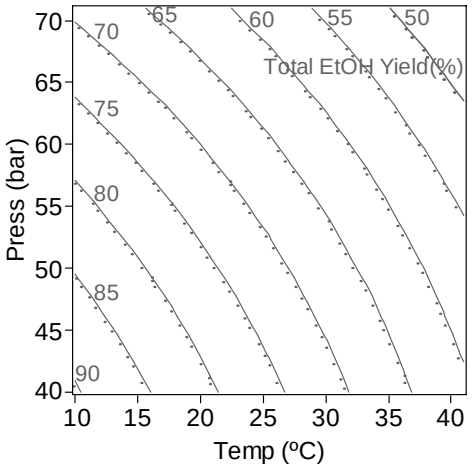

Figure 4.28 Contour plot of Total Yield (%) as function of temperature and pressure at 4200ml/min

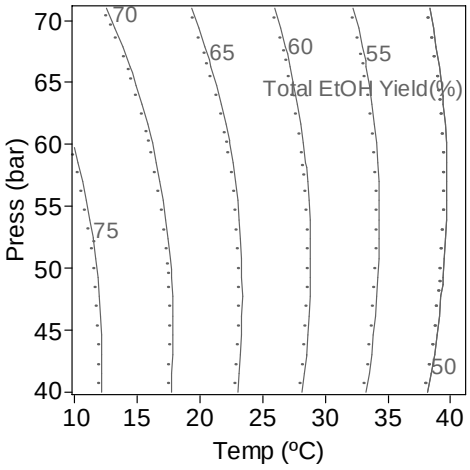

Figure 4.29 Contour plot of Total Yield (%) as function of temperature and pressure at 8400ml/min

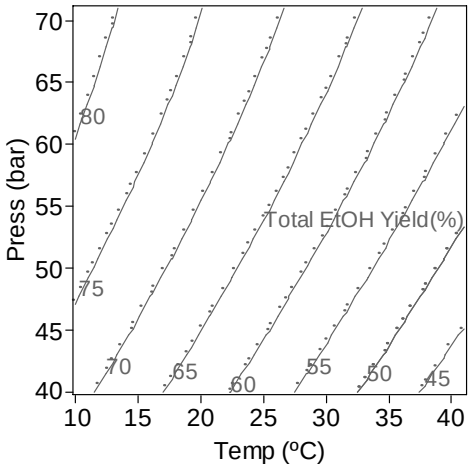

Figure 4.30 Contour plot of Total Yield (%) as function of temperature and pressure at 12600ml/min

4.3.6.4 Response Work of Compression

Temperature and pressure were by far the most important factors that influenced the work of compression needed for ethanol recovery (Table 4.13). The point of minimum work energy consumption was at 40bar, 10^{o}C and 4200ml/min as shown in Figure 4.31. Figures 4.32, 4.33 and 4.34 show compression energy needed ranged from 72,000-160,000kJ/kg total recovered ethanol with 2%(v/v) ethanol in water. For 12%(v/v) ethanol in water, the work of compression requirement ranged from 6,000 to 20,000kJ/kg ethanol recovered. Refrigeration energy break computed for the proposed scheme ranged from 10 to 20% of the work of compression.

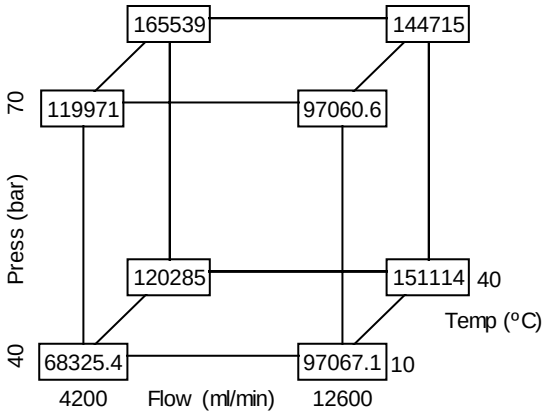

Figure 4.31 Cube Plot showing the Energy consumption (kJ/kg Total Ethanol Recovered) at all extreme parameter conditions

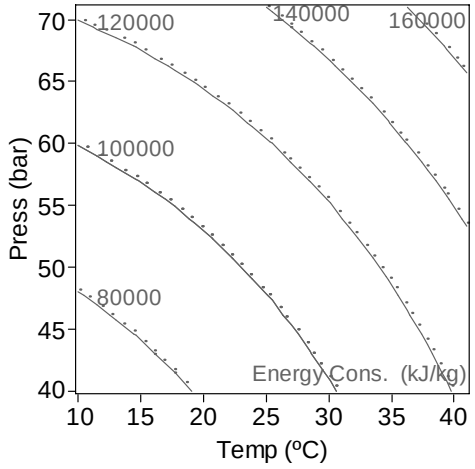

Figure 4.32 Contour plot of Energy consumption (kJ/kg) as function of temperature and pressure at 4200ml/min

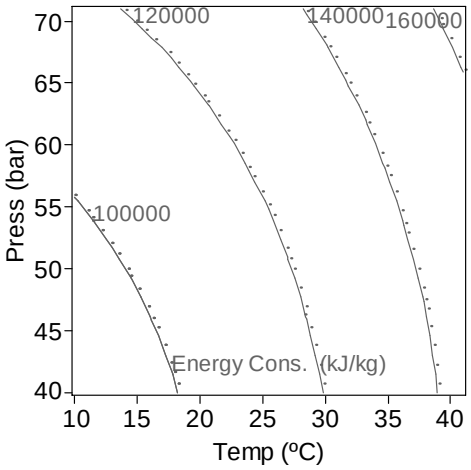

Figure 4.33 Contour plot of Energy consumption (kJ/kg) as function of temperature and pressure at 8400ml/min

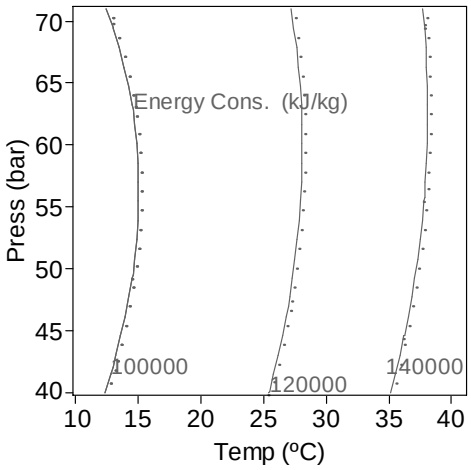

Figure 4.34 Contour plot of Energy consumption (kJ/kg) as function of temperature and pressure at 12600ml/min

4.3.7 Summary of ethanol recovery with the IFTL, RL and the simulated IFTL

For comparison purposes some of the parameters of interest of the two layouts (IFTL and RL) and those simulated are summarized (Table 4.14). The Bottoms ethanol yields or the IFTL were at least 1.6 times those simulated at equilibrium for both 2 and 12% (v/v) ethanol solution in the fermentor. The Bottoms ethanol yield of the IFTL reached a maximum of 80.2%, a 3.8 fold increase over that calculated at equilibrium with a fermentor solution of 2%v/v and 89.5%, a 3.5 fold increase over the simulated value at equilibrium with 12% (v/v) solution in the fermentor. Depending on the chosen temperature and pressure of the flash tank, the Bottoms ethanol yield of the IFTL could vary immensely from a little over one fold increase to almost fourfold increase. The physical state of the Tops (CO_2-rich phase) in the flash tank of the IFTL had a tremendous influence on the Bottoms ethanol yield. As was seen in previous discussions of the IFTL, when the CO_2-rich phase in contact with the aqueous phase in the flash tank

was liquid the Bottoms ethanol yield dropped rapidly approaching the equilibrium values. The maximum Bottoms ethanol yields were measured where the CO_2-rich phase in the flash tank was in the gaseous form as opposed to the liquid form. The experimental maximum Bottoms ethanol recovered with a fermentor solution of 12% (v/v) was approximately 12% higher than the maximum obtained with 2% (v/v) ethanol solution in the fermentor. It is interesting to note that there was a similar increment in the Bottoms ethanol yield of the simulated equilibrium IFTL with 12%v/v over that simulated at 2%v/v. The Bottoms and total ethanol yields of the IFTL increased with increase in the concentration of ethanol in the fermentor and hence the extraction mechanism was more efficient when the concentration of ethanol in the fermentor was high. On the other hand, the maximum total ethanol yield of the RL was 12% lower than the maximum with the IFTL at the same fermentor ethanol concentration.

Table 4.14 Comparison of ethanol yields and concentrations of the IFTL and RL

Parameter	Simulation		Experiment		
	IFTL	IFTL	IFTL	IFTL	RL
Fermentor EtOH (%v/v)	2	12	2	12	12
Flash Tank Press.(bar)	65.9	65.9	40-70	6-55	50-60
Flash Tank Temp.(^oC)	25	25	10-40	15-55	30
Bottom EtOH (%v/v)	5.7	33.0	8.0-14.9	40.0-53.8	49.0-49.3
Bottom EtOH Yield (%)	21.2	25.4	34.9-80.2	48.8-89.5	73.7-78.4
Total EtOH Yield (%)	21.2	25.4	46.0-80.2	57.1-89.5	73.7-78.4
Energy (MJ/kg EtOH)	394	51	84-160	6.4-20.1	15.4

It can be concluded that the compression of the ternary system primarily recovers ethanol into the Bottoms aqueous layer. Compression energy requirement per unit mass of total ethanol recovered showed that energy is saved if the ethanol concentration in the fermentor is high. Compression energy requirement for the extraction of 2% (v/v) ethanol in water was approximately one order of magnitude higher relative to 12% (v/v).

4.3.8 Cost savings with the proposed extraction scheme

Comparison of the traditional state-of-the-art dry grind process of ethanol production form corn with fermentation and *in situ* carbon dioxide gas stripping process by Taylor et al. (2000) showed that the feed sugars entering the fermentor in the gas stripping process could be increased by at least 50%. The capacity to increase the feed sugars into the fermentor resulted in a total saving of $0.03/gallon of ethanol produced from the gas stripping pilot plant. The major equipment difference between the proposed extraction scheme and that carbon dioxide gas stripping used by Taylor et al. (2000) is that instead of the refrigeration system and condensers, we used a carbon dioxide gas compressor to condense the ethanol from the gas stream. Also the packed column over which the fermentation broth was recycled as eliminated in our case. Because simple refrigeration system was expensive, the researchers (Taylor et al. 2000) used a complex network of condensers. The recommended the use of good heat exchanger networking in other work. With the proposed extraction scheme, the investment in heat exchangers and refrigeration is eliminated for a compressor alone which would lead to capital cost savings. The proposed extraction scheme could promise more cost saving if the fermentor is operated at slightly elevated pressures to suppress yeast division and hence effectively convert sugars to product. Using the cooling effect produced by the carbon dioxide for the fermentor or other cooling needs would reduce operating cost as well. The exit temperatures of the carbon dioxide stream from the flashing process in the proposed scheme are lower than those with the condensers and hence ethanol will be effectively condensed from the gas stream. Because the total ethanol yield of the proposed extraction scheme varies mildly and smoothly over a wide range of flash tank pressures (below the

saturation pressure of the CO_2-rich phase), it creates a wide room for operation and fine tuning of the flash tank pressure to optimize the overall operation cost savings.

CHAPTER FIVE

CONCLUSION AND RECOMMENDATION

5.1 Conclusion

It was evident from the results of the experiments that the fast compression of ternary system ($CO_2/C_2H_5OH/H_2O$) transfers the ethanol mostly into the aqueous layer initially at the non equilibrium conditions. Ethanol will tend to move back into the Tops carbon dioxide layer with time towards attaining equilibrium if the Tops and Bottoms are left in contact with each other for extended time. At a particular temperature of the flash tank, the best operating pressure was slightly below the saturation pressure of carbon dioxide. In this way, liquid carbon dioxide with a higher potential of expelling the aqueous phase will likely be formed in the compressor but the Tops in the flash tank would be gas with minimal liquid carbon dioxide to prevent possible entrainment of the lower aqueous phase. Up to 88% total ethanol was recovered from the carbon dioxide gas stream. 10-20% of the work of compression could be recovered as cooling effect of carbon dioxide. The compression energy for the recovery process from a 2%(v/v) ethanol solution ranged from 3-12 times that of a 12%(v/v) solution. For the 2%(v/v) ethanol solutions, the highest total ethanol recovered was 80.2% recorded at 25ºC and 40bar for and at the 12%(v/v) ethanol solutions, the recorded highest was 88.6% at 6ºC and 40bar. The total ethanol yield at for the 12%(v/v) at 25 ºC and 55bar was however 85.7% which was not very far from the highest yield. This extraction scheme could hence attain high ethanol recovery at flash tank temperature of 25 ºC. At this temperature, the flash tank could be cooled with ambient air thus possibly eliminating the need for artificial refrigeration of

the flash tank. Refrigeration energy from throttling carbon dioxide could then be used for other purposes

The total water collected averaged 15 ± 11% more than the equilibrium value for the 2%(v/v) solutions and 39 ± 6% for the 12%(v/v) solution. There was no observed relation of carbon dioxide flow rate with this trend. It appears that not only did water attained thermodynamic equilibrium but was carried in excess of the thermodynamic amounts in carbon dioxide. The high concentration gradient of water across the gas bubbles in the fermentor probably caused an initial rapid super saturation of the gas with water since water partition in the gas phase was fast. This gas potentially exited the fermentor before it could be reduced to the thermodynamic equilibrium value since the gas/liquid interaction times in the fermentor were short. Implementation of the extraction scheme should take into consideration the possible loss of more water than the thermodynamic equilibrium content from the fermentor. Excessive loss of water from the fermentor could possibly have an osmotic effect on the fermentation microorganisms.

The proposed extraction scheme could easily be extended to the recovery of other volatile fermentation products. It would also be useful for recovery of valuable volatile fermentation product where the metabolic evolution of carbon dioxide significantly entrains the product. A major advantage of this process is that it involves only a main compressor and a small pressure tank. There were no other expensive equipment like reinforced fermentors and extraction columns. The ability of this scheme to process more substrate (sugars) if run in a fed batch or continuous mode and at the highest possible non-inhibitive concentration of alcohol can promise increased productivity and compression energy savings. Fed batch or continuous mode operation of the fermentor

could be maintained if at the optimum yeast count and alcohol concentration, the fermentation pressure is increased slightly so stop further cell division so that the continuous substrate stream can be effectively converted to product. Fermentation medium will have to be replaced as some point due to the possible build up of some non volatile by-products like glycerol that sometimes accompanies microorganism fermentation. This process shares several of the advantages of supercritical extraction in that it can be used with fermentation media that has suspended material like with fermentation of sugar substrate from biomass because the gas will not entrain solids from the fermentation medium.

5.2 Recommendation

The choice of compressor for the high pressure recovery of alcohols or other materials should be chosen with care. Small quantities of lubricating material leak into the systems could have a pronounced effect on the quality of the products. The compression phenomenon in the compressors has the ability to fragment and oxidize the lubricating oil during use due to mechanical strain and high temperature similar to that in motor engines (Vazquez-Duhalt 1989). The fragmented long chain hydrocarbon or aromatic species could be oxidized by carbon dioxide into carboxylic acids. In the presence of alcohols, esterification reaction could be triggered. Even though the fraction of alcohol that would be lost through this esterification process would be small, minute quantities of poly aromatic esters species are capable of showing intense color. These colored contaminants could possibly affect the value of the product. Ultimately it would be desired to avoid contamination of any form. Compressors that do not use oil for lubrication will be best suited for the process. Because ethanol itself is completely miscible in liquid carbon

dioxide, contact times between the aqueous and carbon dioxide phases in the flash tank should be kept to the minimum, continuous separation of the aqueous phase from the carbon dioxide phase would promise good recoveries.

REFERENCES

Aldridge GA, Verykios XE, Mutharasan R. 1984. Recovery of Ethanol from Fermentation Broths by Catalytic Conversion to Gasoline .2. Energy Analysis. Industrial & Engineering Chemistry Process Design and Development 23(4):733-737.

Almudi R. 1982. In: Duckworth HE, editor. Proc. Int. Symp. on Ethanol from Biomass. Winniberg, Canada: The Royal Society of Canada.

Arcayledezma GJ, Slaughter JC. 1984. The Response of Saccharomyces-Cerevisiae to Fermentation under Carbon-Dioxide Pressure. Journal of the Institute of Brewing 90(2):81-84.

Baburin LA, Shvinka JE, Viesturs UE. 1981. Equilibrium Oxygen Concentration in Fermentation Fluids. European Journal of Applied Microbiology and Biotechnology 13(1):15-18.

Belanche MI, Soriano E, Zaragoza JL. 1986. Ingenieria Quimica 208:143.

Brignole EA, Andersen PM, Fredenslund A. 1987. Supercritical Fluid Extraction of Alcohols from Water. Industrial & Engineering Chemistry Research 26(2):254-261.

Bungay HR. 1981. Adv. in Biochem. Eng. New York: Springer-Verlag. p 1.

Butler JN. 1982. CO2, Equilibria and their Applications. London: Addison Wesley.

Cardona CA, Sanchez OJ. 2007. Fuel ethanol production: Process design trends and integration opportunities. Bioresource Technology 98(12):2415-2457.

Carioca JOB, Arora HL, Khan AS. 1981. Adv. in Biochem. Eng. New York: Springer-Verlag. p 153.

Christen P, Minier M, Renon H. 1990. Ethanol Extraction by Supported Liquid Membrane During Fermentation. Biotechnology and Bioengineering 36(2):116-123.

Cysewski GR, Wilke CR. 1976. biotechnol. and Bioeng. 18:1297.

Cysewski GR, Wilke CR. 1977. Rapid Ethanol Fermentations Using Vacuum and Cell Recycle. Biotechnology and Bioengineering 19(8):1125-1143.

da Silva FLH, Rodrigues MI, Maugeri F. 1999. Dynamic modelling, simulation and optimization of an extractive continuous alcoholic fermentation process. Journal of Chemical Technology and Biotechnology 74(2):176-182.

Dale MC; 1992. Method of use of a Multi-stage reactor separator with simultaneous product separation Patent: US5141861.

Dale MC, Okos MR, Wankat PC. 1985. An Immobilized Cell Reactor with Simultaneous Product Separation .1. Reactor Design and Analysis. Biotechnology and Bioengineering 27(7):932-942.

Dean JA. 1979. Lange's Handbook of Chemistry. 12 ed. New York: McGraw-Hill.

Defilippi RP, Moses JM. 1982. Extraction of Organics from Aqueous-Solutions Using Critical-Fluid Carbon-Dioxide. Biotechnology and Bioengineering:205-219.

Dixon NM, Kell DB. 1989. The Inhibition by CO2 of the Growth and Metabolism of Microorganisms. Journal of Applied Bacteriology 67(2):109-136.

Dominguez JM, Cao NJ, Gong CS, Tsao GT. 2000. Ethanol production from xylose with the yeast Pichia stipitis and simultaneous product recovery by gas stripping using

a gas-lift loop fermenter with attached side-arm (GLSA). Biotechnology and Bioengineering 67(3):336-343.
Douglas L, Fienberg D. 1983. Evaluation of Non-distillation Ethanol Separation Processes. Solar Energy Research Institute, US Dept. of Commerse(NTIS). Report nr DE83011994

Duboc P, von Stockar U. 1998. Systematic errors in data evaluation due to ethanol stripping and water vaporization. Biotechnology and Bioengineering 58(4):428-439.
Earhart JP, Won KW, Wong HY, Prausnitz JM, King CJ. 1977. Recovery of Organic Pollutants Via Solvent-Extraction. Chemical Engineering Progress 73(5):67-73.
Esplin DW, Capek R, Esplin BA. 1973. An intracellular study of the actions of carbon dioxide on the spinal monosynaptic pathway. Can J Physiol Pharmacol 51(6):424-36.
Fanta GF, Burr RC, Orton WL, Doane WM. 1980. Liquid-Phase Dehydration of Aqueous Ethanol-Gasoline Mixtures. Science 210(4470):646-647.
Fenn WO, Marquisr O. 1968. Growth of Streptococcus faecalis under high hydrostatic pressure and high partial pressures of inert gases. . Journal of General Physiology 52:810-824.
Francis AW. 1954. Ternary systems of liquid carbon dioxide. J. Phys. Chem. 58:1099-1114.
Gan Q, Allen SJ, Taylor G. 2002. Design and operation of an integrated membrane reactor for enzymatic cellulose hydrolysis. Biochemical Engineering Journal 12(3):223-229.
Gill CO, Tan KH. 1979. Effect of Carbon-Dioxide on Growth of Pseudomonas-Fluorescens. Applied and Environmental Microbiology 38(2):237-240.
Gmehling J, Onken U. 1977. Vapor-Liquid Equilibrium Data Collection. Frankfurt, FRG: DECHEMA.
Gryta M, Morawski AW, Tomaszewska M. 2000. Ethanol production in membrane distillation bioreactor. Catalysis Today 56(1-3):159-165.
Gutknecht J, Bisson MA, Tosteson FC. 1977. Diffusion of Carbon-Dioxide through Lipid Bilayer Membranes - Effects of Carbonic-Anhydrase, Bicarbonate, and Unstirred Layers. Journal of General Physiology 69(6):779-794.
Holland CD, Liapis AI. 1983. Computer methods for solving dynamic separation problems. New York: McGraw-Hill. p Appendix 8.
Hong J, Voloch M, Ladisch MR, Tsao GT. 1982. Adsorption of Ethanol-Water Mixtures by Biomass Materials. Biotechnology and Bioengineering 24(3):725-730.
Ikegami T, Kitamoto D, Negishi H, Haraya K, Matsuda H, Nitanai Y, Koura N, Sano T, Yanagishita H. 2003. Drastic improvement of bioethanol recovery using a pervaporation separation technique employing a silicone rubber-coated silicalite membrane. Journal of Chemical Technology and Biotechnology 78(9):1006-1010.
Jones RP, Greenfield PF. 1982. Effect of Carbon-Dioxide on Yeast Growth and Fermentation. Enzyme and Microbial Technology 4(4):210-222.
Joshi DK, Senetar JJ, King CJ. 1984. Solvent-Extraction for Removal of Polar-Organic Pollutants from Water. Industrial & Engineering Chemistry Process Design and Development 23(4):748-754.

Knoche W. 1980. Chemical reactions of CO, in water. In: Bauer C, Gros, G. & Bartels, H., editor. Biophysics and Physiology of Carbon Dioxide. Berlin: Springer-Verlag. p 3-1 1.
Kosaric N, Duvnjak Z, Stewart GG. 1981. Adv. in Biochem. Eng. New York: Springer-Verlag. p 119.
Kosaric N, Wieczorek A, Cosentino GP, Magee RJ, Prenosil JE. 1983. Ethanol Fermentation. In: Dellweg H, editor. Biotechnology. Weinhein: Verlag-Chemie.
Kuhn I. 1980. Alcoholic Fermentation in an Aqueous 2-Phase System. Biotechnology and Bioengineering 22(11):2393-2398.
Kunkee R, .E. , Ouch CS. 1966. Multiplication and fermentation of Saccharomyces cerevisiae under carbon dioxide pressure in wine. Applied Microbiology 14:643-648.
Ladisch MR, Dyck K. 1979. Dehydration of Ethanol - New Approach Gives Positive Energy-Balance. Science 205(4409):898-900.
Ladisch MR, Voloch M, Hong J, Bienkowski P, Tsao GT. 1984. Cornmeal Adsorber for Dehydrating Ethanol Vapors. Industrial & Engineering Chemistry Process Design and Development 23(3):437-443.
Lemmon EW, McLinden MO, Friend DG. 2005. Thermophysical properties of fluid systems. In: Linstrom PJ, Mallard WG, editors. NIST Chemistry WebBook Standard Reference Database Number 69. Gaithersburg, Maryland: National Institute of Standards and Technology(http://webbook.nist.gov).
Lencki RW, Robinson CW, Moo-Young M. 1983. On-Line Extraction of Ethanol from Fermentation Broths Using Hydrophobic Adsorbents. Biotechnol. Bioeng. Symp. Ser. 13:617-628.
Litalien Y, Thibault J, Leduy A. 1989. Improvement of Ethanol Fermentation under Hyperbaric Conditions. Biotechnology and Bioengineering 33(4):471-476.
Lopez-Ulibarri R, Hall GM. 1997. Saccharification of cassava flour starch in a hollow-fiber membrane reactor. Enzyme and Microbial Technology 21(6):398-404.
Loser C, Schroder A, Deponte S, Bley T. 2005. Balancing the ethanol formation in continuous bioreactors with ethanol stripping. Engineering in Life Sciences 5(4):325-332.
Lumsden WB, Duffus JH, Slaughter JC. 1987. Effects of CO2 on Budding and Fission Yeasts. Journal of General Microbiology 133:877-881.
Maiorella BL, Blanch HW, Wilke CR. 1984. Biotechnology report. Economic evaluation of alternative ethanol fermentation processes. Biotechnology and Bioengineering 26:1003–1025.
Mandavilli SN. 2000. Performance characteristics of an immobilized enzyme reactor producing ethanol from starch. Journal of Chemical Engineering of Japan 33(6):886-890.
Matsumura M, Markl H. 1984. Application of Solvent Extraction to Ethanol Fermentation. . Appl. Microbiol. Biotechnol. 20:371-377.
Muller M, Pons MN. 1991. Coupling of Gas Membrane Smooth Pervaporation and Alcoholic Fermentation. Journal of Chemical Technology and Biotechnology 52(3):343-358.

Munson CL, King CJ. 1984. Factors Influencing Solvent Selection for Extraction of Ethanol from Aqueous-Solutions. Industrial & Engineering Chemistry Process Design and Development 23(1):109-115.
Norton JS, Krauss RW. 1972. The inhibition of cell division in Saccharomyces cereuisiae (Meyen) by carbon dioxide. . Plant & Cell PhysioIogy 13:139-149.
Offeman RD, Stephenson SK, Robertson GH, Orts WJ. 2005. Solvent extraction of ethanol from aqueous solutions. I. Screening methodology for solvents. Industrial & Engineering Chemistry Research 44(17):6789-6796.
Oliveira AC, Rosa MF, Cabral JMS, Aires-Barros MR. 1998. Improvement of alcoholic fermentations by simultaneous extraction and enzymatic esterification of ethanol. Journal of Molecular Catalysis B-Enzymatic 5(1-4):29-33.
P.W. A. 1986. Physical chemistry. 3rd ed. New York W.H. Freeman and Company.
Park CH, Geng QH. 1992. Simultaneous Fermentation and Separation in the Ethanol and ABE Fermentation. Separation and Purification Methods 21(2):127-174.
Perry RH, Green DW, Maloney JO. 1997. Perry's chemical engineers' handbook. 7th ed. New York: McGraw-Hill. p 20-21.
Pham CB, Motoki M, Matsumura M, Kataoka H. 1989. Simultaneous Ethanol Fermentation and Stripping Process Coupled with Rectification. Journal of Fermentation and Bioengineering 68(1):25-31.
Pitt WW, Haag GL, Lee DD. 1983. Recovery of Ethanol from Fermentation Broths Using Selective Sorption-Desorption. Biotechnology and Bioengineering 25(1):123-131.
Poole-Wilson PA. 1978. Inhibition of calcium uptake by acidosis in the myocardium of the rabbit [proceedings]. J Physiol 277:79P.
Rachford HH, Rice JD. 1952. Procedure for Use of Electrical Digital Computers in Calculating Flash Vaporization Hydrocarbon Equilibrium. J. Pet. Technol 4:19-20.
Roddy JW. 1981. Distribution of Ethanol-Water Mixtures to Organic Liquids. Industrial & Engineering Chemistry Process Design and Development 20(1):104-108.
Ryan JP, Ryan H. 1972. The role of intracellular pH in the regulation of cation exchanges in yeast. Biochem J 128(1):139-46.
Schumpe A, Deckwer WD. 1979. Estimation of O-2 and CO2 Solubilities in Fermentation Media. Biotechnology and Bioengineering 21(6):1075-1078.
Schumpe A, Quicker G, Deckwer W-D. 1982. Gas solubilities in microbial culture media. Advances in Biochemical Engineering 24:1-38.
Scott JA, Cooke DE. 1995. Continuous Gas (CO2) Stripping to Remove Volatiles from an Alcoholic Beverage. Journal of the American Society of Brewing Chemists 53(2):63-67.
Serra A, Poch M, Sola C. 1987. A Survey of Separation Systems for Fermentation Ethanol Recovery. Process Biochemistry 22(5):154-158.
Shabtai Y, Chaimovitz S, Freeman A, Katchalskikatzir E, Linder C, Nemas M, Perry M, Kedem O. 1991. Continuous Ethanol-Production by Immobilized Yeast Reactor Coupled with Membrane Pervaporation Unit. Biotechnology and Bioengineering 38(8):869-876.

Shen JC, Agblevor FA. 2008. Optimization of enzyme loading and hydrolytic time in the hydrolysis of mixtures of cotton gin waste and recycled paper sludge for the maximum profit rate. Biochemical Engineering Journal 41(3):241-250.
Straskrabova V, Paca J, Kralickova E. 1980. Effect of Aeration and Carbon-Dioxide on Cell Morphology of Candida-Utilis. Applied and Environmental Microbiology 40(5):855-861.
Taylor F, Kurantz MJ, Goldberg N, Craig JC. 1995. Continuous Fermentation and Stripping of Ethanol. Biotechnology Progress 11(6):693-698.
Taylor F, Kurantz MJ, Goldberg N, Craig JC. 1998. Kinetics of continuous fermentation and stripping of ethanol. Biotechnology Letters 20(1):67-72.
Taylor F, Kurantz MJ, Goldberg N, McAloon AJ, Craig JC. 2000. Dry-grind process for fuel ethanol by continuous fermentation and stripping. Biotechnology Progress 16(4):541-547.
Thibault J, Leduy A, Cote F. 1987. Production of Ethanol by Saccharomyces-Cerevisiae under High-Pressure Conditions. Biotechnology and Bioengineering 30(1):74-80.
Vazquez-Duhalt R. 1989. Environmental impact of used motor oil. Sci Total Environ 79(1):1-23.
Walsh PK, Liu CP, Findley ME, Liapis AI, Siehr DJ. 1983. Ethanol Separation from Water in a 2-Stage Adsorption Process. Biotechnology and Bioengineering. Symp. Ser. 13:629-647.
Wilke CR, Maiorella BL, Blanch HW, Cysewski GR; 1982. Patent: US4359533.
Wilke CR, Yang RD, Von Stockar U. 1981. Biotechnol. and Bioeng. Symp. 6:155.
Wilson GM. 1964. J. Amer. Chem. Soc. 86:127-33.
Yagi H, Yoshida F. 1977. Desorption of Carbon-Dioxide from Fermentation Broth. Biotechnology and Bioengineering 19(6):801-819.